

**CALCULATING DEFLECTIONS OF THE
INDIAN RIVER INLET BRIDGE USING
ROTATIONS FROM A STRUCTURAL
HEALTH MONITORING SYSTEM**

by

Ashley Bechtold

A thesis submitted to the Faculty of the University of Delaware in partial fulfillment of the requirements for the degree of Master of Civil Engineering

Spring 2017

© 2017 Bechtold
All Rights Reserved

**CALCULATING DEFLECTIONS OF THE
INDIAN RIVER INLET BRIDGE USING
ROTATIONS FROM A STRUCTURAL
HEALTH MONITORING SYSTEM**

by

Ashley Bechtold

Approved: _____
Michael J. Chajes, Ph.D.
Professor in charge of thesis on behalf of the Advisory Committee

Approved: _____
Harry W. Shenton III, Ph.D.
Chair of the Department of Civil and Environmental Engineering

Approved: _____
Babatunde A. Ogunnaike, Ph.D.
Dean of the College of Engineering

Approved: _____
Ann L. Ardis, Ph.D.
Senior Vice Provost for Graduate and Professional Education

ACKNOWLEDGMENTS

I would like to express my deepest gratitude to my advisors, Dr. Michael Chajes and Dr. Harry “Tripp” Shenton, for their support and guidance throughout this research. Their extensive knowledge and experience in the bridge engineering and structural health monitoring fields were paramount to the completion and accomplishment of this research.

Special thanks are also extended to Hadi Al-Khateeb and Gary Wenczel. Hadi offered endless assistance for numerous aspects of the structural health monitoring system and the finite element analysis bridge model. He was readily available to collaborate when necessary, whether it was to answer questions, brainstorm ideas, or analyze results. Gary was an excellent source of information for all aspects of the structural health monitoring system and had the answers to all of my questions regarding data collection.

I would also like to thank my family and friends for their continuous support and encouragement. Notably, I would like to thank my parents, James and Joanne, for making my structural engineering dreams become a reality. They have stood by my side through each and every step of my studies and reassured me when I needed it most. Lastly, I would like to thank my fiancé, Raymond, for his patience, emotional encouragement, and unconditional love.

TABLE OF CONTENTS

LIST OF TABLES	ix
LIST OF FIGURES	xi
ABSTRACT	xv
Chapter	
1 INTRODUCTION	1
1.1 Research Objective	1
1.2 Thesis Outline	2
2 BACKGROUND	4
2.1 Importance of Monitoring Deflections	4
2.2 Related Studies	5
2.2.1 Measuring Bridge Deflections Using GPS	5
2.2.1.1 Experimental Monitoring of the Humber Bridge Using GPS (Ashkenazi & Roberts, 1997)	5
2.2.1.2 Deflection and frequency Monitoring of the Forth Road Bridge, Scotland, by GPS (Roberts et al., 2012)... 7	
2.2.1.3 Structural Monitoring of Cable-Stayed Bridge: Analysis of GPS Versus Modeled Deflections (Watson, Watson, & Coleman, 2007)	8
2.2.2 Comparison of Laser Doppler Vibrometer with Contact Sensors for Monitoring Bridge Deflection and Vibration (Nassif, Gindy, & Davis, 2005)	10
2.2.3 Using Inclinometers to Measure Bridge Deflection (Hou, Yang, & Huang, 2005)	12
2.3 Contribution of this Research	14
3 DESCRIPTION OF THE BRIDGE AND SYSTEM	16
3.1 Description of the Indian River Inlet Bridge	16
3.2 Description of the Structural Health Monitoring System	18
3.2.1 System Overview	18
3.2.2 Fiber-Optic Tilt Meters	20
3.2.2.1 Introduction	20

3.2.2.2	Placement of Tilt Meters	20
3.3	Description of the Analytical Model for the Indian River Inlet Bridge ..	22
3.3.1	History of FEA Models for the Indian River Inlet Bridge	22
3.3.2	Overview of 3-D CSiBridge Beam Element Model.....	24
3.3.3	Importance of FEA Model for Verification of Results	25
4	GENERAL METHODOLOGY FOR CALCULATING DELFECTIONS FROM ROTATIONS	26
4.1	Elastic Beam Theory	26
4.1.1	Assumptions	26
4.1.2	Derivation of the Basic Differential Equation.....	27
4.2	Double Integration Method	30
5	CONTROLLED LOAD TEST OF THE INDIAN RIVER INLET BRIDGE .	33
5.1	Overview of the Load Testing.....	33
5.2	Load Test 5 Data Collection.....	34
5.2.1	Introduction	34
5.2.2	Measured Deflections through Survey	37
5.2.2.1	Process of Measuring Deflections through Survey	37
5.2.2.2	Importance of Measuring Deflections through Survey	39
5.2.3	Load Pass 0_1 Measured Rotation and Deflections	39
5.2.4	Load Pass 0_2 Measured Rotations and Deflections	41
6	PROCESS FOR CALCULATING DEFLECTIONS FROM IRIB ROTATION DATA.....	44
6.1	Automated Matlab Code for Load Test System Data	44
6.1.1	Introduction	44
6.1.1.1	Importance of Generating an Automated Code.....	45
6.1.2	Preprocessing Steps Used in the Automated Matlab Code	46
6.1.2.1	Extracting System Data	46
6.1.2.2	Demeaning and Smoothing System Data	46

6.1.2.3	Merging System A and System B	48
6.1.3	Utilizing the Matlab Curve Fitting Tool.....	49
6.2	Surface Mounted Tilt Meters for Load Test Data	50
6.2.1	Preprocessing Steps Used for the Surface Mounted Tilt Meters.	50
6.2.1.1	Calibrating the Surface Mounted Tilt Meters.....	50
6.2.1.2	Integrating the Surface Mounted Tilt Meters and the SHM System Data	53
7	CALCULATED DEFLECTIONS USING IRIB ROTATION DATA: PRELIMINARY RESULTS	56
7.1	Automated Matlab Code for Load Test System Data	56
7.1.1	Presentation of Results	56
7.1.1.1	Load Pass 0_1.....	57
7.1.1.2	Load Pass 0_2.....	58
7.1.2	Issues with Results	59
7.1.2.1	Bridge End Deflections	60
7.1.2.2	Bridge Pylon Deflections	60
7.1.3	Adjustments Made to Overcome Issues	61
7.1.3.1	Forcing End Deflections to Zero	61
7.1.3.2	Forcing Pylon Deflections to Zero	62
7.2	Need for Additional Tilt Meters	63
7.2.1	Presentation of Original SHM System Data.....	63
7.2.2	Shortcomings of Results.....	65
7.2.2.1	Need for Surface Mounted Tilt Meters	68
7.2.3	Determining the Location of the Surface Mounted Tilt Meters ..	69
8	CALCULATED DEFLECTIONS USING IRIB ROTATION DATA: FINAL RESULTS	71
8.1	Results from Automated Matlab Code	71

8.1.1	Load Pass 0_1	71
8.1.2	Load Pass 0_2	75
8.2	Results from Surface Mounted Tilt Meters	80
8.2.1	Load Pass 0_1	82
8.2.1.1	Final Rotation and Deflection Profile Plots.....	82
8.2.1.2	Comparison of Deflection Profiles With and Without Surface Mounted Tilt Meters.....	89
8.2.2	Load Pass 0_2	93
8.2.2.1	Final Rotation and Deflection Profile Plots.....	93
8.2.2.2	Comparison of Deflection Profiles With and Without Surface Mounted Tilt Meters.....	97
9	ACCURACY OF CALCULATED DEFLECTIONS	101
9.1	Automated Matlab Code for Load Test System Data	101
9.1.1	Load Pass 0_1	102
9.1.1.1	Comparison to FEA Model	102
9.1.1.2	Comparison to Survey	105
9.1.2	Load Pass 0_2	107
9.1.2.1	Comparison to FEA Model	107
9.1.2.2	Comparison to Survey	110
9.1.3	Comparison of Final Results	112
9.2	Surface Mounted Tilt Meters for Load Test Data	114
9.2.1	Load Pass 0_1	114
9.2.1.1	Comparison to FEA Model	115
9.2.1.2	Comparison to Survey	117
9.2.2	Load Pass 0_2	120
9.2.2.1	Comparison to FEA Model	120
9.2.2.2	Comparison to Survey	123

9.2.3	Comparison of Final Results	125
10	CONCLUSIONS AND RECOMMENDATIONS.....	128
10.1	Conclusions	128
10.2	Recommendations for Future Work	131
	REFERENCES	133
Appendix		
A	LOAD PASS 0_1 RESULTS, INCLUDING SURFACE MOUNTED TILT METERS	134
A.1	Rotation and Deflection Profiles for Loading Scenarios.....	134
B	LOAD TEST 5 TRUCK CONFIGURATIONS.....	139
B.1	Truck Configurations and Respective Load Pass Numbers.....	139
C	AUTOMATED MATLAB CODE USED TO CALCULATE DEFLECTIONS FROM SHM SYSTEM ROTATION DATA.....	142
C.1	Matlab Code Used to Automatically Analyze Load Test Data	142
D	RAW ROTATION DATA COLLECTED DURING LOAD TEST 5.....	161
D.1	Raw Rotation Data from SHM System and Surface Mounted Tilt Meters.....	161
E	PERMISSIONS	162
E.1	Permission to Use Figure 2 and Figure 5	162

LIST OF TABLES

Table 1	Truck Weights Used in Load Test 5.....	35
Table 2	Load Pass Descriptions for Load Test 5.....	36
Table 3	Final Deflection Values for Load Pass 0_1 with Trucks Positioned Above T_E5	75
Table 4	Final Deflection Values for Load Pass 0_2 with Trucks Positioned Above T_E5	78
Table 5	Final Deflection Values for Load Pass 0_1, Including Surface Mounted Tilt Meters, with Trucks Positioned Above T_E5	87
Table 6	Comparison of Final Deflection Values With and Without Surface Mounted Tilt Meters.....	92
Table 7	Final Deflection Values for Load Pass 0_2, Including Surface Mounted Tilt Meters, with Trucks Positioned Above T_E5	96
Table 8	Comparison of Final Deflection Values With and Without Surface Mounted Tilt Meters.....	100
Table 9	Comparison of Load Pass 0_1 Calculated Deflections with FEA Model Deflections	103
Table 10	Comparison of Load Pass 0_1 Calculated Deflections with Survey Deflections.....	105
Table 11	Comparison of Load Pass 0_2 Calculated Deflections with FEA Model Deflections	108
Table 12	Comparison of Load Pass 0_2 Calculated Deflections with Survey Deflections.....	110
Table 13	Comparison of Calculated Load Pass 0_1, Calculated Load Pass 0_2, Survey, and FEA Model Deflections	113
Table 14	Comparison of Load Pass 0_1 Calculated Deflections, Including Surface Mounted Tilt Meters, with FEA Model Deflections	115
Table 15	Comparison of Load Pass 0_1 Calculated Deflections, Including Surface Mounted Tilt Meters, with Survey Deflections.....	118

Table 16	Comparison of Load Pass 0_2 Calculated Deflections, Including Surface Mounted Tilt Meters, with FEA Model Deflections	120
Table 17	Comparison of Load Pass 0_2 Calculated Deflections, Including Surface Mounted Tilt Meters, with Survey Deflections.....	123
Table 18	Comparison of Calculated Load Pass 0_1, Calculated Load Pass 0_2, Survey, and FEA Model Deflections	127
Table D.1	Raw Rotation Data from Load Pass 0_1 and Load Pass 0_2	161

LIST OF FIGURES

Figure 1	Location of the Indian River Inlet Bridge	17
Figure 2	Sensor Layout for the Indian River Inlet Bridge (Al-Khateeb, 2016).....	19
Figure 3	Elevation View of the Bridge Indicating Tilt Meter Locations (Shenton, Fernandez, Ramanna, Chajes, & Wenczel, 2013)	21
Figure 4	Elevation View of the Bridge Indicating Location of System and Surface Mounted Tilt Meters	22
Figure 5	3-D CSiBridge Model with Beam Elements for the IRIB (Al-Khateeb, 2016).....	24
Figure 6	Loads Applied Perpendicular on a Straight Simple Beam (Hibbeler, 2012).....	27
Figure 7	The Straight Simple Beam Cross Section Before and After Deformation (Hibbeler, 2012).....	28
Figure 8	Truck Configuration for Load Pass 0	37
Figure 9	Layout of Survey Prisms and Tilt Meter Locations	38
Figure 10	Schematic of Survey Reading Locations.....	40
Figure 11	Rotation and Deflection Profile Plots from Load Pass 0_1 With Trucks Located Above Tilt Meter T_E4	41
Figure 12	Rotation and Deflection Profile Plots from Load Pass 0_2 With Trucks Located Above the Midspan Location	43
Figure 13	Example of the Surface Mounted Tilt Meter Lab Setup	52
Figure 14	Raw Voltage Data from Surface Mounted Tilt Meters	54
Figure 15	Rotation and Deflection Profiles for Load Pass 0_1 with Trucks Positioned AboveT_E5.....	58
Figure 16	Rotation and Deflection Profiles for Load Pass 0_2 with Trucks Positioned Above T_E5.....	59
Figure 17	Rotation Profile of the IRIB from the November 2012 Load Test	64

Figure 18	Deflection Profile of the IRIB from the November 2012 Load Test	65
Figure 19	Rotation Profile Comparison Between November 2012 Load Test and Model.....	66
Figure 20	Deflection Profile Comparison Between November 2012 Load Test and Model.....	67
Figure 21	Comparison Between May 2016 Load Test Rotation Points and FEA Model Rotation Profile	70
Figure 22	Final Rotation and Deflection Profiles for Load Pass 0_1 with Trucks Positioned Above T_E5.....	73
Figure 23	Final Deflection Profile for Load Pass 0_1 with Trucks Positioned Above T_E5	74
Figure 24	Final Rotation and Deflection Profiles for Load Pass 0_2 with Trucks Positioned Above T_E5.....	76
Figure 25	Final Deflection Profile for Load Pass 0_2 with Trucks Positioned Above T_E5	77
Figure 26	Comparison of Load Pass 0_1 and Load Pass 0_2 Deflection Profiles ..	79
Figure 27	Comparison of Rotation Profiles from the November 2012 Load Test, May 2016 Load Pass 0_1, and May 2016 Load Pass 0_2.....	81
Figure 28	Rotation and Deflection Profiles for Load Pass 0_1, Including Surface Mounted Tilt Meters, with Trucks Positioned Above T_E4.....	83
Figure 29	Final Deflection Profile for Load Pass 0_1, Including Surface Mounted Tilt Meters, with Trucks Positioned Above T_E4.....	84
Figure 30	Rotation and Deflection Profiles for Load Pass 0_1, Including Surface Mounted Tilt Meters, with Trucks Positioned Above T_E5.....	85
Figure 31	Final Deflection Profile for Load Pass 0_1, Including Surface Mounted Tilt Meters, with Trucks Positioned Above T_E5.....	86
Figure 32	Rotation and Deflection Profiles for Load Pass 0_1, Including Surface Mounted Tilt Meters, with Trucks Positioned Above T_E6.....	88
Figure 33	Final Deflection Profile for Load Pass 0_1, Including Surface Mounted Tilt Meters, with Trucks Positioned Above T_E6.....	89

Figure 34	Rotation Profile Comparison Between Inclusion of Surface Mounted Tilt Meters and Exclusion of Surface Mounted Tilt Meters	90
Figure 35	Deflection Profile Comparison Between Inclusion of Surface Mounted Tilt Meters and Exclusion of Surface Mounted Tilt Meters	91
Figure 36	Final Rotation and Deflection Profiles for Load Pass 0_2, Including Surface Mounted Tilt Meters, with Trucks Positioned Above T_E5	94
Figure 37	Final Deflection Profile for Load Pass 0_2, Including Surface Mounted Tilt Meters, with Trucks Positioned Above T_E5	95
Figure 38	Comparison of Load Pass 0_1 and Load Pass 0_2 Deflection Profiles, Including Surface Mounted Tilt Meters	97
Figure 39	Deflection Profile Comparison Between Inclusion of Surface Mounted Tilt Meters and Exclusion of Surface Mounted Tilt Meters	98
Figure 40	Deflection Profile Comparison Between Inclusion of Surface Mounted Tilt Meters and Exclusion of Surface Mounted Tilt Meters	99
Figure 41	Graphical Comparison of Load Pass 0_1 Calculated Deflections and FEA Model Deflections.....	104
Figure 42	Graphical Comparison of Load Pass 0_1 Calculated Deflections and Survey Deflections	106
Figure 43	Graphical Comparison of Load Pass 0_2 Calculated Deflections and FEA Model Deflections.....	109
Figure 44	Graphical Comparison of Load Pass 0_2 Calculated Deflections and Survey Deflections	111
Figure 45	Comparison of Calculated Load Pass 0_1, Calculated Load Pass 0_2, Survey, and FEA Model Deflections	112
Figure 46	Graphical Comparison of Load Pass 0_1 Calculated Deflections, Including Surface Mounted Tilt Meters, and FEA Model Deflections .	116
Figure 47	Graphical Comparison of Load Pass 0_1 Calculated Deflections, Including Surface Mounted Tilt Meters, and Survey Deflections.....	119
Figure 48	Graphical Comparison of Load Pass 0_2 Calculated Deflections, Including Surface Mounted Tilt Meters, and FEA Model Deflections .	122

Figure 49	Graphical Comparison of Load Pass 0_2 Calculated Deflections, Including Surface Mounted Tilt Meters, and Survey Deflections.....	124
Figure 50	Comparison of Calculated Load Pass 0_1, Calculated Load Pass 0_2, Survey, and FEA Model Deflections	126
Figure A.1	Rotation and Deflection Profiles for Trucks Positioned Above Tilt Meter T_E4.....	134
Figure A.2	Rotation and Deflection Profiles for Trucks Positioned Above Tilt Meter SM_1.....	135
Figure A.3	Rotation and Deflection Profiles for Trucks Positioned Above Tilt Meter T_E5.....	136
Figure A.4	Rotation and Deflection Profiles for Trucks Positioned Above Tilt Meter SM_2.....	137
Figure A.5	Rotation and Deflection Profiles for Trucks Positioned Above Tilt Meter T_E6.....	138

ABSTRACT

As the age of bridges worldwide increase, and their structural integrities decrease, the need for ways to evaluate and monitor the ever changing structural health of bridges has become more crucial. One monitoring method that has recently gained popularity worldwide is the use of structural health monitoring systems. Structural health monitoring systems allow bridge owners to continuously monitor parameters that can be used to assess a bridge's structural health. Two such parameters are strain and rotation. While structural health monitoring systems have advanced over the years, bridge owners still lack simple methods for analyzing certain types of structural health monitoring data in order to evaluate the structural integrity of their bridges. One example is the monitoring and evaluation of bridge rotations. While rotations can offer insight into a bridge's deflections, they have not been thoroughly investigated and introduced to the bridge industry.

In this research, rotation data from a structural health monitoring system on the Indian River Inlet Bridge, and two additional surface mounted tilt meters, was analyzed and used to calculate bridge deflections. The methodology behind calculating bridge deflections from rotation data is based on elastic beam theory and the double integration method. In order to obtain the rotation data for the analyses, a controlled load test was conducted on the Indian River Inlet Bridge in May of 2016. During that load test, a survey crew was onsite to measure the deflection of the bridge. The deflections that were calculated using structural health monitoring system rotation data were compared to the measured defections. The final calculated Load Pass 0_1 midspan deflection was off from the survey midspan deflection by about 16%. The final calculated Load Pass 0_2 midspan deflection was off from the survey midspan

deflection by about 14%. Through these comparisons of calculated deflections to survey deflections, the methodology used to calculate deflections from rotation data was validated. The deflections that were predicted by a validated finite element analysis (FEA) of the bridge were also compared to measured survey deflections. The FEA model midspan deflection was off from the survey midspan deflection by about 9%, which suggests that FEA can be used to produce both rotations and deflections.

Chapter 1

INTRODUCTION

1.1 Research Objective

As more and more long-span bridges are built, the search for ways to efficiently evaluate their in-service performance has become a growing area of research. In recent years, structural health monitoring systems have been increasing in use as a way to aid bridge owners in evaluating their bridges. Structural health monitoring systems employ various types of sensors including strain gauges, accelerometers, and tilt meters. While each type of sensor is important for monitoring and evaluating certain aspects of a bridge, some sensor types are more commonly used and their applications are better defined than others. Tilt meters have not been as widely utilized in existing structural health monitoring systems. Because of this, their use for bridge evaluation is not well defined. Since deflections are one of the key parameters that can be used to evaluate the overall condition of a bridge, and since deflections can be found from rotations, the monitoring of rotations holds promise as one parameter that can be monitored and used in the bridge evaluation process.

The primary objective of this research was to develop a method for using the rotation data collected by the structural health monitoring system on the Indian River Inlet Bridge to determine bridge deflections. The method used to calculate deflections from rotations, which is based on elastic beam theory and the double integration method, holds promise for use by transportation agencies as a way of monitoring and evaluating overall bridge health. This research could pave the way for further research

in the area of structural health monitoring, in terms of both rotation and deflection analyses and monitoring.

1.2 Thesis Outline

The following outline discusses the contents of the remainder of this thesis.

Chapter 2 – Background discusses the importance of monitoring structural deflections and describes several related studies that involve calculating and monitoring bridge deflections. Additionally, the contribution of this research to the area of study is introduced.

Chapter 3 – Description of the Bridge and System provides a description of the Indian River Inlet Bridge and the Structural Health Monitoring system that has been installed on the bridge. Towards the end of the chapter, the finite element analysis model used to analyze the Indian River Inlet Bridge is introduced.

Chapter 4 – General Methodology for Calculating Deflections from Rotations describes the theory behind calculating deflections from rotations, which consists of elastic beam theory and the double integration method.

Chapter 5 – Controlled Load Test of the Indian River Inlet Bridge provides an overview of the load testing that was conducted on the Indian River Inlet Bridge. Load Test 5, which is the test from which the analyzed data came from, is described in detail, including an overview of the load test and the data collection process.

Chapter 6 – Process for Calculating Deflections from IRIB Rotation Data describes the process for calculating deflections from rotation data. An automated Matlab code is introduced, followed by a description of the preprocessing steps that are used and the curve fitting tool that is applied in Matlab. The initial deflection calculations were based on rotation data collected solely by the structural health

monitoring system. At the end of the chapter, the process for analyzing rotation data from both the structural health monitoring system and additional surface mounted tilt meters is introduced.

Chapter 7 – Calculated Deflections Using IRIB Rotation Data: Preliminary Results presents the preliminary deflection calculation results computed based on the original SHM system rotation data. Based on the preliminary deflection results, modifications to the computation process to account for known boundary condition values are developed and described. In the second half of the chapter, deflection calculation results using the modified process are presented. These results indicate a need for additional tilt meters to improve the accuracy of the deflection calculations. This leads to a discussion of the benefit of adding two surface mounted tilt meters, and the optimal location for those additional tilt meters.

Chapter 8 – Calculated Deflections Using IRIB Rotation Data: Final Results first presents the final deflection results computed based only on rotation data collected by permanently mounted tilt meters, followed by deflection results computed based on rotation data collected by both permanently mounted tilt meters and two additional surface mounted tilt meters.

Chapter 9 – Accuracy of Calculated Deflections focuses on comparing the calculated deflections found using rotation data to deflections predicted by a finite element analysis and also to actual deflections measured through surveying during Load Test 5.

Chapter 10 – Conclusions and Recommendations starts by discussing the conclusions that are drawn from this research. The second half of the chapter provides recommendations for future work.

Chapter 2

BACKGROUND

This chapter provides insight on the importance of monitoring bridge deflections. Some related studies on bridge deflection monitoring are also introduced in this chapter, which consist of monitoring bridge deflections using GPS, monitoring bridge deflections using laser Doppler vibrometers, and monitoring bridge deflections using inclinometers. Lastly, the contribution of this research to the topic of bridge deflection monitoring is discussed towards the end of this chapter.

2.1 Importance of Monitoring Deflections

As the safety requirements of long-span bridges becomes more stringent, structural health monitoring of these bridges is becoming more prevalent. Bridge structural health monitoring is commonly used as a simple approach to measure the overall integrity and stability of the structure. Because deflections are one of the key parameters that can be used to assess the overall integrity and stability of the bridge, monitoring deflections of long-span bridges can be quite useful. Bridge deflections can be caused by dead loads, live loads, and thermal effects. All types of deflections are useful to measure and monitor as long-term changes in deflections can indicate changes in the bridge stiffness, which ultimately can indicate a change in the bridge condition. Comparing the measured deflections to the allowable deflection limits will allow for reductions in the occurrence of crack formations and any other structural damage. This could ultimately result in the reduction of bridge failures, and even allow for the prediction of bridge failures before they could occur.

The deflection measurements obtained through structural health monitoring are also useful for the validation of any finite element models used for a bridge. While

finite element models are created to accurately analyze a bridge, they can often be extremely complex for cable-stayed bridges, which will be discussed in Section 3.3. Therefore, validating models using deflection measurements obtained from structural health monitoring is extremely advantageous and allows for additional verification.

2.2 Related Studies

While the importance of monitoring bridge deflections is widely understood, the process of monitoring bridge deflections has not been extensively researched. Some recent studies on monitoring bridge deflections are discussed in the following sections. The main processes that will be discussed include monitoring bridge deflections using GPS, monitoring bridge deflections using laser Doppler vibrometers, and monitoring bridge deflections using inclinometers.

2.2.1 Measuring Bridge Deflections Using GPS

The use of Global Positioning System (GPS) for monitoring bridge deflections is a method that continues to advance since its recent development in the 1990s. It has been recognized as a reliable and efficient structural health monitoring application. While GPS monitoring is useful for various types of structures, it has frequently been applied to structural health monitoring of bridges, specifically cable-stayed and suspension bridges. Some of the GPS monitoring studies conducted on long-span bridges are discussed in the following sections.

2.2.1.1 Experimental Monitoring of the Humber Bridge Using GPS (Ashkenazi & Roberts, 1997)

The Humber Bridge, located in England, has a total length of about 2,220 m. The bridge was designed to endure deformations of as high as 4 m, in either the

positive or negative direction. Because the predicted deflections of the bridge were so large, there was an interest in monitoring the actual bridge deflections. Monitoring of the bridge deflections was done using kinematic GPS. Separate GPS antennas were placed at specific points along the bridge deck and the bridge towers. A reference receiver was placed about 1.5 m from the bridge, which was used as a benchmark relative to the GPS antennas. The resolution of the GPS system was ± 1 mm in the horizontal direction and ± 3 mm in the vertical direction, which was determined through a zero-baseline test.

The GPS receiver used for the Humber Bridge was placed on the west side rail of the bridge deck, as this location would hypothetically experience the largest deflection. The deflections in the longitudinal, vertical, and lateral directions were measured for the Humber Bridge. Focusing on solely the vertical deflection of the bridge, the maximum deflection experienced on the bridge deck was about 40 cm. This deflection was likely due to a heavy traffic load on the bridge, as the typical vertical deflections experienced were around 15 cm.

The results from the GPS monitoring of the Humber Bridge deflection compared closely to the expected deflections of the bridge. While there are some errors introduced due to vibrations in the receiver poles, overall the use of GPS to monitor deflections is seen as a credible method that provides fairly accurate results. Because of this, GPS monitoring has been introduced to many other bridges in England

2.2.1.2 Deflection and frequency Monitoring of the Forth Road Bridge, Scotland, by GPS (Roberts et al., 2012)

The Forth Road Bridge in Scotland, which crosses the Firth of Forth, has a total length of about 2.5 km. The bridge has structural stiffening in the towers, as well as a stiffening truss below the deck. The structural stiffening helps the bridge carry over 23 million vehicles each year, with a current weight limit of 44 tons. This study focused on monitoring the deflection and frequency of the Forth Road Bridge.

Deflection monitoring of the Forth Road Bridge was done using GPS. Two reference GPS stations were positioned on the Forth Road Bridge, which were located on the southern viewing platform off of the bridge. Five GPS receivers were attached to the bridge deck and two were attached to the southern bridge tower. The five GPS receivers located on the bridge deck were positioned along the length of the bridge so that they were dispersed fairly evenly, to ensure that a complete deflection profile of the bridge could be obtained. The reference receivers served as benchmarks for each of the seven GPS receivers.

Bridge loading trials were conducted on the Forth Road Bridge in order to collect GPS data to monitor the deflections of the bridge. Six of the seven GPS receivers collected data at a frequency of 10 Hz, while the other GPS receiver collected data at a frequency of 20 Hz. A sequence of load trials with two 40 ton trucks were conducted, during which the configuration and location of the trucks were known. Other load trials with random daily traffic were conducted as well.

Once the data was collected from the GPS receivers, the data was converted to a coordinate system relative to the bridge. This ultimately resulted in displacements in the lateral, longitudinal, and vertical directions. In order to obtain the most accurate

deflection measurements, a zero-baseline test was conducted on the bridge as well, which would be used to analyze and compare results from the load trials.

The results from the load trials were compared to the results predicted by a finite element model (FEM) of the bridge. The maximum deflection for the FEM of the Forth Road Bridge was about 280 mm. The mean deflection from the GPS receiver at the same location along the bridge compared extremely well to the FEM deflection, at about 280 mm. The overall maximum vertical deflection experienced during the load trials was about 400 mm.

Because the deflection results of the GPS receivers compared very well to the deflection results from the FEM for the Forth Road Bridge, the GPS method used for the bridge can serve as a foundation for structural monitoring GPS systems. Structural monitoring GPS systems can now serve many important purposes, including validating models and assessing bridge behavior.

2.2.1.3 Structural Monitoring of Cable-Stayed Bridge: Analysis of GPS Versus Modeled Deflections (Watson, Watson, & Coleman, 2007)

The Batman Bridge in northern Tasmania is a cable-stayed bridge that was built in 1968. The steel bridge was one of the first cable-stayed truss bridges in the world. The uniqueness of the Batman Bridge makes structural health monitoring of the bridge particularly important, in order to monitor the performance of the bridge and determine any necessary maintenance or repairs for the bridge.

The study conducted on the Batman Bridge focused on collecting deflection data using GPS and comparing the observed data to results obtained from a structural analysis model of the bridge. The monitored deflections were used to quantify both deflections caused by thermal changes and deflections caused by vehicle loads. The

purpose of the study was to verify the methodology used to monitor deflections using GPS, as well as to verify the model created for the bridge.

The GPS system that was set up for the study consisted of three GPS antenna receivers, one of which was a GPS reference site and two of which were GPS rover sites. The reference site was positioned on the eastern abutment of the bridge. The two rover sites were positioned on the top of the bridge tower and on the bridge deck where the maximum deflection was expected to occur. The frequency of data collection from the GPS system was restricted to 1 Hz. The data that was collected using the GPS system was converted into a local coordinate system for the bridge. The results from this conversion were time-stamped coordinate data that could then be used to analyze the thermal and vehicle loading responses that were targeted.

The model for the bridge was produced using Space Gass software. For this study, the estimated vehicle weight that was used for the structural analysis was 300 kN. Model deflections were determined at one second increments, in order to correlate with the data collected from the GPS system. The bridge deflection produced from the model consisted of a downward deck deflection at the midpoint of the main span and a resultant longitudinal deflection at the bridge tower.

The results from the observed GPS data collection and the predicted model analysis were compared, for both the bridge deck deflection and the bridge tower deflection. For the bridge deck deflection, the results from the GPS system agreed very well with the results from the model, in terms of both the magnitude of the deck deflection and the shape of the deflection profile. The maximum deck deflection for the Batman Bridge with a 300 kN load was about 54 mm. The shape of the deflection profile followed a trend where the maximum midspan deflection was a negative peak,

and as the ends of the bridge neared, the deflection became positive before returning back to zero.

For the bridge tower deflection, the results from the model underestimated the results from the GPS system. While the general shapes of the deflection profiles agreed well with each other, the magnitude of the model tower deflection was about half of the magnitude of the GPS tower deflection. The maximum tower deflection experienced from the GPS data was about 17 mm, whereas the model predicted a maximum tower deflection of only about 8 mm. It was determined that this discrepancy was likely caused by an incorrect mass load or a simplification in the model configuration.

It can be seen from the above-mentioned study of the Batman Bridge that GPS was effectively used to determine deck and tower deflections. The observed GPS deflections provided a means of verifying the structural analysis model of the bridge. While there are some discrepancies in the comparisons of the model and GPS deflections, the approach of using GPS to monitor bridge deflections and verify model deflections has been confirmed as useful and effective.

2.2.2 Comparison of Laser Doppler Vibrometer with Contact Sensors for Monitoring Bridge Deflection and Vibration (Nassif, Gindy, & Davis, 2005)

The Doremus Avenue Bridge in New Jersey is an essential part of the roadway system that provides access to the air and sea ports of Newark City. Because the bridge is so significant, it was determined that it was important to monitor the deflections of the bridge. In order to do this, a Laser Doppler Vibrometer (LDV) system was placed on the bridge. The LDV system uses laser interferometry to measure surface vibrations of the bridge. The surface vibrations were used to record

both displacement and velocity. The LDV does this by detecting the Doppler shift of the laser light. The LDV system controls were set up below the bridge, to ensure that the controls did not experience any vibrations. Because of this, the LDV system was only used for short-term monitoring as a temporary setup.

A Linear Variable Differential Transformer (LVDT)-cable system was also placed on the bridge, as a more permanent monitoring option. The LVDT-cable system consists of a stainless steel aircraft reference cable and an LVDT, which are installed on the girder that experiences the heaviest northbound traffic. The reference cable is attached to both ends of the bridge support girder. The LVDT is attached at the centerline of the girder, at the position where the maximum moment occurs. The displacement is measured as the distance between the reference cable and the LVDT changes due to traffic loads. The output of the LVDT-cable system is a voltage output. The voltage outputs are recorded using a solar powered data logger and transmitted to a computer using a wireless data link transceiver.

Controlled dynamic load tests were conducted on the Doremus Avenue Bridge to collect data using both the LDV system and the LVDT-cable system. A loaded 5-axle truck, with a known weight, was driven across the bridge in three different configurations. Using three different configurations allowed for a more thorough comparison of results between the two systems.

After the controlled load tests, the data from the LDV system and the permanent LVDT-cable system were analyzed and compared. The bridge deflection profiles generated using the data from the two systems correlated extremely well, both in terms of deflection profile shapes and deflection magnitudes. The maximum positive and negative deflections during the controlled load tests were about 10 mm

and 4 mm, respectively. Because the deflection measurements from the two systems compared very well, it was concluded that the LDV system is an efficient non-contact method of measuring bridge deflections that provides accurate and repeatable results.

2.2.3 Using Inclometers to Measure Bridge Deflection (Hou, Yang, & Huang, 2005)

Model QY Inclometers were installed on the Taolaizhao Bridge over the Songhua River in China. The inclinometers were developed by the Measuring Instrument Division, the Institute of Engineering Mechanics, and the China Earthquake Administration. Model QY Inclometers measure angles of rotation and output the angles in proportionate voltages. The inclinometers were installed on the bridge, at the sixth and tenth spans, to measure both static and dynamic deflections. Ten inclinometers were installed for the static deflection measurements, whereas seven inclinometers were installed for the dynamic deflection measurements.

Once data collection was complete and the raw data was obtained from the Model QY Inclometers, the voltages were used to determine the corresponding angles, and ultimately calculate the resulting deflections. In order to calculate the resulting deflections, an algorithm was developed, which is presented below in Equation 2.1. Equation 2.1 is used to calculate the deflection curve of the bridge span solely for the dynamic deflection cases, while the algorithm for the static deflection cases can be obtained by simply omitting the time parameter in the algorithm.

$$y(x, t_0) = A(x) \sum_{j=1}^{n-1} X_j(t_0) g_j(x) \quad \text{Equation 2.1}$$

Where,

$y(x,t_0)$ = deflection curve of the bridge span

$A(x)$ = chosen function that makes the deflection curve satisfy boundary conditions

$X_j(t_0)$ = undetermined coefficient

$g_j(x)$ = appropriately selected function group

The deflection curve of the bridge span is determined by defining the angular values of the span as $\theta_i(t_0)$. The angular values can be calculated using Equation 2.2, which is presented below.

$$\left[A'(x) \sum_{j=1}^{n-1} X_j(t_0) g_j(x) + A(x) \sum_{j=1}^{n-1} X_j(t_0) g'_j(x) \right] \Big|_{x=x_i} = \theta_i(t_0) \quad \text{Equation 2.2}$$

Where,

x_i = coordinate of the i th inclinometer

$A'(x)$ = first differentiation of $A(x)$

$g'_j(x)$ = first differentiation of $g_j(x)$

$X_j(t_0)$ = undetermined coefficient that can be determined using the least-square method

More details about the dynamic deflection algorithm and its parameters can be found in (Hou et al., 2005).

Once the deflection curve of the bridge span is determined, the whole deflection time history can be calculated as well. Understandably, the larger the number of inclinometers installed, the greater the precision of the calculated bridge

deflection. In general, it is suggested that at least five inclinometers be installed along the length of the bridge to obtain reliable results.

The data from the Model QY Inclinometers for the Taolaizhao Bridge was verified using a photoelectric bridge deflection measurement gauge. The results from the Model QY Inclinometers compared relatively well to the results from the photoelectric bridge deflection measurement gauge, with relative errors less than five percent. It was evident that the Model QY Inclinometers underestimated the deflection measurements of the Taolaizhao Bridge when compared to the photoelectric bridge deflection measurement gauge. However, in the end, the described method of measuring bridge deflections using inclinometers is a promising technique that has the potential to provide substantial engineering value.

2.3 Contribution of this Research

The various studies mentioned in the area of bridge deflection monitoring represent a few very different methods of monitoring or calculating deflections. For the most part, the previously mentioned studies have not involved permanent structural health monitoring systems, likely due to the up and coming nature of the subject. Therefore, there is a need for focus on how permanent structural health monitoring systems can be used to monitor bridge deflections. While many bridges throughout the United States do not currently have permanent structural health monitoring systems in place, it is expected that as the cost of the systems come down, the number of permanent structural health monitoring systems will increase due to the vast benefits associated with them. With the rise of structural health monitoring systems on bridges, determining the most efficient and reliable ways to monitor bridge deflections using such systems become important.

The Indian River Inlet Bridge has the first identified permanent fiber optic structural health monitoring system on a cable-stayed bridge in the United States. The rotation data obtained from the structural health monitoring system on the Indian River Inlet Bridge is projected to be utilized to monitor the rotation and deflection of the bridge for the remainder of its service life. This research aims to introduce a new method of monitoring bridge deflections for the Indian River Inlet Bridge, which consists of calculating deflections using rotation data from the structural health monitoring system. There is anticipation that this research will also serve as a foundation for a reliable and efficient deflection monitoring method that could be used for other bridges with structural health monitoring systems.

Chapter 3

DESCRIPTION OF THE BRIDGE AND SYSTEM

The following chapter consists of background information regarding the Indian River Inlet Bridge, including the location of the bridge and design details. This chapter also introduces the Structural Health Monitoring (SHM) system that was installed on the bridge, with a detailed explanation of the tilt meters used to measure rotation. The Finite Element Analysis (FEA) model used to analyze the Indian River Inlet Bridge is also discussed in this chapter.

3.1 Description of the Indian River Inlet Bridge

The Charles W. Cullen Bridge at the Indian River Inlet, commonly referred to as the Indian River Inlet Bridge (IRIB), is a cable-stayed bridge located on State Route 1, connecting Rehoboth Beach and Bethany Beach in Southern Delaware. The location of the bridge is shown in Figure 1. The bridge is bordered by the Atlantic Ocean on the east and the Indian River Bay on the west.

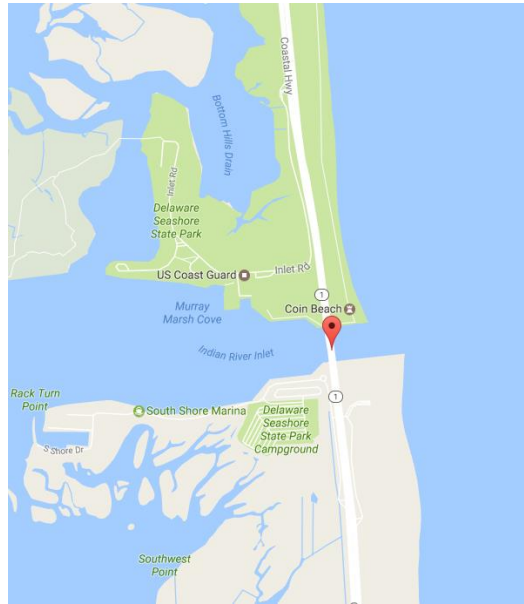


Figure 1 Location of the Indian River Inlet Bridge (Google Maps, 2017)

The IRIB consists of three spans, with a center span of 950 feet and two back spans of 400 feet each. Four lanes of traffic are carried by the bridge, as well as two shoulders and a pedestrian walkway on the east side of the bridge, resulting in an out-to-out width of 106.17 feet. The bridge has a horizontal clearance across the inlet of 900 feet to accommodate potential future widening of the 500-foot wide inlet.

The superstructure of the bridge is comprised of cast-in-place concrete edge girders, precast and cast-in-place concrete transverse floor beams, and a cast-in-place concrete deck. The two continuous edge girders are 6 feet deep and 5 feet wide. The transverse floor beams are approximately I-shaped and spaced at 12 feet. The cable system is comprised of a total of 152 stays, with 19 stays stemming from each side of the four pylons in order to support the edge girders. The stay cables are comprised of 0.62-inch diameter strands, with a range of 19 to 61 strands per cable. The strands are

wax coated and encased inside high-density polyethylene (HDPE) sheathing in order to enhance corrosion resistance. The stays are enclosed in an HDPE pipe to further protect the stays and also to diminish vibrations induced by rain and wind.

The pylons are cast-in-place reinforced concrete hollow towers. The width of the pylons is constant below the deck level, but then tapers to the top of the pylons. The height of the pylons measures roughly 248 feet above ground level. The stays are secured to the towers using steel anchorage boxes. The pylon towers are connected together via a grade beam at the footing level. All piers for the bridge were constructed outside of the inlet in hopes of preventing problems related to extreme tides and scour that haunted the previous bridges over the inlet.

3.2 Description of the Structural Health Monitoring System

3.2.1 System Overview

The Indian River Inlet Bridge was constructed with a fiber-optic sensor network. A DeIDOT grant to the University of Delaware for the design and installation of the system funded the project. Chandler Monitoring Systems, Inc. and Cleveland Electric Labs worked with the University of Delaware team on designing, acquiring, and installing the components of the structural health monitoring (SHM) system for the bridge. The SHM system consists of 144 fiber-optic sensors, including accelerometers, displacement gauges, tilt meters, chloride sensors, strain gauges, and anemometers. Some of the sensors are embedded into the concrete structures and others are mounted on the surface of the bridge components. The locations and types of sensors are shown in Figure 2.



Figure 2 Sensor Layout for the Indian River Inlet Bridge (Al-Khateeb, 2016)

The fiber-optic sensors are triggered by a light pulse that is produced by an interrogator, manufactured by Micron Optics. The light pulse travels along an optical fiber and returns the measurement data to the interrogator in the form of reflected wavelengths of light. The fiber-optic network leads back to a command hut located under the bridge. The system can be controlled locally at the command hut or remotely through a secure internet connection.

The SHM system is capable of producing 1,000 readings per second. The frequency of the sensor readings can be adjusted according to the type of data required and the occurrence of special events, such as hurricanes and nor'easters.

The data obtained from the SHM system will serve as an indication of the behavior of the bridge over time and can be used for early detection of any potential structural problems. The SHM system is expected to collect data and monitor the bridge throughout its lifetime.

3.2.2 Fiber-Optic Tilt Meters

3.2.2.1 Introduction

The inclination, or tilt, of the bridge deck is measured using optical Fiber Bragg Grating (FBG) tilt meters. The FBG-TI-310 Model tilt meters have a measurement range of about ± 10 degrees and a sensitivity of about 200 pm/deg. The response time of the tilt meters is about 20 seconds, which indicates that the tilt meters are effective in measuring only static behavior. This means the tilt meters can be used to capture rotations due to stationary trucks on the bridge or due to slow changes over time like those caused by changes in temperature. The tilt sensors are single axis sensors that measure the rotation of the deck about an axis that is perpendicular to the direction of traffic.

3.2.2.2 Placement of Tilt Meters

The SHM system has a total of nine tilt meters along the length of the bridge. The tilt meters are situated on the top of the east edge girder and are spaced fairly evenly along the length of the edge girder. They are positioned at each end of the bridge, at each of the two pylons, at the midspan of the bridge's main span, at the midspan of the each of the back spans, and at each of the quarter points of the main span. The locations of the nine tilt meters are shown on the elevation sketch of the bridge in Figure 3, with each tilt meter labeled with an "E" and the respective tilt meter number. The location of each tilt meter is also labeled with a corresponding station number in feet.

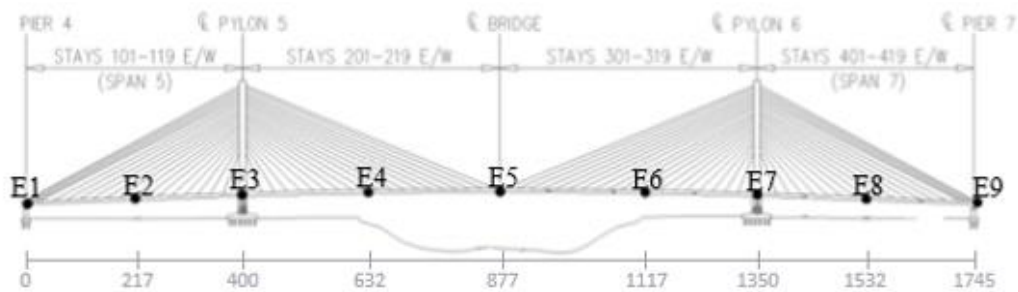


Figure 3 Elevation View of the Bridge Indicating Tilt Meter Locations (Shenton, Fernandez, Ramanna, Chajes, & Wenczel, 2013)

The number of tilt meters and their locations were based solely on engineering judgement and prior experience. Because the bridge was constructed under a design-build contract, the University of Delaware team did not have access to a completed bridge design when the SHM system was designed. As such, detailed analyses could not be used to determine optimal locations for the tilt meters. While the system tilt meters initially installed provide fairly comprehensive information, the research described herein has indicated that the accuracy of computed midspan deflections based on rotations can be significantly improved if two additional tilt meters are added.

Since it requires a good deal of effort to add tilt meters to the system, and since the number and placement of the additional tilt meters became part of the ongoing research project, additional surface mounted tilt meters were utilized during the most recent load test. Two Geokon MEMS surface mounted tilt meters, with measurement ranges of about ± 15 degrees and resolutions of about ± 0.02 mm/m, were placed on the bridge, one on each side of the midspan system tilt meter. The location of the additional surface mounted tilt meters is shown in Figure 4, with the red circles

representing the original system tilt meters and the blue circles representing the new surface mounted tilt meters. The work supporting the decision to add two surface mounted tilt meters, at the chosen locations of 734 feet and 1010 feet, will be presented in Section 7.2.

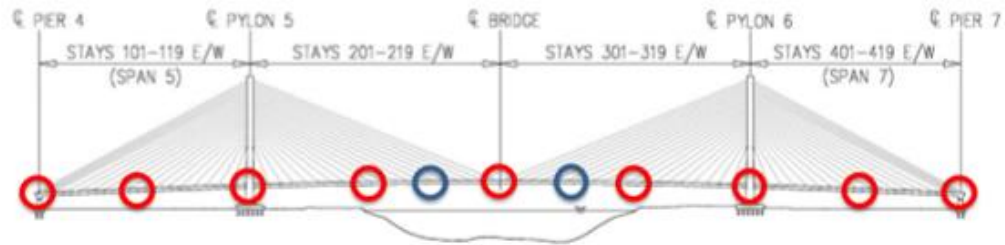


Figure 4 Elevation View of the Bridge Indicating Location of System and Surface Mounted Tilt Meters

3.3 Description of the Analytical Model for the Indian River Inlet Bridge

Due to the complex behavior of cable-stayed bridges like the IRIB, the Finite Element (FE) method and computer technology are commonly used for the analyses of such bridges. Through FE analysis (FEA), the static and dynamic behavior of cable-stayed bridges can be analyzed rather quickly, when compared to previous methods of analysis. Because of this, FEA models were developed for the IRIB and have been habitually used for analyses of the bridge.

3.3.1 History of FEA Models for the Indian River Inlet Bridge

Since the original models used by the designer of the IRIB were not available, researchers at the University of Delaware had to create their own FEA models. The first model created for the IRIB was a 2-D STAAD Pro model created by Pablo Marquez. This 2-D model focused specifically on the west side of the bridge, because

the pedestrian walkway on the east side of the bridge caused slightly less load on the east side of the bridge compared to the traffic loads on the west side of the bridge. More details about the 2-D STAAD Pro model can be found in (Marquez, 2013).

From the 2-D STAAD Pro model, a 2-D SAP2000 beam element model was created by Hadi Al-Khateeb. This model was created using the section properties, material types, geometry, and boundary conditions specified in the as-built drawings provided by the designer. The three types of members used in the 2-D SAP2000 model are frame elements, cable elements, and joint springs. More details about the 2-D SAP2000 beam element model can be found in (Al-Khateeb, 2016).

Although the 2-D STAAD Pro model and the 2-D SAP2000 model produced results that compared very well with each other, there were still some limitations to the 2-D models. One limitation of the 2-D models is that the 2-D models could not accurately represent trucks moving across the bridge in a way that compared to the actual bridge. For this reason, it was determined that a 3-D model was necessary in order to accurately analyze the overall behavior of the bridge.

The first 3-D model created by Al-Khateeb was a 3-D CSiBridge model with shell elements. The shell elements were used to model the bridge deck, while the remainder of the bridge was modeled using the frame elements, cable elements, and joint springs previously mentioned for the 2-D SAP2000 model. In order to create the 3-D CSiBridge model with shell elements, many assumptions had to be made regarding geometry, element types, materials, boundary conditions, and section properties. An in-depth explanation of each aspect of the assumptions can be found in (Al-Khateeb, 2016).

Following the 3-D CSiBridge model with shell elements, a new 3-D CSiBridge model with beam elements was created by Al-Khateeb. The main purpose of creating the model with beam elements was to decrease the computation time and the size of the output files. The 3-D CSiBridge model with beam elements is briefly described below.

3.3.2 Overview of 3-D CSiBridge Beam Element Model

In the 3-D CSiBridge model with beam elements, the separate shell and edge girder elements were replaced with a single edge girder element. The edge girder element acts similarly to a composite member, where the edge girder and the deck essentially act together. The assumptions that were previously used in the 3-D CSiBridge model with shell elements were also adopted for the 3-D CSiBridge model with beam elements. A three-dimensional view of the 3-D CSiBridge model with beam elements is shown in Figure 5.

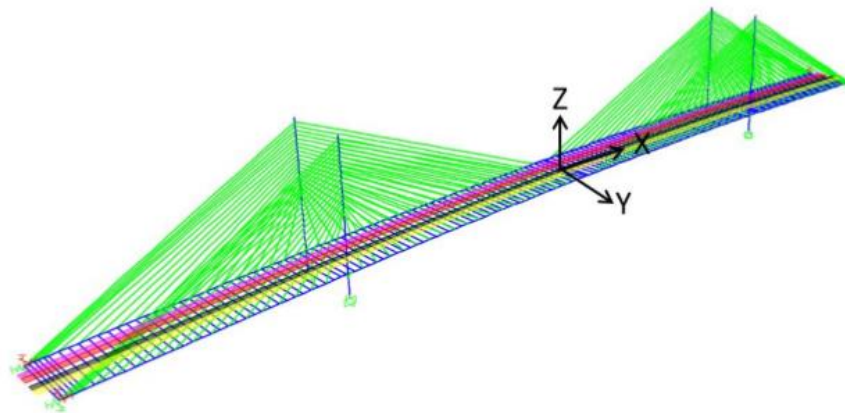


Figure 5 3-D CSiBridge Model with Beam Elements for the IRIB (Al-Khateeb, 2016)

The 3-D CSiBridge model with beam elements has a total of 453 nodes, 590 frame elements, and 152 cable elements. By reducing the number of nodes in the new model, compared to the 3-D CSiBridge model with shell elements, live load analyses can now be completed in about 10 to 12 minutes. The model compares very well with the measured data obtained during controlled load tests. Because of this, the 3-D CSiBridge model with beam elements was utilized for the research conducted herein. Additional details regarding the 3-D CSiBridge model with beam elements can be found in (Al-Khateeb, 2016).

3.3.3 Importance of FEA Model for Verification of Results

As stated previously, FEA models greatly improve the accuracy and efficiency of cable-stayed bridge analyses. FEA analyses provide the opportunity to verify calculated or measured results. Because of this, FEA models can be used to analyze rotations and deflections of cable-stayed bridges, as well as many other structures. Often times, FEA models are the only available verification method.

For the purpose of this research, FEA models are one of the main ways to verify results, along with verification through the use of survey data. The FEA model can replicate any loading on the bridge, which allows for various different analyses of the bridge. As is documented extensively in (Al-Khateeb, 2016), the 3-D CSiBridge model with beam elements has been validated by numerous comparisons with experimental data. Therefore, the model will be used to verify edge girder rotations and deflections used throughout each step of the analysis process. Specifically, the FEA model is commonly used to verify load test rotation data, to determine optimal locations of additional tilt meters, and as a benchmark to compare computed deflection values using the developed methodology.

Chapter 4

GENERAL METHODOLOGY FOR CALCULATING DEFLECTIONS FROM ROTATIONS

This chapter describes the methodology used to calculate deflections from rotation data. In this case, the rotation data was obtained from the SHM system on the Indian River Inlet Bridge. The process used to calculate deflections from rotation data is based on classical Elastic Beam Theory. The assumptions that must be made in order to use Elastic Beam Theory are discussed in this chapter, and the basic differential equation governing the deflection of a beam is introduced. Lastly, the Double Integration Method is described. This is the method used in this research to calculate deflections.

4.1 Elastic Beam Theory

Classical Elastic Beam Theory is commonly used to determine important response parameters of a loaded beam, such as the rotation and deflection of the beam. Because of the many assumptions associated with Elastic Beam Theory, which will be described in the following section, it becomes a special case of Timoshenko Beam Theory. Elastic Beam Theory is widely used in engineering practice because of its simplicity and that is why it was selected for use in this research.

4.1.1 Assumptions

In order to use Elastic Beam Theory, a few assumptions must be made. First, it must be assumed that Hooke's Law applies, meaning that stress is proportional to strain. In other words, the Elastic Beam Theory can only be used for beams that are stressed up to or below the elastic limit. Second, it must be assumed that the slope of the elastic curve at any point is very small. Since the slope of the elastic curve for

most structures is small, it must also be assumed that the deflections are, therefore, very small. This is the third assumption. These two assumptions will apply only to displacements of the elastic curve solely in the vertical direction, not the horizontal direction. Lastly, it must be assumed that deflections due to shear deformations are very small and therefore can be neglected. In other words, only deflections due to bending are considered when using the Elastic Beam Theory.

4.1.2 Derivation of the Basic Differential Equation

The derivation of the basic differential equation governing the deflection of a beam is based on a straight simple beam that is elastically deformed by loads applied perpendicular to the beam, as shown in Figure 6. The deflection of the simple beam is caused by the bending moment and the shear force within the beam. However, only the bending moment will be considered for the derivation of the basic differential equation.

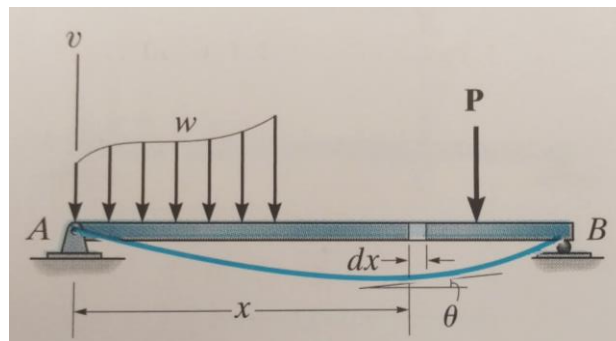


Figure 6 Loads Applied Perpendicular on a Straight Simple Beam (Hibbeler, 2012)

When the bending moment, M , causes the beam to deform, an angle forms between the plane cross sections of the beam, which is referred to as $d\theta$. The part of the elastic curve that intersects the neutral axis for each of the plane cross sections is referred to as dx . The arc that is formed is defined by its radius of curvature, ρ . The properties of the deformed beam cross section are pictured in Figure 7.

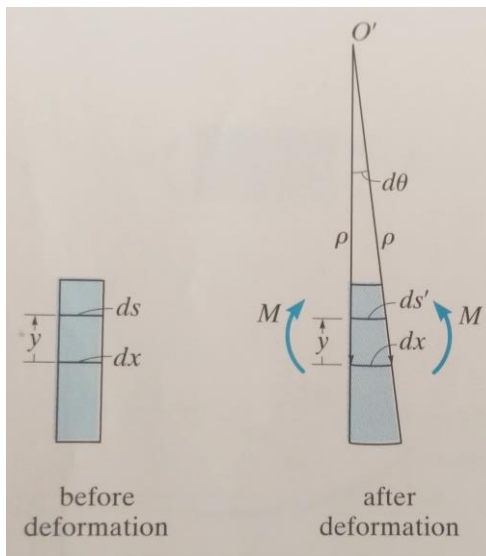


Figure 7 The Straight Simple Beam Cross Section Before and After Deformation (Hibbeler, 2012)

Using the geometry of the deformed beam in Figure 7, the following relationship is developed, which is denoted as Equation 4.1. Although Figure 7 shows a clear distinction between ds and ds' , Equation 4.1 simply uses ds since the slope in actual beams is very small, resulting in ds approximately equaling ds' and dx .

$$ds = dx = \rho d\theta \quad \text{Equation 4.1}$$

By simplifying and rearranging Equation 4.1, the relationship for the curvature can be rewritten as shown in Equation 4.2.

$$\frac{d\theta}{dx} = \frac{1}{\rho} \quad \text{Equation 4.2}$$

Any arc on the beam cross section, with the exception of dx , is subjected to a normal strain, ϵ , at a specific distance, y , from the neutral axis. Knowing this, and using the relationship between displacement and curvature, Equation 4.3 is developed.

$$\frac{1}{\rho} = -\frac{\epsilon}{y} \quad \text{Equation 4.3}$$

By using the assumption that Hooke's Law applies, which means that the material is homogeneous and performs linear elastically, Equation 4.4 is developed using the stress-strain relationship presented by Hooke's Law. In Equation 4.4, σ represents the stress in the beam and E represents the material's modulus of elasticity.

$$\frac{1}{\rho} = -\frac{\sigma}{Ey} \quad \text{Equation 4.4}$$

Equation 4.4 can be further expanded by taking into account the flexure formula, which describes the relationship between the flexural stress at the top of the beam cross section and the internal moment. The expanded equation, Equation 4.5, is shown below, where I represents the beam's moment of inertia.

$$\frac{1}{\rho} = \frac{M}{EI} \quad \text{Equation 4.5}$$

The relationship shown in Equation 4.1 can be used to rearrange Equation 4.5 in terms of $d\theta$ and dx , which is expressed as Equation 4.6.

$$d\theta = \frac{M}{EI} dx \quad \text{Equation 4.6}$$

Finally, the basic differential equation governing the deflection of a beam is developed by expressing rotation in terms of deflection, v . The basic differential equation is shown below as Equation 4.7.

$$\frac{d^2v}{dx^2} = \frac{M}{EI} \quad \text{Equation 4.7}$$

This equation relates the internal moment in a simple beam to the displacement of its elastic curve. Equation 4.7 is the foundation of various deflection methods that are commonly used for simple beams. One such deflection method is the Double Integration Method, which is described in the following section.

4.2 Double Integration Method

The Double Integration Method, often referred to as Direct Integration, is a very powerful method for calculating the rotation and deflection of a beam. Once the internal moment in the beam is expressed as a continuous function over the length of the beam, direct integration can be applied to determine both the rotation and deflection of the beam as a function of the position along the beam, x . In order to do this, Equation 4.7 is rearranged to a more suitable form, which is expressed as Equation 4.8.

$$EI \frac{d^2v}{dx^2} = M_0 \quad \text{Equation 4.8}$$

Equation 4.8 can be integrated to determine the slope, or rotation, of the loaded simple beam. When integrating, it is necessary to introduce a constant of integration, C_1 , in order to attain a unique solution to the specific beam problem. The process of evaluating this constant of integration will be discussed later in this section. The slope of the loaded beam, dv/dx , also commonly expressed as θ , generally has units of either radians or degrees. The equation used to calculate the slope of the loaded beam is shown below, as Equation 4.9.

$$EI \frac{dv}{dx} = M_0x + C_1 \quad \text{Equation 4.9}$$

In order to calculate the deflection of the loaded simple beam, Equation 4.9 must be integrated. Again, it is necessary to introduce a constant of integration, C_2 , when integrating. The deflection of the loaded beam, v , is commonly expressed in units of inches. The equation used to calculate the deflection of the loaded beam is shown below, as Equation 4.10.

$$EIv = \frac{M_0x^2}{2} + C_1x + C_2 \quad \text{Equation 4.10}$$

The constants of integration are determined using boundary conditions. Boundary conditions are known conditions, either slope or deflection, at specific points along the beam. By incorporating the boundary conditions into the

corresponding slope or deflection functions (Equation 4.9 or Equation 4.10), the constants of integration can be determined.

In situations where a single known point along the beam cannot be used to express the beam's slope or deflection functions, continuity conditions must be used to determine the constants of integration. Continuity conditions describe the idea that the slope and deflection of the beam must be continuous between consecutive segments of the beam. By using boundary conditions and/or continuity conditions, all constants of integration can be determined and the functions describing the slope and deflection of the beam can be defined and used to calculate the slope and deflection at any point along the beam.

Chapter 5

CONTROLLED LOAD TEST OF THE INDIAN RIVER INLET BRIDGE

This chapter provides an overview of the controlled load tests that have been conducted on the IRIB, including the schedule, goal, and procedure of the load tests. The controlled load tests are an experimental way to obtain the necessary data, specifically rotations in the case of the research being reported herein, needed to validate new analytical methodologies. Load Test 5 is explained in greater detail, with emphasis specifically on Load Pass 0. During Load Pass 0, a survey was utilized to measure the actual vertical deflection of the bridge. These measurements were used to validate the developed methodology for calculating deflections from rotations. The procedure used to measure the deflection of the bridge through the survey is discussed in this chapter.

5.1 Overview of the Load Testing

Several controlled load tests have been conducted since the opening of the bridge. The timeline of such load tests includes just prior to the bridge opening, 6 months after the bridge opening, at the 1-year anniversary, at the 2-year anniversary, and at the 4-year anniversary, with the load tests named Load Test 1 through Load Test 5, respectively. The plan is to continue conducting load tests every two years for the remainder of the bridge's service life. The load tests are used for various reasons, ranging from calibrating and confirming proper operation of the system to investigating the performance of the bridge by comparing its response to the baseline behavior.

Each of the five load tests were conducted through the night, to ensure that the impacts on traffic were minimized. The load tests typically began between 10:00 pm

and 11:00 pm on weeknights, when the traffic volumes are generally low. A police crew and Maintenance of Traffic (MOT) crew were on scene throughout the entire load test procedure, in order to ensure all safety and traffic concerns were diminished.

DelDOT provided a maximum of six fully loaded 3-axle dump trucks for the load tests, which were weighed before the tests began. During the load tests, the dump trucks drove over the bridge at various speeds and configurations, depending on the specific load pass, while data was recorded by the SHM system. The load passes were broken up into small groups in order to ensure that the bridge was closed to traffic for no longer than 15 minutes at a time, as traffic was prohibited on the bridge while the load passes were taking place.

5.2 Load Test 5 Data Collection

5.2.1 Introduction

Load Test 5 occurred on the night of May 18, 2016. The test began around 10:00 pm and ended by about 2:00 am. Six fully loaded dump trucks were used for the load test in order to simulate a controlled live load on the bridge. The dump trucks were weighed by DelDOT offsite and verified onsite using portable scales prior to the start of the load test. The average weight of the six dump trucks was 63.07 kips. The gross weights of each of the six dump trucks are presented in Table 1.

Table 1 Truck Weights Used in Load Test 5

Truck #	Gross Weight (kips)
2904	63.57
2771	63.12
2677	62.81
2829	62.77
2943	63.17
2783	63.00
Average	63.07

A total of 26 load passes were conducted during Load Test 5. The number of trucks on the bridge during these load passes ranged from one to six trucks, with various different configurations. There were two main types of load passes, quasi-static and high speed passes. During the quasi-static passes, the trucks were travelling at an average speed of about 5-10 mph, and during the high speed passes, the trucks were travelling at an average speed of about 55 mph. Descriptions of each of the load passes can be found in Table 2. The formations of the load passes are further described in diagrams located in Appendix A.

Table 2 Load Pass Descriptions for Load Test 5

Pass	Identifier	Description
Six trucks		
Zero (0)	New	Side by side, one in each lane and shoulder
One truck		
1,7	1e	Southbound shoulder
2,8	1a	Southbound slow-lane
3,9	1b	Southbound fast-lane
6,12	1f	Northbound shoulder
5,11	1d	Northbound slow-lane
4,10	1c	Northbound fast-lane
Four trucks		
13,14	4a	Side by side, one in each lane
Six trucks		
15,16	6b	Side by side, one in each lane and shoulder
One truck high speed passes		
17,18	1a	Southbound, slow-lane
New Passes		
One truck high speed passes		
19-22	1a,1b,1c,1d	Repeat 2, 3, 4, and 5 high speed
Truck-trains		
23	New	Two truck-train in southbound slow-lane
24	New	Three truck-train in southbound slow-lane
25	New	Repeat 23 (two truck-train in southbound slow-lane)
26	New	Four truck-train in southbound slow-lane

This paper specifically focuses on Load Pass 0 from Load Test 5. Load Pass 0 was broken into two passes, which are referred to as Load Pass 0_1 and Load Pass 0_2. These two load passes focused on obtaining rotation measurements at various locations along the bridge, in order to investigate the deflection of the bridge at certain points. Load Pass 0 consisted of 6 fully loaded dump trucks travelling northbound across the bridge side-by-side, with a truck in each lane including the shoulders. A diagram of Load Pass 0 can be seen in Figure 8. Load Pass 0_1 and Load Pass 0_2 were the only passes from Load Test 5 that utilized survey equipment and the two

additional surface mounted tilt sensors, which will be described in the following sections.

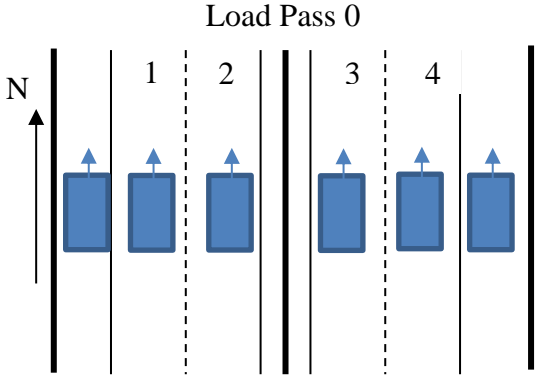


Figure 8 Truck Configuration for Load Pass 0

5.2.2 Measured Deflections through Survey

5.2.2.1 Process of Measuring Deflections through Survey

For the May 2016 Load Test, a survey crew was on site during the load test to take survey measurements at specified locations along the bridge. The survey measurements were taken during both Load Pass 0_1 and Load Pass 0_2 only, which will each be described in the following sections. For Load Pass 0, the survey crew set up nine prisms along the bridge, which were strategically placed according to the project team at the University of Delaware. It was determined that the prisms were needed at each system tilt meter location, with the exception of the two pylon tilt meter locations. The deflection at the pylon locations should be zero, and therefore did not need to be measured. In addition to the prisms at the seven selected tilt meter

locations, one additional prism was placed at the location of each of the two surface mounted tilt meters. The locations of the prisms and tilt meters are shown in Figure 9.

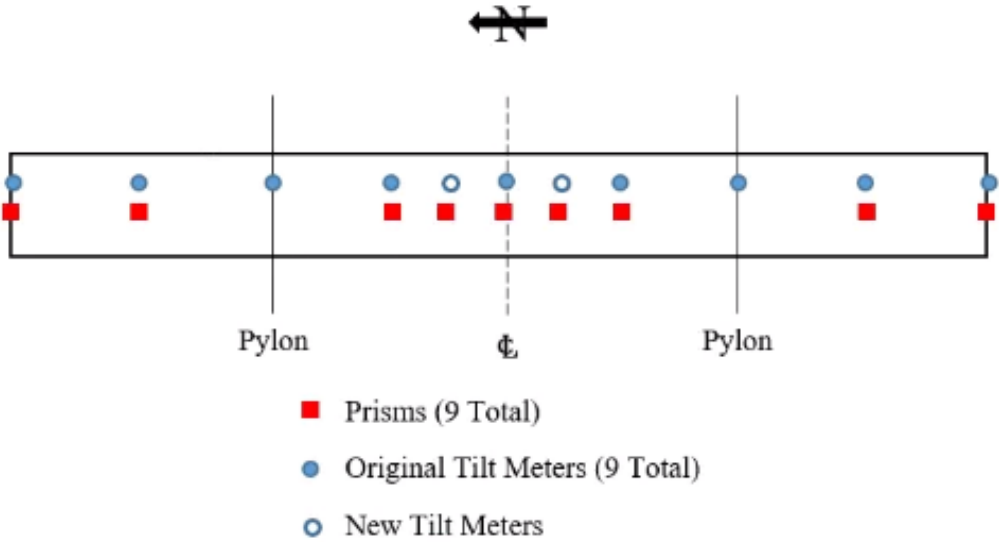


Figure 9 Layout of Survey Prisms and Tilt Meter Locations

Before the dump trucks began driving across the bridge, initial survey measurements were taken for each prism location. These represent the baseline profile against which deflections can be measured. While the trucks were on the bridge, particular survey measurements were taken at specified locations along the bridge, which will be described in further detail in the following sections. Once the dump trucks were done driving across the bridge, final survey measurements were taken for each prism location, to ensure that the survey readings went back to the initial baseline values. After the load test was complete, the survey crew used the initial survey measurements and the recorded measurements to calculate the deflection of the bridge deck at each prism location.

5.2.2.2 Importance of Measuring Deflections through Survey

Being able to conduct the survey measurements during the May 2016 Load Test was critical for this work. The survey results provide accurate and reliable deflections for the bridge due to the applied truck loading. These deflections enable the research team to validate the proposed methodology for computing deflections using rotation measurements, as well as to further validate the FEA model. To the authors knowledge, it is uncommon to have survey deflection measurements for long span bridges under controlled loads. As such, these deflection measurements, in themselves, represent valuable information for the bridge community.

5.2.3 Load Pass 0_1 Measured Rotation and Deflections

Load Pass 0_1 focused on investigating the rotation and deflection of the bridge at each tilt meter location, rather than simply at the maximum midspan location. In order to do this, with no other traffic on the bridge, the trucks stopped adjacent to each tilt meter location for an average of about one minute while travelling across the bridge. The trucks stopped for about one minute at each location in order to allow the bridge to stop oscillating due to the movement of the trucks (recall that the tilt meters are designed to take readings of static situations).

In total there were seven stops along the bridge. Although there were nine system tilt meters and two surface mounted tilt sensors, totaling 11 tilt meter locations, the system tilt meters at the two pylons and the two expansion joints towards the ends of the bridge were not investigated since no deflections were expected at these locations. A schematic of the tilt meter locations and the corresponding prism locations is shown in Figure 10.

location of tilt meter T_E4, is shown in Figure 11. The rotation and deflection profile plots for the remainder of the reading numbers can be found in Appendix B, and the plots will be presented and analyzed in Chapters 9 and 10, respectively.

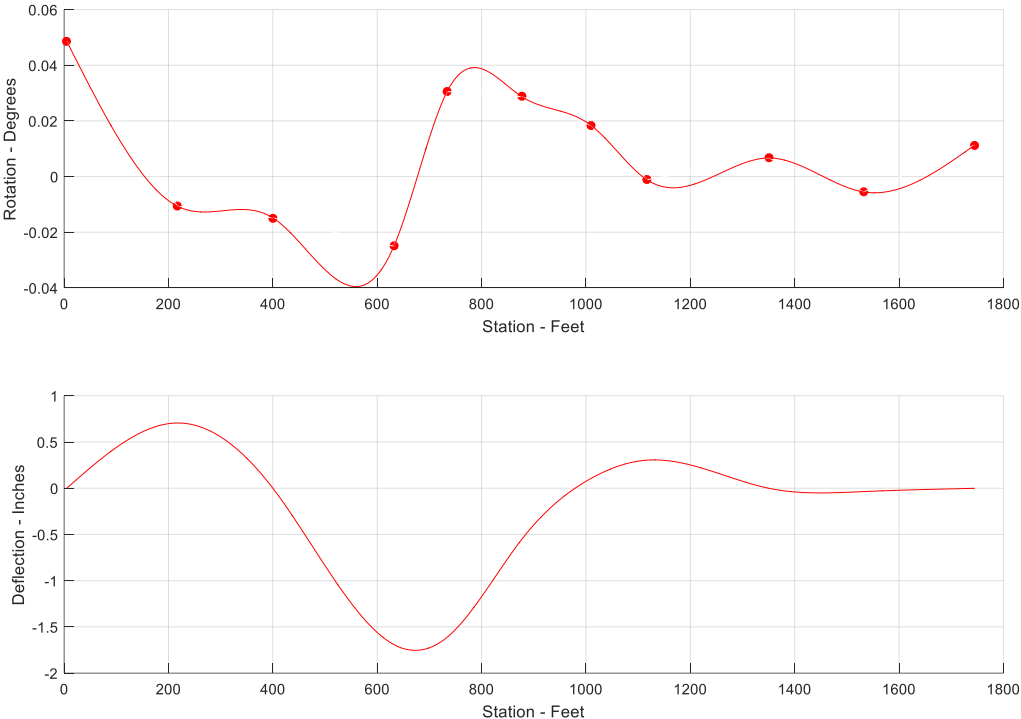


Figure 11 Rotation and Deflection Profile Plots from Load Pass 0_1 With Trucks Located Above Tilt Meter T_E4

5.2.4 Load Pass 0_2 Measured Rotations and Deflections

Load Pass 0_2 focused on investigating the midspan deflection of the bridge, and associated rotations. Although the midspan deflection and associated rotations could have been investigated using the data from the prior load pass, the repeatability and reliability of the readings were established by duplicating the midspan deflections and associated rotations during Load Pass 0_2. Comparisons of the deflection profiles

from Load Pass 0_1 and Load Pass 0_2 will be shown in Section 8.1.2 and Section 8.2.2.1, in order to demonstrate the repeatability of the results.

During Load Pass 0_2, the trucks drove to the midspan location, stopped for about 5 minutes, and then continued across the remainder of the bridge. The SHM system and the surface mounted tilt sensors were collecting data during the entire load pass, from before the trucks drove onto the bridge until the trucks drove off the other end of the bridge. While the trucks were stopped at the midspan location, the survey crew took survey readings at all of the seven tilt meter locations described previously for Load Pass 0_1, in order to obtain a deflection profile of the bridge associated with the six trucks being positioned at the midspan location. This deflection profile is the most significant and the only one considered during this load pass, because the midspan deflection is the largest and most crucial deflection to monitor. The peak midspan deflection can be seen in the final rotation and deflection profile plots from Load Pass 0_2, which are shown in Figure 12. The deflection plot will be presented again and analyzed in Chapters 9 and 10, respectively.

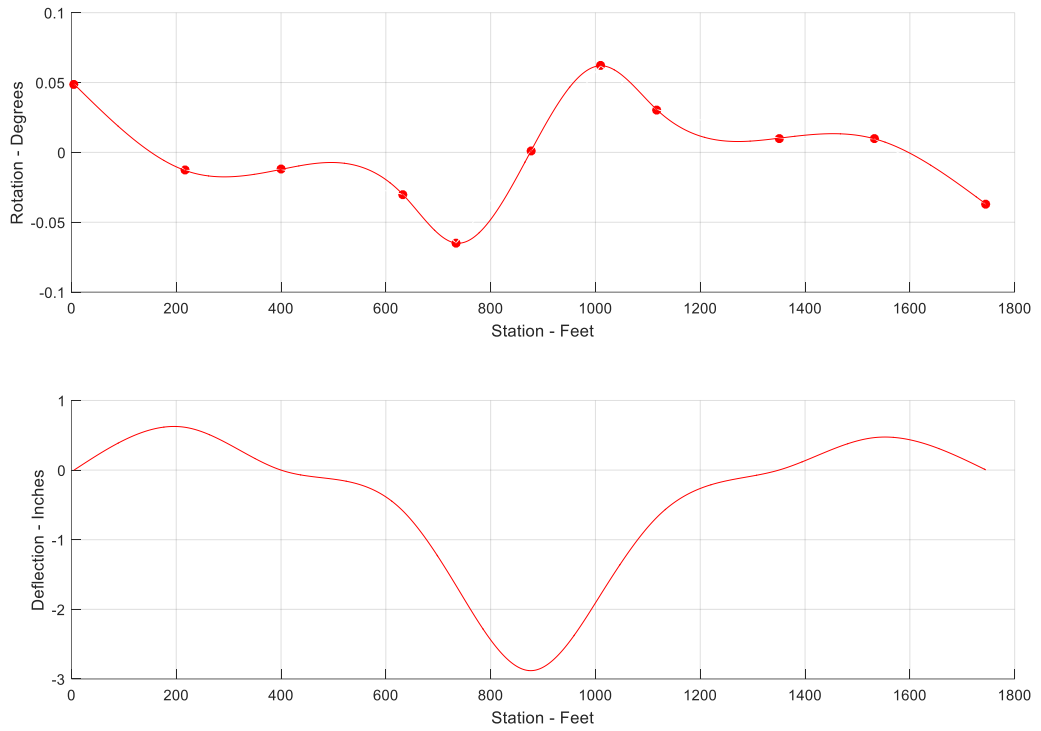


Figure 12 Rotation and Deflection Profile Plots from Load Pass 0_2 With Trucks Located Above the Midspan Location

Chapter 6

PROCESS FOR CALCULATING DEFLECTIONS FROM IRIB ROTATION DATA

In this chapter, the process for calculating deflections from SHM system data is discussed. First, the Matlab code used to calculate the deflections is introduced, with a focus on the need for having a fully automated code. The main preprocessing steps used in the automated Matlab code are then discussed, which include extracting the system data, demeaning and smoothing the system data, and merging the data from System A and System B of the SHM system. The main tool used in the automated Matlab code will then be discussed.

The second part of this chapter focuses on the process used to include the data from the surface mounted tilt meters into the deflection calculation process. The main preprocessing steps used for this analysis are discussed. These preprocessing steps include calibrating the surface mounted tilt meters and integrating the surface mounted tilt meters and the SHM system data.

6.1 Automated Matlab Code for Load Test System Data

6.1.1 Introduction

Matlab was used to analyze the rotation data obtained from the SHM system. It was determined that Matlab would be a better tool to use than other more basic software programs such as Microsoft Excel due to Matlab's available add-ons and advanced computational abilities. Although Matlab is not as commonly used and user-friendly as Microsoft Excel, Matlab's key benefit of providing more advanced options and more powerful data processing capabilities led to the decision to use Matlab for this research.

The final output of the Matlab code includes a rotation profile plot, a deflection profile plot, and a table of the final deflection values at each tilt meter location. The code typically takes no more than a few minutes to run, but does depend on the size of the selected data files. The automated Matlab code used to analyze load test system data can be found in Appendix C. While the code may seem extensive and complex, each segment of the code is described in detail at the beginning of the corresponding segment in the code.

6.1.1.1 Importance of Generating an Automated Code

As stated previously, Matlab is not as commonly used as other software programs, and therefore can be intimidating to new users. Keeping this in mind, and noting that DeIDOT will ultimately be the primary user of this code, it was important to generate an automated code to ensure that DeIDOT will be able to operate the code effectively. Generating an automated code allows users to run the code by only hitting a few key buttons, while reading instruction messages throughout the entire process. It is important to note that Matlab normally operates in an automatic manor, so the automated code referred to in this research implies that the code is a one-step code. Once the user hits a few key buttons, Matlab conducts all of the calculations at once, rather than the user needing to complete several different calculations in several separate Matlab codes. By following the instructions provided in the automated Matlab code, and referring to a manual if further instruction is needed, it is anticipated that any person involved with the Indian River Inlet Bridge will be able to run the automated code.

6.1.2 Preprocessing Steps Used in the Automated Matlab Code

There are a few main preprocessing steps that are used in the automated Matlab code. These steps are essential to ensure that the final results of the analysis are accurate and complete.

6.1.2.1 Extracting System Data

In order for the SHM system data to be analyzed, it must first be imported into the Matlab code. The system data is stored by the SHM system as CSV files. Therefore, it is important to note that the user must save the CSV files as Excel Workbook files before running the code. The data files that are produced from the SHM system contain copious amounts of data, which include strain data, temperature data, and rotation data. Because the automated Matlab code only analyzes rotation data, the rotation data needs to be extracted from the system data files.

Once the user selects the Excel Workbook files that are to be analyzed, after being prompted to do so, Matlab will extract the rotation data from the vast data files that were originally selected by searching the data files for each of the tilt meter names. Extracting only the rotation data for use during the analysis shortens the computation time of the code and ensures that only the necessary information is presented.

6.1.2.2 Demeaning and Smoothing System Data

The raw data from System A and System B of the SHM system are not calibrated and zeroed to the same baseline. Additionally, the raw data from the SHM system generally contains a considerable amount of noise in the signal. Therefore, the raw data has to be zeroed demeaned and smoothed before the data can be utilized for further analyses and calculations.

In order to zero the data, the data from the initial ten readings is averaged in Matlab and recorded as the initial average for the individual sensor under consideration. This initial average, denoted as AverageT_E1 for example, represents the data collected before trucks drive onto the bridge. In the notation for the tilt sensors, such as T_E1, the T represents the type of sensor as a tilt sensor, the E represents the location of the sensor on the east edge girder, and the numeric at the end represents the tilt sensor number. Refer to Figure 3 for the layout of the tilt sensors and their corresponding numbers. The calculated average is then subtracted from each data point in the data series for the particular sensor being considered. Subtracting the initial average from each data point accounts for the fact that the strain and rotation of the bridge should be zero when there is no traffic on the bridge. This process is completed for each sensor in order to obtain zeroed data for the entire data collection set, which is denoted as DemeanT_E1 for example (demeaned is what the zeroed data will be referred to as).

In order to smooth the data, the demeaned data is used with Matlab's smoothing average function. Smoothing the data eliminates much of the noise in the data. The smoothing span used for the smoothing average function is set to five, because it was determined that this provided sufficient results for the majority of the frequencies used for data collection. A smoothing span of five means that an average is taken over five data points. For data that is recorded at a frequency of 1 Hz, with one data point recorded every second, a smoothing span of five means that an average is taken for every five seconds of data. Once the data is zeroed (or demeaned) and smoothed, the individual data from each system, System A and System B, is ready for analysis.

6.1.2.3 Merging System A and System B

The SHM system has two data acquisition systems, System A and System B. The system tilt meters are split up between the two systems, with tilt meters TE_2 through TE_8 on System A and tilt meters TE_1 and TE_9 on System B. Therefore, in order to obtain all of the rotation readings for the bridge, both System A and System B must be considered. Because the two systems need to be manually started to collect data during load tests, the timestamps on the two systems are different and must be made to match each other when analyzing data. Sometimes the difference in timestamps for the two systems is small and doesn't have much affect; however, sometimes the difference is very large and requires adjustments.

In order to account for the difference in timestamps, the system readings must be shifted according to the time differences in the manual starts of the systems and the frequency differences for which the systems are acquiring data. The system readings are shifted by evaluating the difference in the beginning timestamp values from System A and System B, which is shown in Equation 6.1.

$$SystemDiff = TimestampA(1) - TimestampB(1) \quad \text{Equation 6.1}$$

This system difference is then divided by the frequency of System B, which is shown in Equation 6.2.

$$ShiftB = \frac{SystemDiff}{\frac{TimestampB(end) - TimestampB(1)}{size(TimestampB)}} \quad \text{Equation 6.2}$$

This ultimately results in the amount that System B needs to be shifted, in order to match up with System A. Once the shifting is done, the System A and System B data are merged and used as needed.

6.1.3 Utilizing the Matlab Curve Fitting Tool

The main tool used in the automated code to calculate deflections from the load test system data is Matlab's Curve Fitting Tool. The Curve Fitting Tool is a graphical user interface, which is commonly used to conduct parametric or nonparametric data fitting, as well as determine a goodness of fit and extrapolate data. Because the Curve Fitting Tool is an add-on to Matlab, it must first be purchased before running the automated code.

For the purpose of this study, the Curve Fitting Tool was used to conduct nonparametric data fitting. Nonparametric data fitting is commonly used when there is a desire to fit a smooth curve through data, without the need to interpret any corresponding curve parameters. The automated Matlab code specifically uses smoothing splines as a nonparametric fitting method. Smoothing splines use a smoothing parameter to adjust the smoothness of the corresponding fitted curve. The smoothing parameter is varied in order to vary the fitted curve from a least-squares straight line to a cubic spline curve.

In the automated Matlab code, a smoothing spline was fit through the rotation data and station data from the SHM system, with the rotation data on the y-axis and the station data on the x-axis. Units of both degrees and radians were used for the rotation data in the Curve Fitting Tool. The rotation data in degrees was used to fit a smoothing spline through the data and simply display a rotation profile of the bridge. The rotation data in radians was used to fit a smoothing spline through the data that

could then be integrated into deflections, in order to ultimately display a deflection profile of the bridge. A constant smoothing parameter of 0.4 was used for all analyses, as it was determined that a smoothing parameter of 0.4 or higher resulted in an Adjusted-R square value of 1.0 for all situations.

6.2 Surface Mounted Tilt Meters for Load Test Data

Although the surface mounted tilt meters were used during the May 2016 Load Test, they are not included in the automated code that was developed for load test data. This is because the surface mounted tilt meters may not be used for all future load tests. In the future, the goal is to add two tilt meters permanently to the SHM system. The automated code could be updated accordingly to include the new system tilt meters. Once the two system tilt meters are installed, the surface mounted tilt meters will no longer be needed in the specified locations. Therefore, to simplify any necessary adjustments to the automated code in the future, the surface mounted tilt meters are analyzed with load test system data separately in a manual code.

6.2.1 Preprocessing Steps Used for the Surface Mounted Tilt Meters

Since the surface mounted tilt meters are not part of the SHM system, there are a few preprocessing steps that need to be conducted in order to include the surface mounted tilt meter data in the analyses of load test data. These steps, which are described below, are crucial to ensure that the final results of the analyses are accurate and complete.

6.2.1.1 Calibrating the Surface Mounted Tilt Meters

Tilt sensor calibration sheets were provided with each of the two surface mounted Geokon MEMS tilt meters. The calibration sheets specified the deflection

gage factor, $G_{\sin\theta}$, and the tilt gage factor, G_{tilt} , for each of the tilt meters, as well as the conditions in which the tilt meters were calibrated and the data that was used for the calibration calculations. The provided gage factors were used along with the voltage readings in order to calculate the tilt or inclination in question.

Before utilizing the Geokon MEMS tilt meters for the load test, the calibration of the tilt meters was verified. In order to do this, multiple tests were conducted in the lab at the University of Delaware. The tests consisted of propping a 25-foot aluminum beam on wooden blocks, one block on each end, and securing the tilt meters to the beam at different locations. The beam was propped on the wooden blocks to avoid discrepancies in the data due to an uneven floor in the lab. The tilt meters were secured to the beam using clamps. The tilt meters were then connected to a DC 12V battery as a power source and a multimeter to measure voltage. An example of the lab setup is shown in Figure 13, which shows one of the tilt meters secured to the aluminum beam and the multimeter recording voltage outputs. After the initial tests, a data acquisition device was used with QuickDAQ on a laptop in order to record the voltage change throughout the entire duration of the tests. The data acquisition device with QuickDAQ was used for recording purposes to increase the accuracy of the voltage output, as the voltage changes were small.



Figure 13 Example of the Surface Mounted Tilt Meter Lab Setup

The voltage was recorded at zero inclination before the beam was raised on one end, which was documented as R_0 , the initial reading. As the beam was incrementally raised on one end, by inserting thin sheets of aluminum between the beam and the wooden block, the voltages were recorded at each angle increment and documented as R_1 , the subsequent readings. Using the initial reading, the subsequent readings, and the gage factor, the calculated tilt for each angle increment could be calculated using Equation 6.3.

$$\text{Calculated Tilt} = G(R_1 - R_0) \quad \text{Equation 6.3}$$

Because the angle increments, or calculated tilts, were known for the test, Equation 6.3 was rearranged in order to calculate the gage factors, or calibration factors, based on the specific testing conditions. The new equation is presented as Equation 6.4, and it allowed for verification of the gage factors that were provided with the MEMS tilt meters.

$$G = \frac{\text{Calculated Tilt}}{(R_1 - R_0)} \quad \text{Equation 6.4}$$

Because the testing conditions in the lab were different than the testing conditions at Goekon's lab, the provided gage factors and the calculated calibration factors differed slightly. The provided gage factors for the surface mounted tilt meters were 3.624 and 3.620, while the calculated calibration factors were 3.7122 and 3.6063, respectively. For all lab tests and load tests conducted after the surface mounted tilt meters were calibrated, the calculated calibration factors were used in order to calculate tilts rather than the provided gage factors.

6.2.1.2 Integrating the Surface Mounted Tilt Meters and the SHM System Data

After the calculated calibration factor for each surface mounted tilt meter was determined, it was used in Equation 6.3, as G , to calculate angles of rotation for the corresponding tilt meter. The initial reading and subsequent readings, R_0 and R_1 respectively, came from the raw data obtained from QuickDAQ. The raw data from QuickDAQ is saved in the form of a CSV file, which was imported into Matlab in order to compute and analyze the rotation data. An example of the raw voltage data collected during Load Test 5 using QuickDAQ is shown in Figure 14.

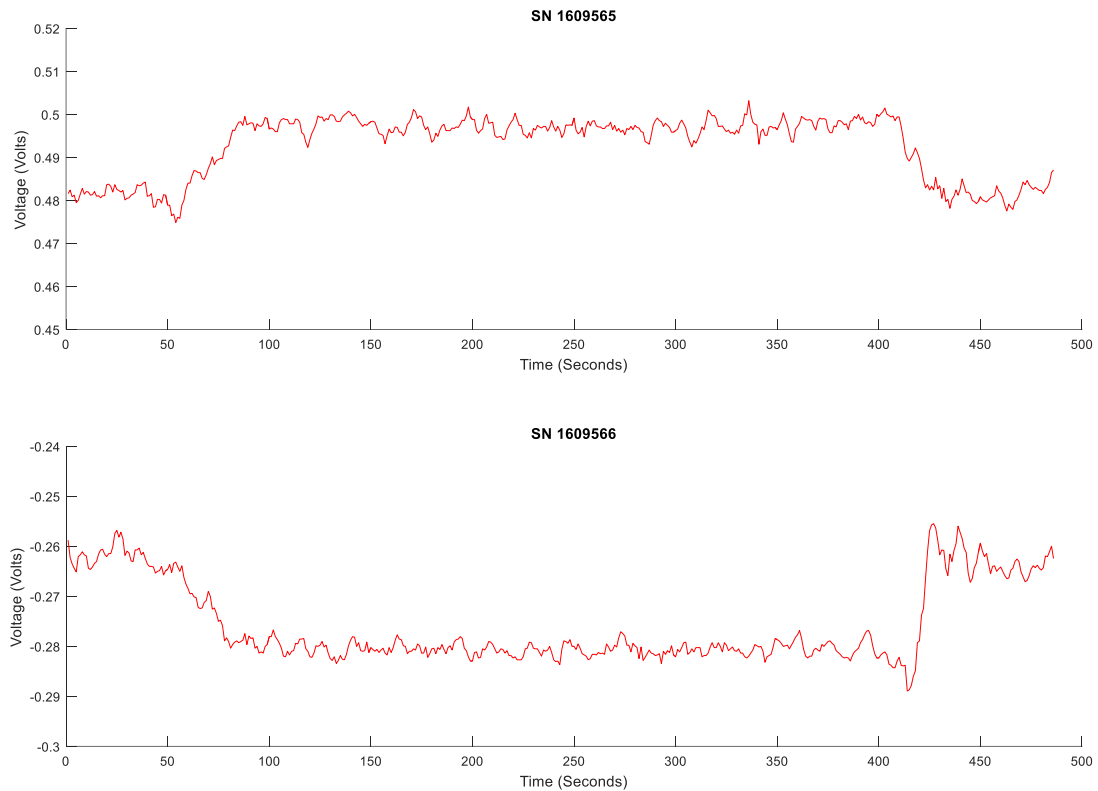


Figure 14 Raw Voltage Data from Surface Mounted Tilt Meters

From the raw voltage data, an initial voltage, represented by R_0 , was obtained by averaging the first 30 seconds of data. This data represents the voltage when there is no traffic on the bridge. The subsequent voltages, represented by R_1 , were obtained by averaging the raw data between 100 and 400 seconds. The data in that timeframe represents the voltage when the trucks were positioned at the midspan location on the bridge.

Using Equation 6.3, along with the initial voltage, subsequent voltage, and calculated calibration factor, the final angle of rotation for each surface mounted tilt

meter was determined. The final rotation values, in degrees, could then be included with the system tilt meter rotations in order to obtain a complete rotation profile of the bridge. This was done by recording the station and final rotation value for each surface mounted tilt meter. The recorded values were then inserted into the SHM system data files, which followed the same format of including station and final rotation values. The complete set of data, which consisted of 11 rotation values, could then be analyzed to obtain a complete rotation profile and deflection profile of the bridge.

Chapter 7

CALCULATED DEFLECTIONS USING IRIB ROTATION DATA: PRELIMINARY RESULTS

This chapter focuses on presenting preliminary results of calculating deflections using rotation data from the SHM system. The results from the automated Matlab code will be presented for both Load Pass 0_1 and Load Pass 0_2 of Load Test 5. Results from both an initial code, and one which was modified to account for known boundary conditions are discussed. The preliminary results presented indicate a distinct benefit of having two additional surface mounted tilt meters for calculating midspan deflections. Finally, the process used to determine the optimal location of the two additional surface mounted tilt meters is discussed.

7.1 Automated Matlab Code for Load Test System Data

As stated previously, in Chapter 6, an automated Matlab code is used to analyze the load test data. The code ultimately provides the user with a rotation profile plot, a deflection profile plot, and a table of the final deflection values at each tilt meter location. The Matlab code can be used to analyze load test data efficiently and easily, whether it be past load test data or load test data that will be collected in the future.

7.1.1 Presentation of Results

The results from Load Pass 0 during the May 2016 Load Test are presented in the following sections. It is important to note that tilt meters T_E2 and T_E8 were not working properly during the load test, and as a result did not collect any data. Therefore, the automated Matlab code results presented in the following two sections only include data from the remaining seven system tilt meters.

7.1.1.1 Load Pass 0_1

As discussed in Chapter 5, Load Pass 0_1 focused on investigating the rotation and deflection of the bridge at each tilt meter location. Although Load Pass 0_1 focused on the rotation and deflection at each tilt meter location, the automated Matlab code only focuses on analyzing the rotation profile and calculating the deflection at the midspan location. This is because the midspan location is the most critical location to monitor, as it is expected to experience the largest deflection along the bridge. Therefore, the results from the automated Matlab code for Load Pass 0_1 only consist of a rotation and deflection profile for the loading scenario when the trucks are positioned above tilt meter T_E5, as this causes the largest midspan deflection. The rotation and deflection profiles for the remaining loading scenarios, when the trucks are above the remaining tilt meters, will be presented and analyzed in the following chapter.

The rotation and deflection profiles when the trucks were positioned above tilt meter T_E5, the midspan tilt meter, are shown in Figure 15. From the deflection profile for this loading situation, it can be seen that the maximum peak deflection is approximately -1.40 inches and occurs around the 870 ft location along the bridge. This maximum deflection location corresponds very well with the location of the trucks above tilt meter T_E5, which is the 877 ft location along the bridge.

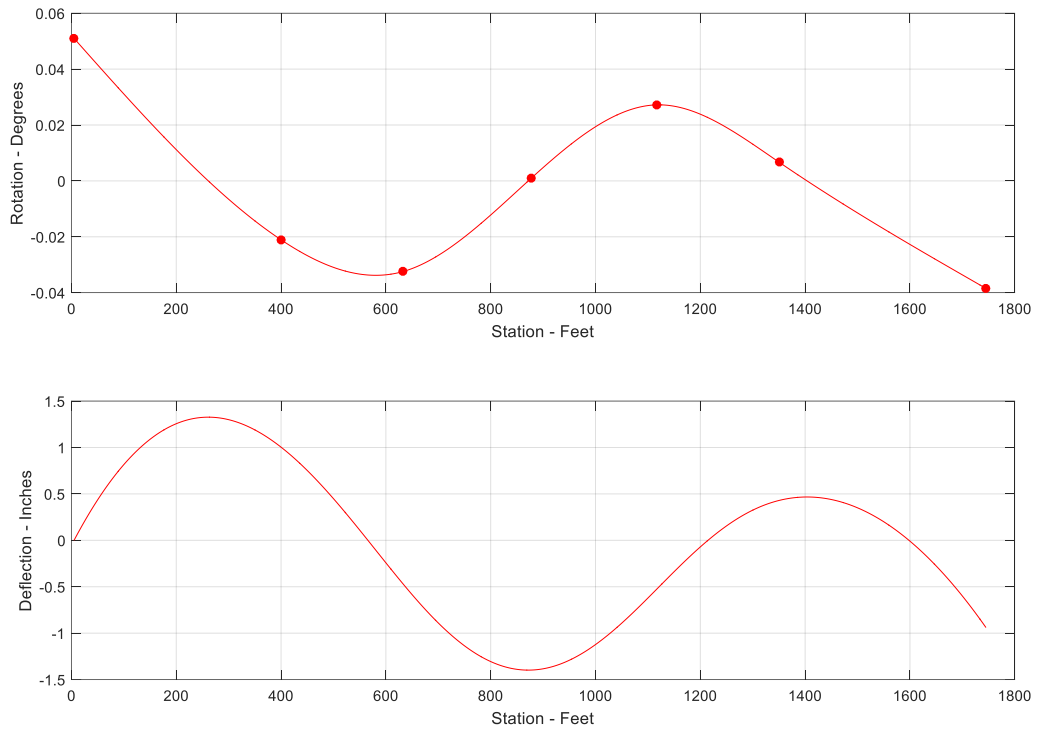


Figure 15 Rotation and Deflection Profiles for Load Pass 0_1 with Trucks Positioned Above T_E5

It is important to keep in mind that the actual collected rotation data is indicated by the dots on the rotation profile. The curve through the collected data points is a curve fit, and the deflection profile is integrated from that rotation curve fit.

7.1.1.2 Load Pass 0_2

As discussed in Chapter 5, Load Pass 0_2 focused on investigating the midspan rotation and deflection of the bridge. The results from Load Pass 0_2 consist of a rotation profile and deflection profile of the bridge at the critical midspan location, above tilt meter T_E5. The rotation and deflection profiles when the trucks were positioned above tilt meter T_E5 are shown in Figure 16. From the deflection

profile for this loading situation, it can be seen that the maximum peak deflection is approximately -1.37 inches and occurs around the 892 ft location along the bridge. As expected, this maximum deflection location corresponds well with the location of the trucks above tilt meter T_E5, which is the 877 ft location along the bridge.

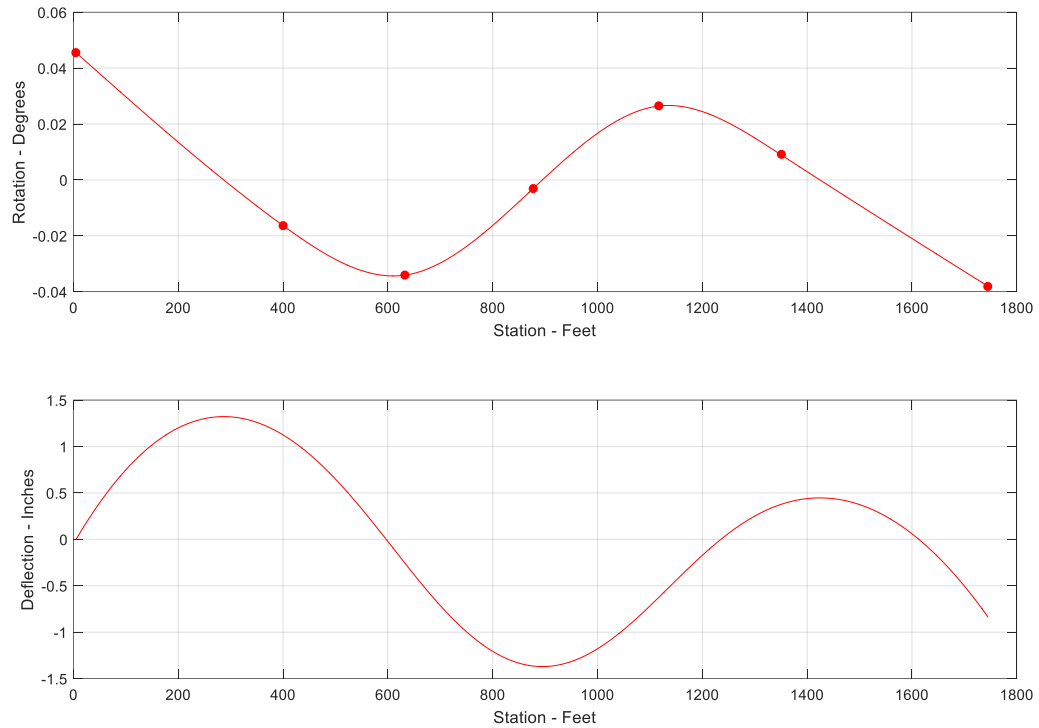


Figure 16 Rotation and Deflection Profiles for Load Pass 0_2 with Trucks Positioned Above T_E5

7.1.2 Issues with Results

After analyzing the data from Load Pass 0 of Load Test 5, it was observed that there were some issues with the results. While these issues do not come from the SHM system data, and instead come from the data analysis processes, they still need to be addressed in order to obtain accurate deflection results. The primary issues that were

identified and need to be addressed relate to the fact that the bridge end deflections and the bridge pylon deflections need to be forced to zero. The treatment of these issues is described in further detail in the following two sections.

7.1.2.1 Bridge End Deflections

As with any bridge, the IRIB has end supports that control the behavior of the bridge at those corresponding locations. Specifically, for the IRIB, the end supports ensure that the bridge does not experience any deflection at the ends of the bridge. This means that the bridge cannot experience any vertical deflection at the locations of tilt meters T_E1 and T_E9. After reviewing the preliminary calculated deflection results from both Load Pass 0_1 and Load Pass 0_2, it was evident that deflections were being computed at the far end of the bridge (the 1,745 ft location). This bridge end deflection was as big as ± 1 inch in some situations, which is a considerable amount of deflection for a location that actually has zero deflection.

It is important to note that the bridge end deflection was only experienced at the far end of the bridge, because the integration used to calculate the deflection began at the opposite end of the bridge, near the 5 ft location. Therefore, the deflection at the beginning of the bridge was forced to remain at zero for each integration calculation. It was determined that accumulated numerical error in the computation process leads to the non-zero end deflection.

7.1.2.2 Bridge Pylon Deflections

The two pylons on the IRIB also act as supports for the bridge and control the behavior of the bridge at their corresponding locations, just as the end supports do. The pylons ensure that the bridge does not experience any vertical deflection at their

respective locations, which are the locations of tilt meters T_E3 and T_E7. After reviewing the preliminary calculated deflection results from both Load Pass 0_1 and Load Pass 0_2, it was evident that deflections were also present at the two pylon locations (at the 400 ft location and the 1,350 ft location). At the 400 ft location, the bridge pylon deflections were as large as 1.5 inches in some situations. At the 1,350 ft location, the bridge pylon deflections were as large as 1 inch in some situations. These are significant deflections relative to the computed midspan deflections and certainly not accurate for the pylon locations. Again, these computed non-zero deflection are due to accumulated numerical integration errors.

7.1.3 Adjustments Made to Overcome Issues

After realizing the above-mentioned issues with numerical computation error, a method for overcoming the issues was sought in order to obtain more accurate results. While Matlab itself has many available options and capabilities, there are limitations to some of Matlab's built-in functions. Specifically, for this research, Matlab's built-in integration function was used, which has limitations that must be accounted for during the analysis process. The adjustments made to account for the known zero bridge end deflections and bridge pylon deflections will be described in the following two sections.

7.1.3.1 Forcing End Deflections to Zero

As stated previously, Matlab's built-in integrate function has limitations, one of which is the lack of boundary condition options. As introduced in Section 7.1.2.1, the deflection boundary condition of the integration segment did not equal zero when the integration was complete. This implies that the deflection at the end of the bridge

was not zero after completing the calculations. Knowing that the deflection at both ends of the bridge must be zero, given that there are supports at those locations, it was evident that additional measures must be taken to force the end deflections to zero.

In order to force the end deflections to zero, a linear regression was used. A linear fit was placed through the two end points of the deflection curve. The slope of the linear fit was then subtracted from the initial rotation profile (the units were radians). The new rotation profile was then integrated in Matlab in order to obtain the final deflection profile of the bridge, with the end deflections appropriately equaling zero.

7.1.3.2 Forcing Pylon Deflections to Zero

Matlab's built-in integrate function also does not allow the option to include initial conditions. Because of this, the final deflection profile created by the Matlab code did not produce zero deflection at the two pylon locations. In order to correct this, it was determined that the integration would need to be split up into three sections. The integration was split into sections so that each individual section would end and begin at either a bridge end or a pylon. The three sections are the southern backspan section from 5 to 400 feet, the mainspan section from 400 to 1,350 feet, and the northern backspan section from 1,350 to 1,745 feet.

The linear regression approach introduced in the previous section, for forcing the end deflections to zero, was also adopted to force the end deflections of each integration section to zero. This would ultimately ensure that the pylon deflections equal zero, as well as the bridge end deflections.

For the boundary locations that overlap between individual sections, the 400 feet and 1,350 feet locations, continuity conditions were used to ensure that the same

rotation values were used for corresponding stations in all integration sections. This ultimately ensured that the final deflection profile, after combining the deflection profiles from each individual section, was smooth and continuous.

7.2 Need for Additional Tilt Meters

Aside from devising a method for incorporating the known boundary conditions in the Matlab code used to compute the deflection profile, the overall shapes of the deflection profiles were also investigated in order to verify their accuracy. After comparing rotation and deflection results from previous load tests, specifically the November 2012 Load Test, to the results from the FEA model for the IRIB, it was determined that additional tilt meters would greatly increase the accuracy of the computed midspan deflection. The results that led to the decision to include additional tilt meters will be presented and discussed in the following sections. Additionally, the decision to add surface mounted tilt meters and the process used to determine the location of the additional surface mounted tilt meters will be discussed towards the end of this chapter.

7.2.1 Presentation of Original SHM System Data

The November 2012 Load Test serves as a baseline load test for the IRIB. This test was conducted six months after the bridge opened to traffic. It has been classified as the baseline test since the bridge was still very early in its lifespan, and because it was the first to utilize six fully-loaded dump trucks as the maximum loading (the prior test utilized only four fully-loaded dump trucks). Since the November 2012 Load Test is the baseline load test, the results from that load test were compared to the results from the model when evaluating how well the SHM system captures the overall

rotation of the bridge deck. The rotation profile of the bridge from the November 2012 Load Test, with a loading of six trucks positioned side-by-side at the midspan location, is shown in Figure 17. It is important to note that the rotation profile presented in Figure 17 differs from the rotation profiles shown in Figure 15 and Figure 16. The difference is because there were no rotation values for tilt meters T_E2 and T_E8 during the May 2016 Load Test. Therefore, the rotation profile shown in Figure 17 is a more accurate rotation profile.

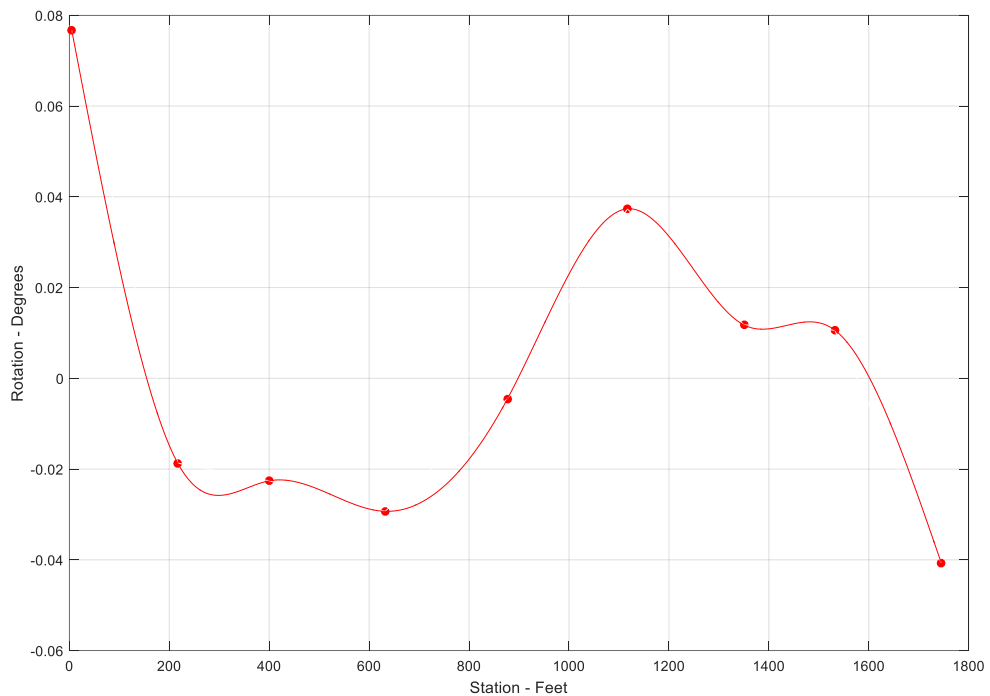


Figure 17 Rotation Profile of the IRIB from the November 2012 Load Test

The rotation profile from the November 2012 Load Test was integrated, using the methodology and processes described previously in Chapters 4 and 6, respectively, in order to obtain the deflection profile of the bridge. The final deflection profile of the

bridge from the November 2012 Load Test due to six trucks at midspan is shown in Figure 18.

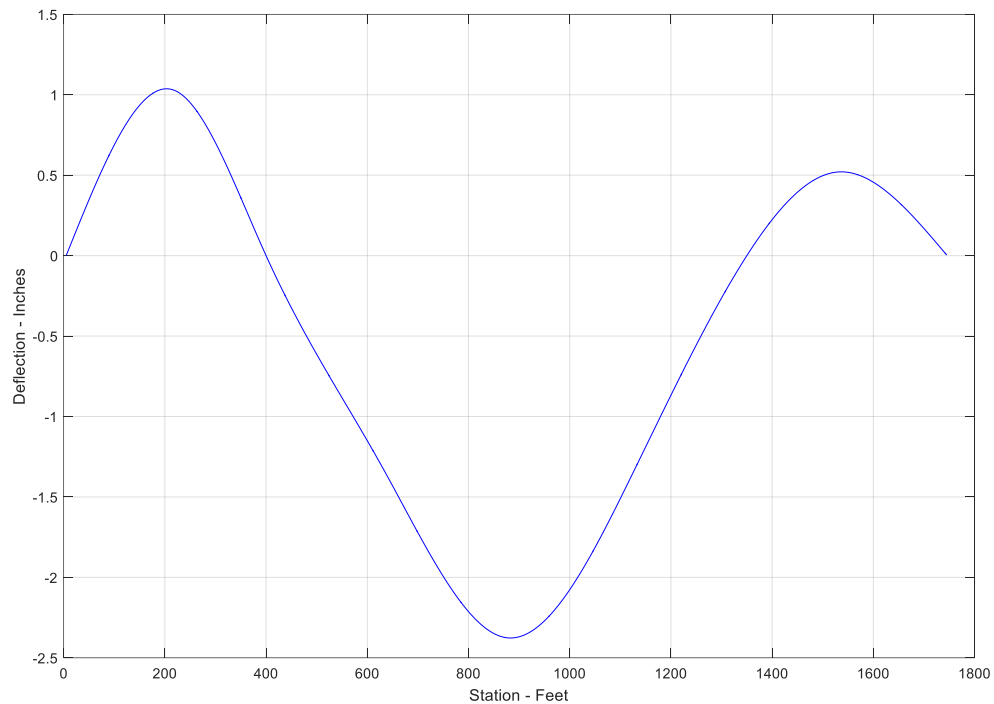


Figure 18 Deflection Profile of the IRIB from the November 2012 Load Test

7.2.2 Shortcomings of Results

As stated previously, the benefit of additional tilt meters was established by comparing the rotation and deflection profiles of the bridge from the FEA model to previous load tests, specifically the November 2012 Load Test. Through this comparison, it was observed that the data from the November 2012 Load Test, and more importantly the resulting curve fit generated from that data to form a rotation profile, could not capture the rotation peaks in the profile that occur at 782 and 984

feet that are predicted by the FEA model. The difference in the rotation profiles can be seen in Figure 19.

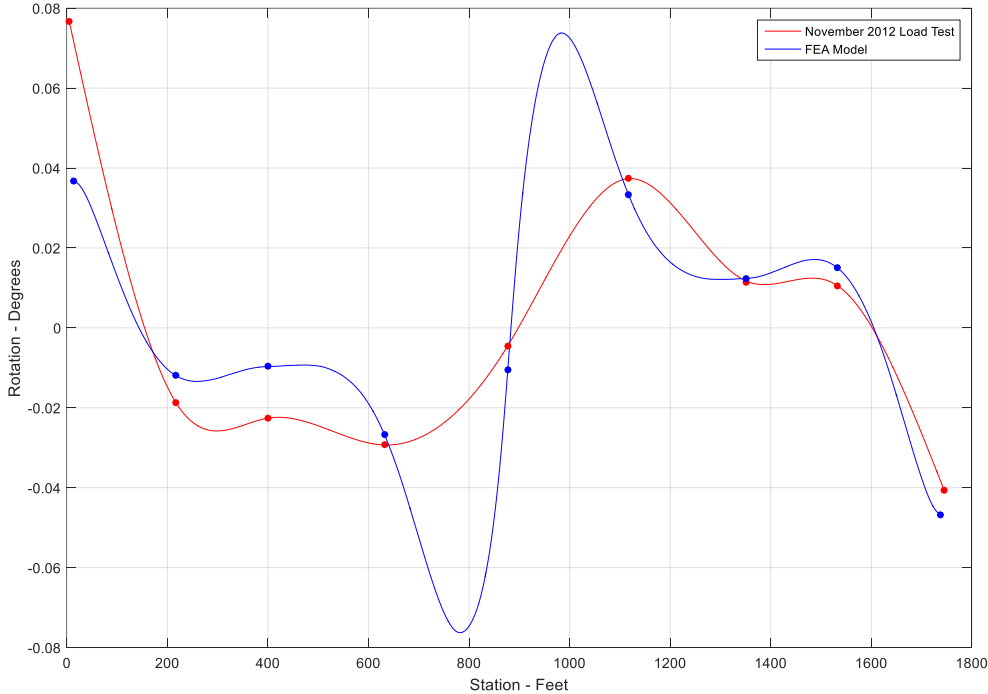


Figure 19 Rotation Profile Comparison Between November 2012 Load Test and Model

The peak rotations at 675 and 1120 feet in the November 2012 Load Test rotation profile, indicated by the red solid line, are approximately -0.029 degrees and 0.037 degrees, whereas the corresponding peak rotations in the model rotation profile, indicated by the solid blue line, are approximately -0.076 degrees and 0.074 degrees. Since the peak rotations for the November 2012 Load Test are much smaller than they are for the FEA model rotation profile, the resulting peak deflection at the midspan

location, predicted by the integration, is also smaller. A comparison of the deflection profiles is shown in Figure 20.

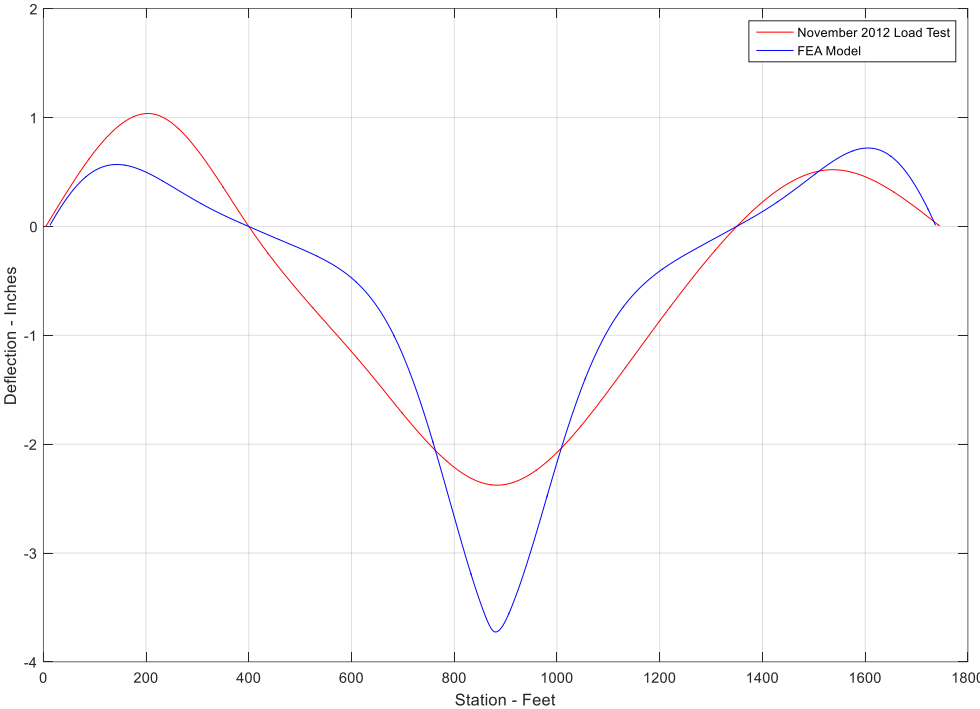


Figure 20 Deflection Profile Comparison Between November 2012 Load Test and Model

The peak midspan deflection in the November 2012 Load Test deflection profile, indicated again by the red solid line, is approximately -2.39 inches, whereas the peak midspan deflection in the model deflection profile, indicated again by the blue solid line, is approximately -3.73 inches. This results in a relative error of about 35.9% when comparing the November 2012 Load Test midspan deflection to the model midspan deflection. Therefore, from this relative error, it was concluded that the nine tilt meters that are currently integrated into the SHM system are not capable

of obtaining highly accurate predictions of the peak deflection at midspan. Because the midspan deflection caused by heavy trucks at midspan is the most crucial deflection to monitor, it was determined that additional tilt meters were needed to capture more accurate rotations of the bridge, which would ultimately result in a more accurate deflection profile of the bridge. In particular, tilt meters were needed near the peaks in the FEA model predicted rotation at 782 and 984 feet. It should be noted that sensors at these locations will be perfectly situated to capture peak rotations due to trucks located at midspan and not necessarily other loading configurations.

7.2.2.1 Need for Surface Mounted Tilt Meters

After determining the benefit of having additional tilt meters, it was necessary to determine how the tilt meters would be added to the existing SHM system. While it is possible to install additional tilt meters and integrate them into the existing SHM system, it is something that requires a reasonable amount of effort. Because of this, and because the research behind adding the tilt meters was in the early stages, permanently installing the tilt meters and integrating them into the SHM system did not seem like the most practical initial option. Instead, surface mounted tilt meters appeared to be the most practical first option given the circumstances, as they are temporary and can collect data on their own. The surface mounted tilt meters do not require any hardwiring into the existing SHM system, which therefore saves a considerable amount of time and effort. Once the research behind the addition and location of the additional tilt meters is complete, the ultimate goal is to integrate the tilt meters permanently into the SHM system so the data collection and analysis processes can be completed more easily.

7.2.3 Determining the Location of the Surface Mounted Tilt Meters

In order to determine the location of the additional tilt meters, the FEA model results were again utilized. From comparing the November 2012 Load Test rotation profile to the FEA model rotation profile, which can be referred back to in Figure 19, it was evident that the overall shape of the rotation profiles compared well with each other. Additionally, it was evident that the rotation profiles for the two backspans compared better than the rotation profiles for the mainspan. By focusing on the mainspan, it was concluded that the smaller peaks in the November 2012 Load Test rotation profile were due to lack of sensors near the locations of the peaks in the FEA model rotation profile. Therefore, the decision was made to add two additional tilt meters close to the locations of the peaks in the model rotation profile. Since the surface mounted tilt meters were only going to be temporary, and the study regarding the placement of the tilt meters was in the early stages, the locations of the tilt meters were estimated using the May 2016 Load Test. For the May 2016 Load Test, the two surface mounted tilt meters were placed at locations of 734 feet and 1,010 feet along the bridge, as these locations were fairly close to the peaks in the model rotation profile. The surface mounted tilt meters were not placed at the exact locations of the peaks in the model rotation profile, because at the time, the chosen locations were the most convenient locations for installation. The locations of all of the tilt meters used during the May 2016 load test are indicated by the red dots in Figure 21, while the rotation profile obtained through the FEA model is shown as the blue solid line.

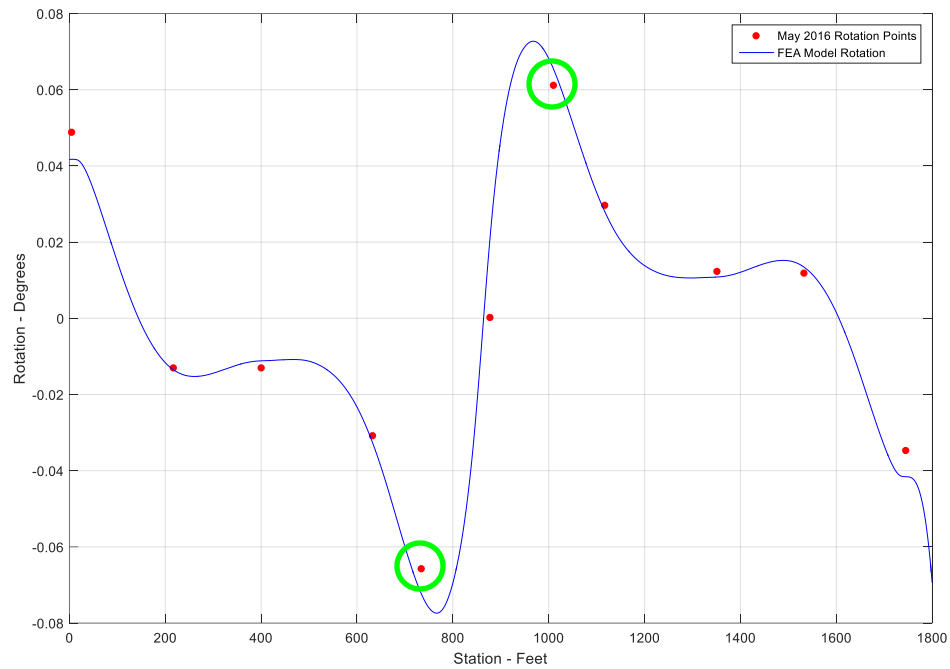


Figure 21 Comparison Between May 2016 Load Test Rotation Points and FEA Model Rotation Profile

The two red dots that are circled in green represent the two surface mounted tilt meters. It can be seen that the surface mounted tilt meters are positioned fairly closely along the length of the bridge to the local peaks in the FEA model rotation profile, and the measured rotation data matches the model predictions very well. Although the surface mounted tilt meters were not positioned in the exact locations of the peak model rotations, the results from the May 2016 Load Test, which will be presented in Chapter 8, compared very well with the model results. During future load tests, the surface mounted tilt meters should be positioned in locations closer to the peak model rotations.

Chapter 8

CALCULATED DEFLECTIONS USING IRIB ROTATION DATA: FINAL RESULTS

In this chapter, the final calculated deflections using rotation data from the SHM system are presented. The deflection results obtained using the automated Matlab code are presented for both Load Pass 0_1 and Load Pass 0_2 of Load Test 5. Results obtained incorporating the surface mounted tilt meters are similarly presented for both Load Pass 0_1 and Load Pass 0_2. Results with and without the surface mounted tilt meter data are compared towards the end of the chapter.

8.1 Results from Automated Matlab Code

After noticing the errors introduced by the original numerical integration procedure (computed nonzero support displacements) presented in Chapter 7, and applying the necessary adjustments to account for the zero displacement boundary support conditions, the automated Matlab code was used to re-analyze the Load Pass 0_1 and Load Pass 0_2 data from Load Test 5. The final results from Load Pass 0 during the May 2016 Load Test are presented in the following sections. As stated in Chapter 7, it is important to note that tilt meters T_E2 and T_E8 were not working properly during the load test. Consequently, the final results from the automated Matlab code will only include data from the remaining seven system tilt meters.

8.1.1 Load Pass 0_1

As described previously, the focus of Load Pass 0_1 was to investigate the rotation and deflection of the bridge at each tilt meter location when the six side-by-side trucks were located at that tilt meter location. Because the case of most interest was the midspan deflection resulting from the six loaded trucks being positioned at

midspan, that is what the Matlab code computed. Because of this, only data from the trucks positioned above tilt meter T_E5 could be analyzed using the automated Matlab code, and therefore, rotation and deflection profiles are only available for that loading situation.

The data from Load Pass 0_1 was reanalyzed with the necessary adjustments that were introduced in Chapter 7, in order to account for the deflection boundary conditions at the bridge end and bridge pylon locations. Therefore, the results presented in this section are produced from the boundary condition corrected calculation using data from seven system tilt meters. Similar to the results presented in Chapter 7, the final results of Load Pass 0_1 consist of a rotation profile and deflection profile of the bridge resulting from test trucks being located at the midspan location, where tilt meter T_E5 is located. These profiles are shown in Figure 22.

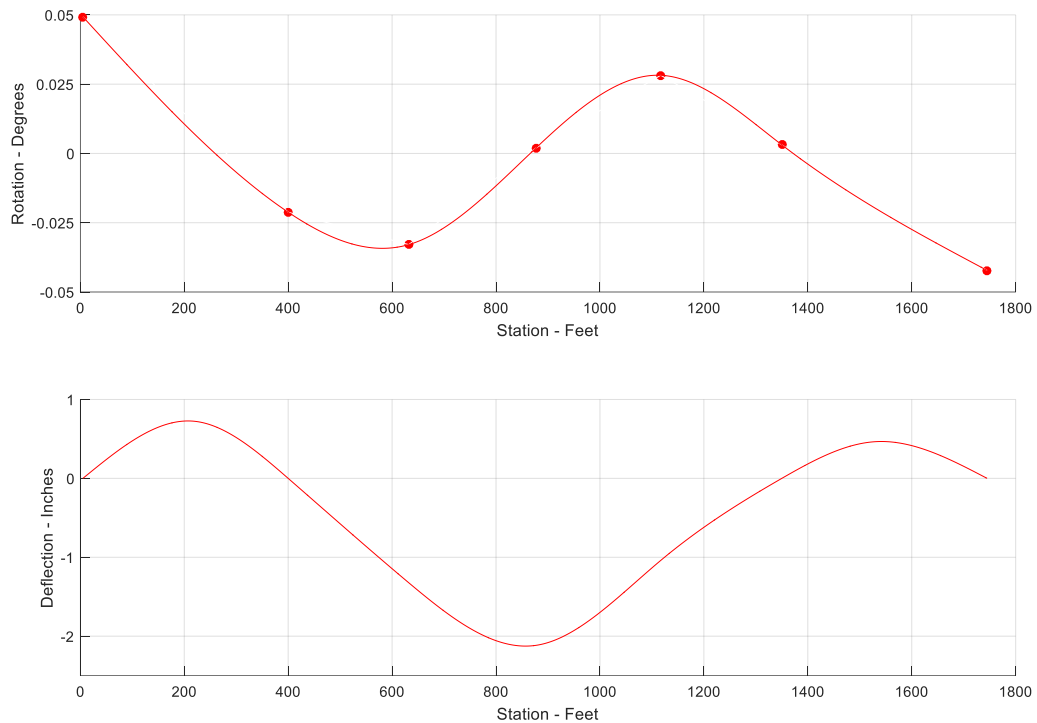


Figure 22 Final Rotation and Deflection Profiles for Load Pass 0_1 with Trucks Positioned Above T_E5

From the deflection profile for this loading situation, it can be seen that the deflections at the pylons, the 400 ft and 1,350 ft locations, are now zero. Additionally, the deflections at the bridge ends are now zero. With these corrections to the original preliminary results, shown in Figure 15, the final deflection profile of the bridge for Load Pass 0_1 is now more accurate and complete. It is important to keep in mind that the actual collected rotation data is indicated by the dots on the rotation profile. The curve through the collected data points is a curve fit, and the deflection profile is integrated from that rotation curve fit.

In order to better see the details of the deflection profile, and in order to better visualize the known boundary condition deflection corrections, the original deflection profile and the final deflection profile are presented in Figure 23.

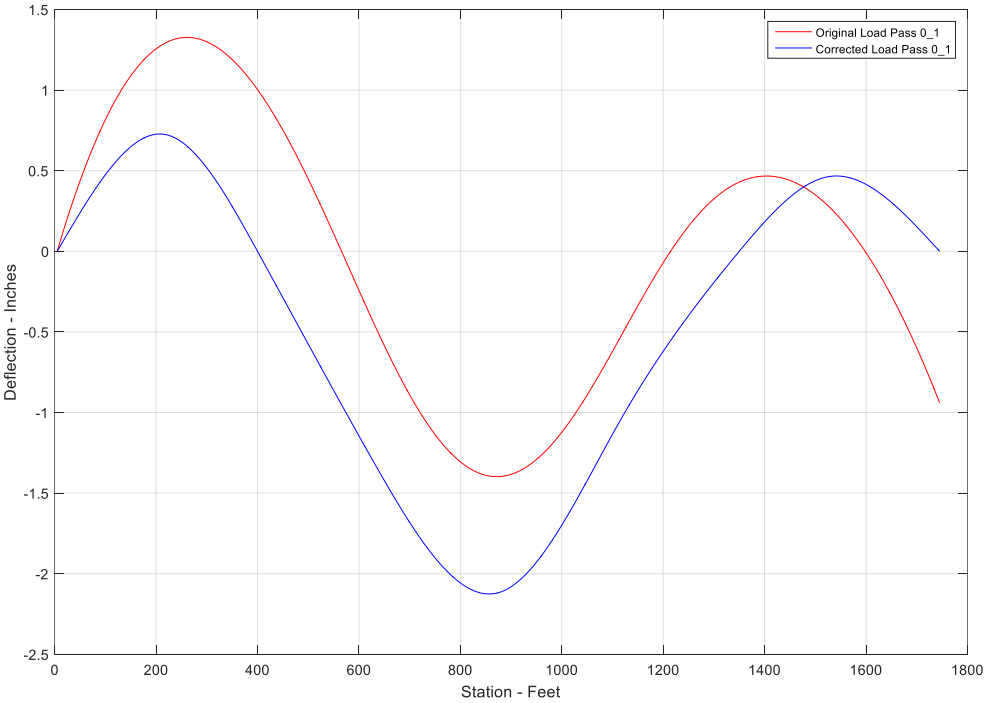


Figure 23 Final Deflection Profile for Load Pass 0_1 with Trucks Positioned Above T_E5

From the final corrected deflection profile, it can be seen that the deflection profile follows the expected deflection shape and corresponds well with the shape of the model deflection presented in Figure 20. The maximum peak deflection occurs near the midspan location, which is the location of tilt meter T_E5, as expected. The deflection values from the automated Matlab code are shown for each tilt meter location in Table 3. Although deflection values are only shown at the tilt meter

locations, deflection values can be computed at all locations along the length of the bridge.

Table 3 Final Deflection Values for Load Pass 0_1 with Trucks Positioned Above T_E5

Tilt Location (Feet)	Deflection (Inches)
5	0
217	0.725
400	0
632	-1.32
877	-2.12
1117	-1.04
1350	0
1532	0.466
1745	0

From the tabulated deflection values, it can be seen that the maximum peak deflection at the midspan location is approximately -2.12 inches. This peak deflection will be compared with deflections from the FEA model and from a survey in Section 9.1.1.1 and Section 9.1.1.2, respectively.

8.1.2 Load Pass 0_2

As described previously, Load Pass 0_2 involved taking rotation and deflection data only when the trucks were located at midspan. Similar to Load Pass 0_1, the data from Load Pass 0_2 was reanalyzed with the necessary adjustments that were introduced in Chapter 7. The results presented in this section are produced from the boundary condition corrected calculation using data from seven system tilt meters. Similar to the preliminary results presented in Chapter 7, the final results from Load

Pass 0_2 consist of a rotation profile and deflection profile of the bridge caused by six load trucks being located at midspan (the location of tilt meter T_E5). The rotation and deflection profiles when the trucks were stationary above tilt meter T_E5 are shown in Figure 24.

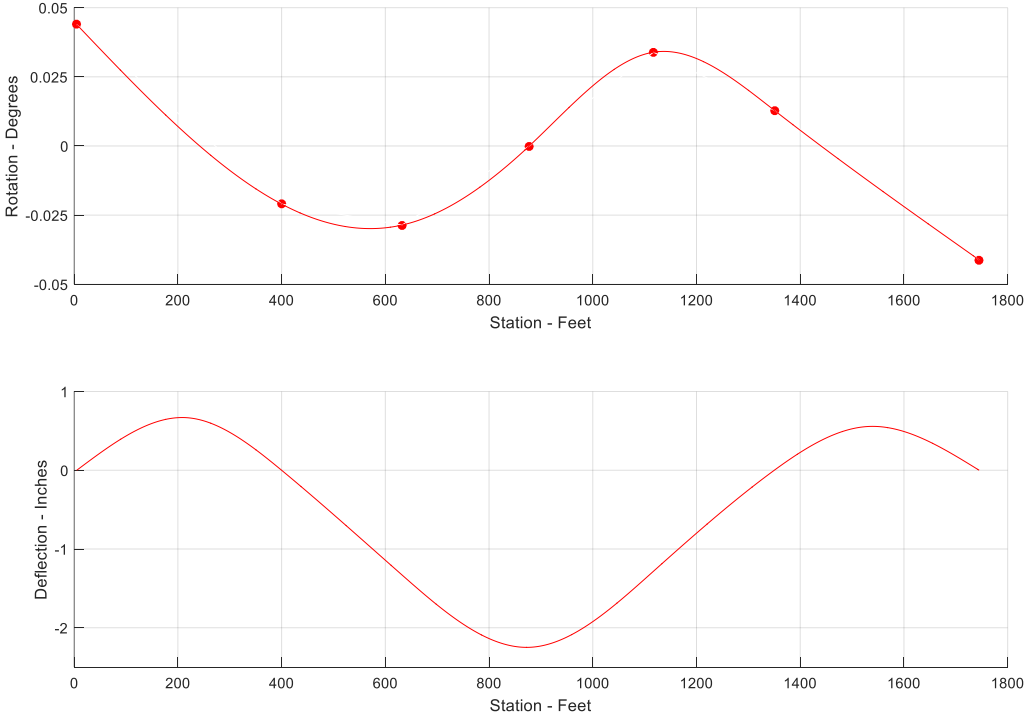


Figure 24 Final Rotation and Deflection Profiles for Load Pass 0_2 with Trucks Positioned Above T_E5

From the deflection profile for this loading situation, it can be seen that the deflections at the pylons are zero, just as they were for Load Pass 0_1. Additionally, the deflections at the bridge ends are zero. With these corrections to the original preliminary results, shown in Figure 16, the final deflection profile of the bridge for Load Pass 0_2 is now more accurate and complete. In order to better see the details of

the deflection profile, and in order to better visualize the known boundary condition deflection corrections, the original deflection profile and the final deflection profile are presented in Figure 25.

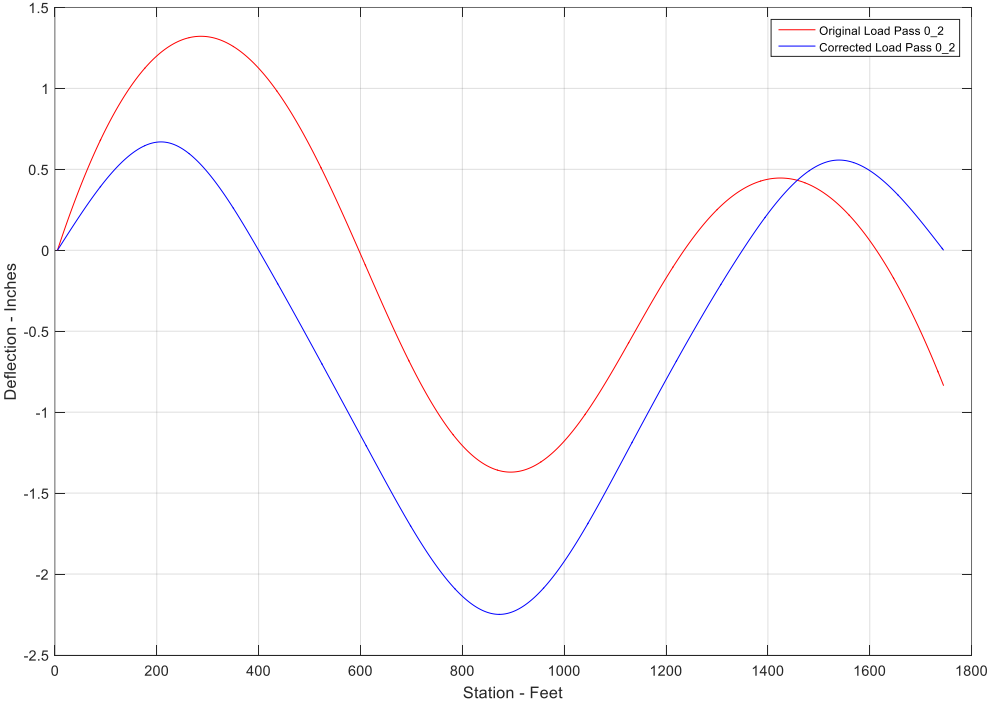


Figure 25 Final Deflection Profile for Load Pass 0_2 with Trucks Positioned Above T_E5

From the final corrected deflection profile, it can be seen that the deflection profile follows the expected shape and corresponds well with the shape of the model deflection presented in Figure 20. The maximum peak deflection occurs at the midspan location, which is the location of tilt meter T_E5, as expected. Similar to Load Pass 0_1 results, the deflection values for Load Pass 0_2 from the automated Matlab code are shown for each tilt meter location in Table 4.

Table 4 Final Deflection Values for Load Pass 0_2 with Trucks Positioned Above T_E5

Tilt Location (Feet)	Deflection (Inches)
5	0
217	0.667
400	0
632	-1.33
877	-2.25
1117	-1.28
1350	0
1532	0.556
1745	0

From the tabulated deflection values, it can be seen that the maximum peak deflection at the midspan location is approximately -2.25 inches. This peak deflection will be compared with that of the FEA model and survey in Section 9.1.2.1 and Section 9.1.2.2, respectively.

As introduced in Section 5.2.4, the repeatability and reliability of the data collected during the May 2016 Load Test were established by duplicating the midspan deflections and associated rotations. While Load Pass 0_1 and Load Pass 0_2 were conducted differently, the data used to compute the deflection profiles in both load passes came from a loading scenario of trucks located at the midspan location. Therefore, Load Pass 0_1 and Load Pass 0_2 are essentially replicates of each other. In order to demonstrate the repeatability of the results, a comparison of the deflection profiles from Load Pass 0_1 and Load Pass 0_2 is shown in Figure 26.

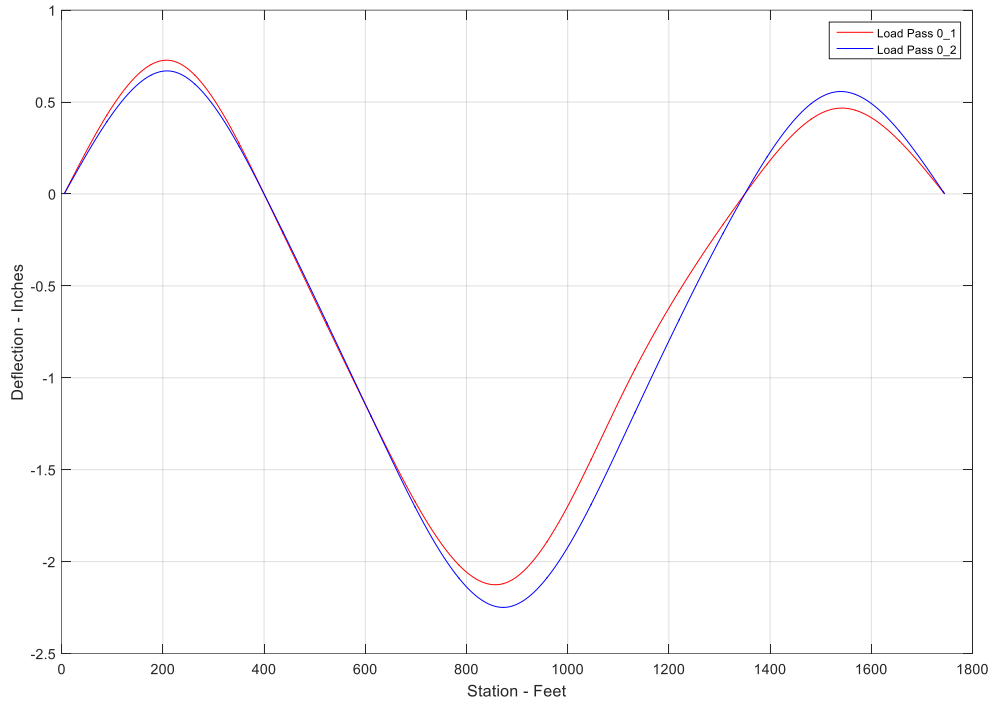


Figure 26 Comparison of Load Pass 0_1 and Load Pass 0_2 Deflection Profiles

While there are some inconsistencies between the two deflection profiles, the shapes of the deflection profiles compare very well. The percent difference between the midspan deflection values is about 6.1%, with midspan deflection values for Load Pass 0_1 and Load Pass 0_2 of -2.12 inches and -2.25 inches, respectively. While the deflection results from Load Pass 0_1 and Load Pass 0_2 are very similar, they are not identical, which is common when replicate tests are conducted. The difference in the loading processes for the two load passes could have led to the difference in the midspan deflection values.

8.2 Results from Surface Mounted Tilt Meters

As previously mentioned in Chapter 7, two surface mounted tilt meters were added for the May 2016 Load Test in an effort to capture additional rotation data that would allow more accurate deflections to be calculated. Surface mounted tilt meters, as opposed to permanently mounted tilt meters, were utilized because of their ease of operation and ability for temporary use and possible future relocation.

Because the surface mounted tilt meters were not integrated into the SHM system, they were analyzed differently than the original system data. In other words, the surface mounted tilt meter data cannot be pre-processed through the automated Matlab code. Therefore, the deflection results presented in the following sections, for both Load Pass 0_1 and Load Pass 0_2, were analyzed using a separate Matlab script, rather than using the automated Matlab code (which both pre-processes the data and conducts the numerical integration). Because of the way the results were analyzed using Matlab, missing rotation values for tilt meters T_E2 and T_E8 could be estimated and inserted into the data sets, in order to obtain more complete rotation and deflection profiles of the bridge. The rotation values for tilt meters T_E2 and T_E8 were estimated by applying a scaling factor to the November 2012 Load Test rotation values for tilt meters T_E2 and T_E8. The scaling factor was determined by calculating the ratio of truck weights from the May 2016 Load Test and the November 2012 Load Test. A comparison of the rotation profiles from the November 2012 Load Test, May 2016 Load Pass 0_1, and May 2016 Load Pass 0_2 is shown in Figure 27. The rotation data used in the November 2012 Load Test rotation profile was scaled to a loading consistent with the May 2016 Load Test prior to creating the plot.

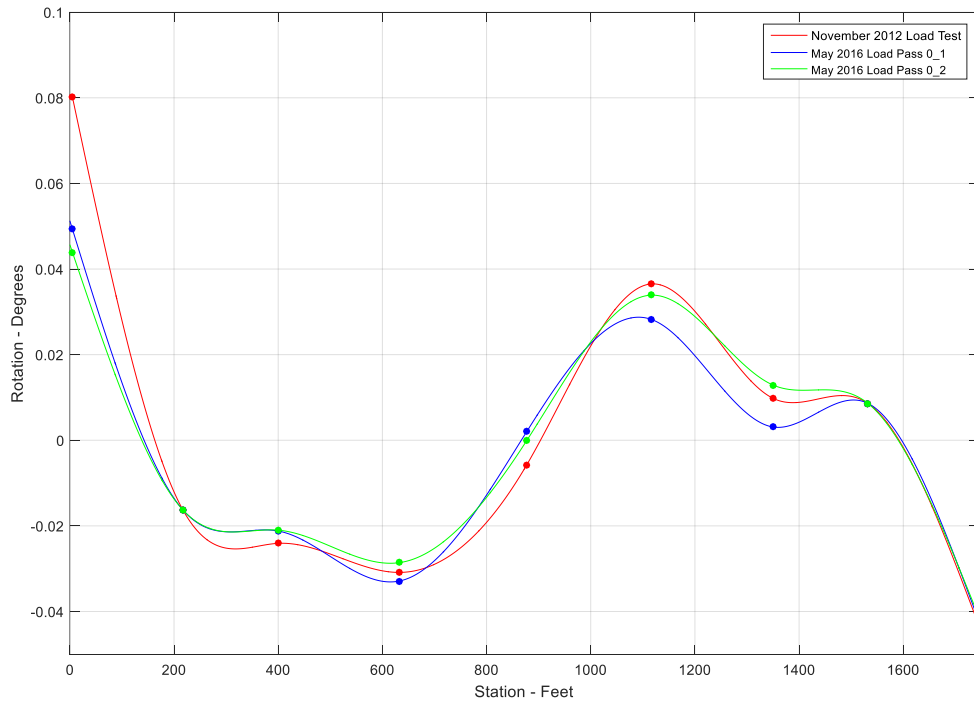


Figure 27 Comparison of Rotation Profiles from the November 2012 Load Test, May 2016 Load Pass 0_1, and May 2016 Load Pass 0_2

From the rotation profile comparison shown in Figure 27, it can be seen that there are slight differences in the rotation values at each tilt meter location. The differences in the rotation values vary at each tilt meter location, indicating that the scaling method used to estimate rotation values works better at some locations along the bridge than others. Because the differences in the rotation values at each tilt meter location are slight, the scaling method used to estimate rotation values is satisfactory for the purpose of this research. For future data analyses, a more appropriate method for estimating rotation values may be developed.

8.2.1 Load Pass 0_1

As mentioned before, Load Pass 0_1 focused on investigating the deflection of the bridge at each tilt meter location. In order to obtain a more complete set of rotation data to analyze, the system data from Load Pass 0_1 was combined with the surface mounted tilt meter data and the estimated rotation data for tilt meters T_E2 and T_E8. The combined rotation data was then analyzed using the necessary adjustments that were introduced in Chapter 7, in order to account for the known boundary conditions (zero deflection) at the bridge end and pylon supports. Therefore, the results presented in the following section are produced from the boundary condition corrected calculation using data from both system tilt meters and surface mounted tilt meters.

The results with the inclusion of the surface mounted tilt meters consist of rotation and deflection profiles at the locations of tilt meters T_E4 through T_E6, which are located on the mainspan of the bridge. The tilt meters at the ends of the bridge and at the pylon locations were not analyzed, and tilt meters T_E2 and T_E8 were not operating during the May 2016 Load Test. Therefore, rotation and deflection profiles could not be generated for those tilt meter locations. Following the presentation of the final rotation and deflection profiles, the results when surface mounted tilt meter data is included will be compared to the results when only permanently mounted tilt meters are used.

8.2.1.1 Final Rotation and Deflection Profile Plots

The rotation and deflection profiles when the trucks were positioned above tilt meter T_E4 are shown in Figure 28. From the rotation profile for this loading situation, it can be seen that the location of zero rotation occurs around the 677 ft location. This location is close to the location of the trucks above tilt meter T_E4,

which is the 632 ft location. This corresponds well with the rotation behavior that is expected, as it is expected that the rotation would be zero close to where the trucks are located.

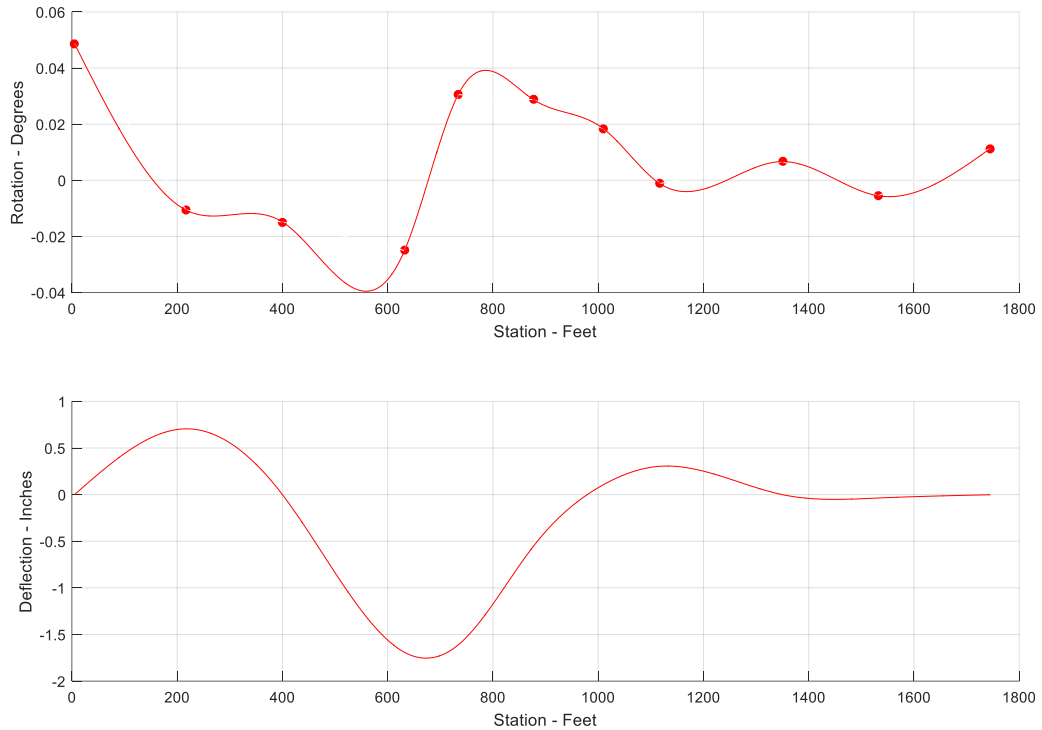


Figure 28 Rotation and Deflection Profiles for Load Pass 0_1, Including Surface Mounted Tilt Meters, with Trucks Positioned Above T_E4

From the deflection profile for this loading situation, it can be seen that the maximum peak deflection is approximately -1.75 inches and occurs around the 672 ft location along the bridge. As expected, this maximum deflection location is close to the location of the trucks above tilt meter T_E4. In order to better see the details of the final deflection profile, the deflection profile including the surface mounted tilt meters is presented individually in Figure 29.

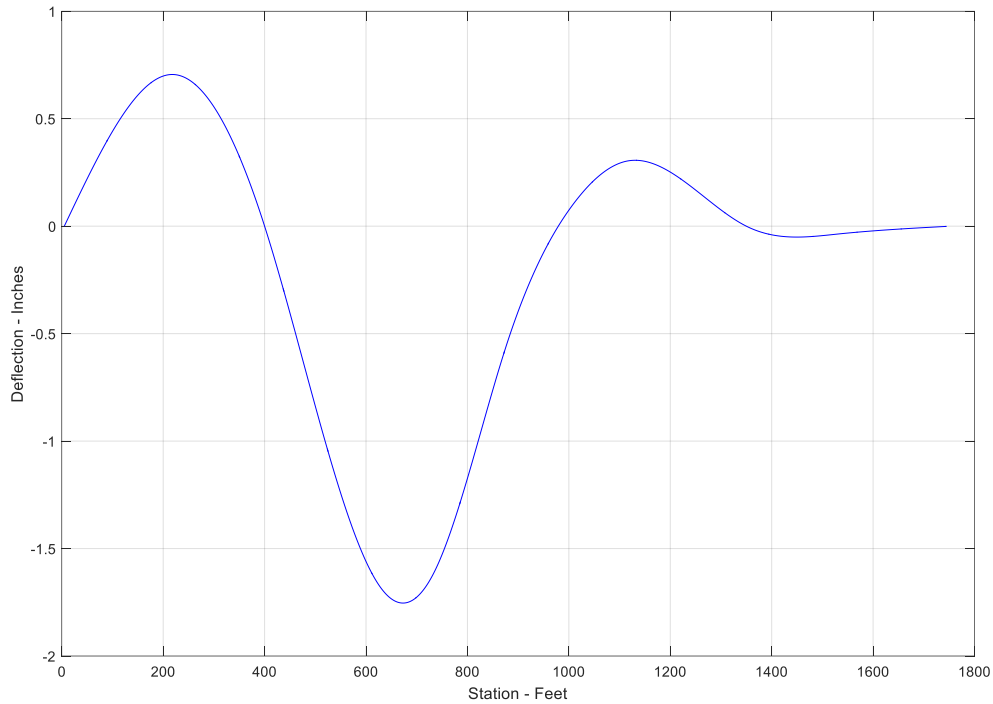


Figure 29 Final Deflection Profile for Load Pass 0_1, Including Surface Mounted Tilt Meters, with Trucks Positioned Above T_E4

It can be seen from the deflection profile presented in Figure 29 that the peak deflection of -1.75 inches occurs slightly to the right of the location of tilt meter T_E4, which is located at the 632 ft location. This is expected as this is not a symmetric load case and the peak deflection will occur at a location slightly towards midspan.

The rotation and deflection profiles when the trucks were positioned above tilt meter T_E5, the midspan tilt meter, are shown in Figure 30. From the rotation profile for this loading situation, it can be seen that the location of zero rotation occurs around the 872 ft location. This location is very close to the location of the trucks above tilt meter T_E5, which is the 877 ft location. This again corresponds well with the rotation

behavior that is expected, as it is expected that the rotation be zero at the location of loading (midspan in this case).

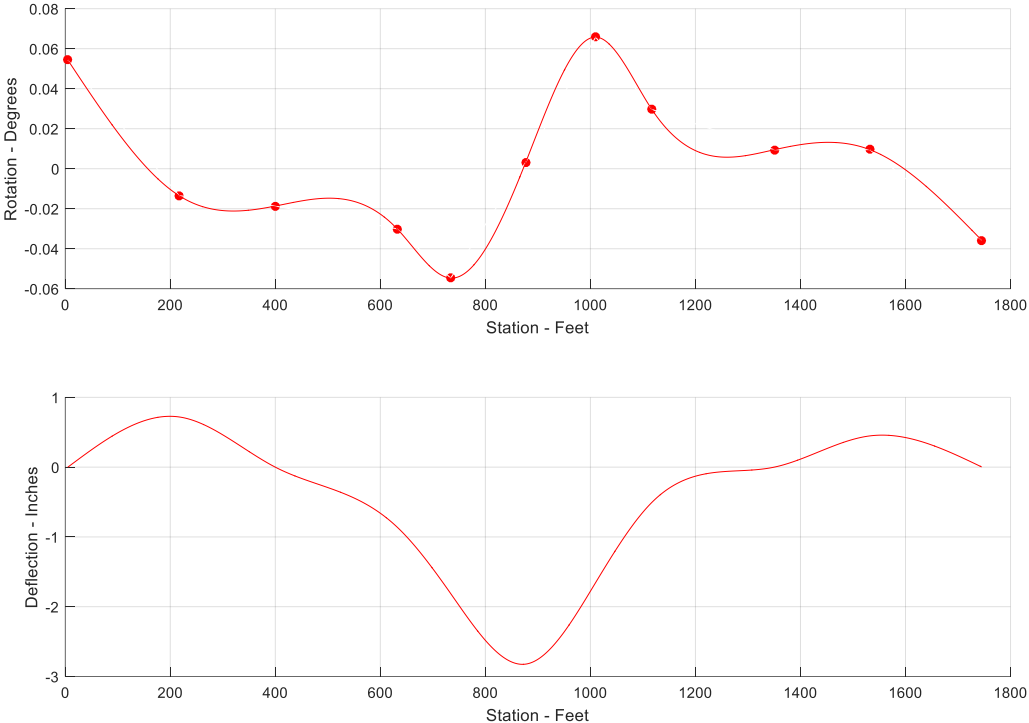


Figure 30 Rotation and Deflection Profiles for Load Pass 0_1, Including Surface Mounted Tilt Meters, with Trucks Positioned Above T_E5

From the deflection profile for this loading situation, it can be seen that the maximum peak deflection is approximately -2.83 inches and occurs around the 870 ft location along the bridge. As expected, this maximum deflection location corresponds very well with the location of the trucks above tilt meter T_E5. In order to better see the details of the final deflection profile, the deflection profile including the surface mounted tilt meters is presented individually in Figure 31.

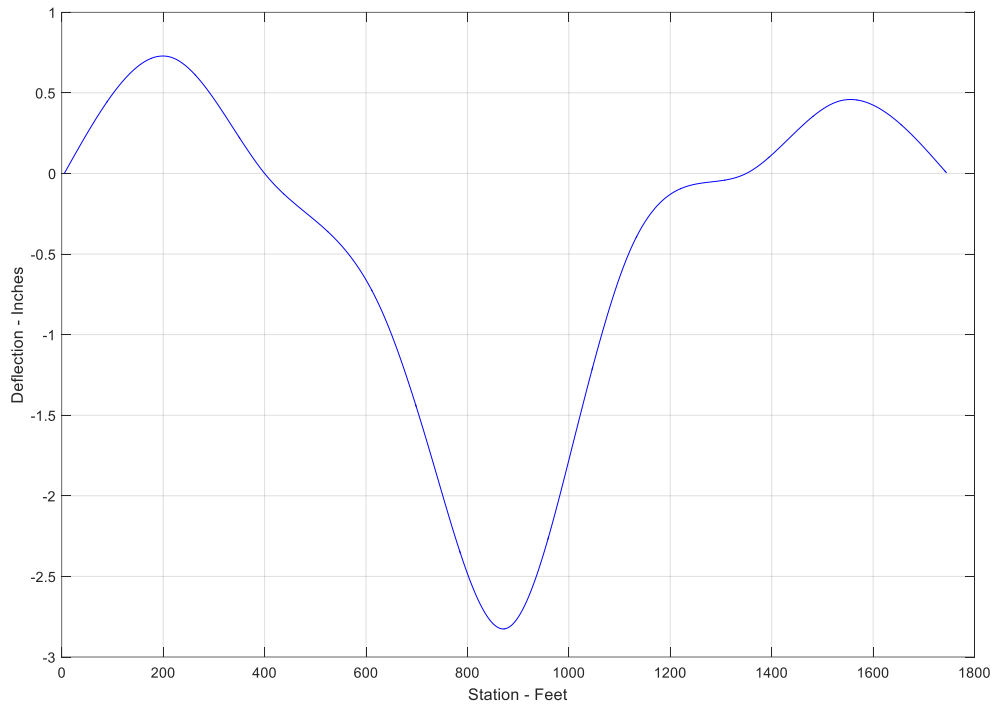


Figure 31 Final Deflection Profile for Load Pass 0_1, Including Surface Mounted Tilt Meters, with Trucks Positioned Above T_E5

It can be seen from the deflection profile in Figure 31 that the peak deflection of -2.83 inches occurs just to the left of the location of tilt meter T_E5. The deflection at the location of tilt meter T_E5 is approximately -2.82 inches, which is approximately a 0.4% difference. The deflection values at each of the tilt meter locations are presented in Table 5.

Table 5 Final Deflection Values for Load Pass 0_1, Including Surface Mounted Tilt Meters, with Trucks Positioned Above T_E5

Tilt Location (Feet)	Deflection (Inches)
5	0
217	0.719
400	0
632	-0.859
734	-1.81
877	-2.82
1010	-1.66
1117	-0.506
1350	0
1532	0.447
1745	0

The rotation and deflection profiles when the trucks were positioned above tilt meter T_E6 are shown in Figure 32. From the rotation profile for this loading situation, it can be seen that the location of zero rotation occurs around the 1,064 ft location. This location is close to the location of the trucks above tilt meter T_E6, which is the 1,117 ft location. This again corresponds well with the rotation behavior that is expected.

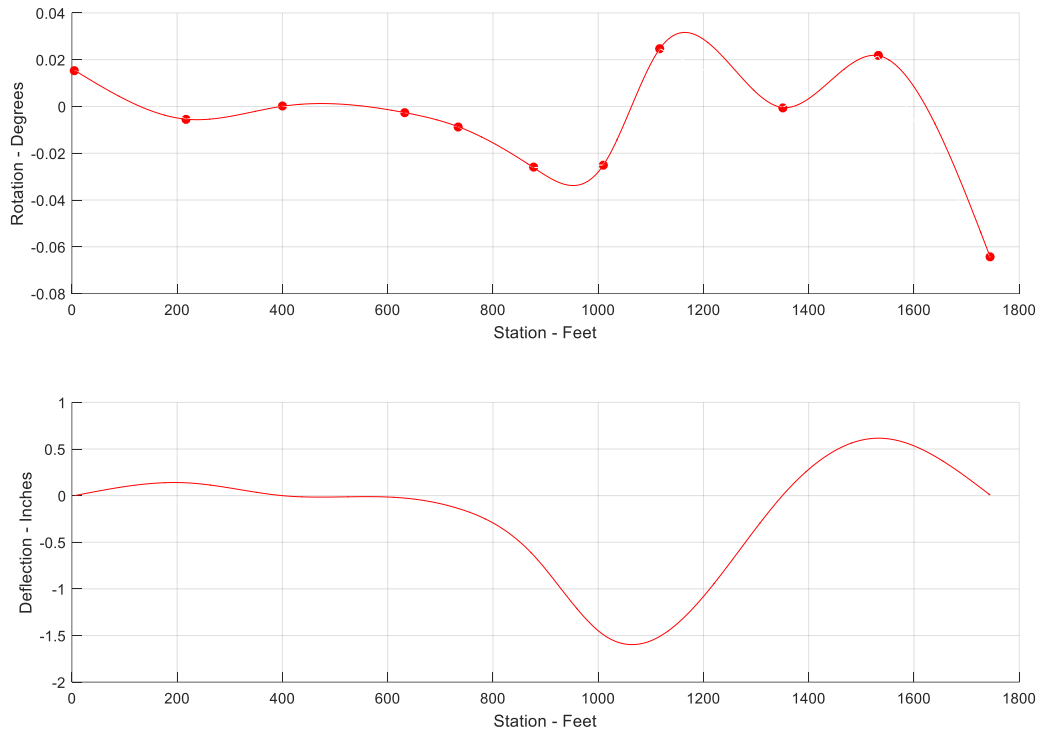


Figure 32 Rotation and Deflection Profiles for Load Pass 0_1, Including Surface Mounted Tilt Meters, with Trucks Positioned Above T_E6

From the deflection profile for this loading situation, it can be seen that the maximum peak deflection is approximately -1.60 inches and occurs around the 1,065 ft location along the bridge. As expected, this maximum deflection location is close to the location of the trucks above tilt meter T_E6. In order to better see the details of the final deflection profile, the deflection profile including the surface mounted tilt meters is presented individually in Figure 33.

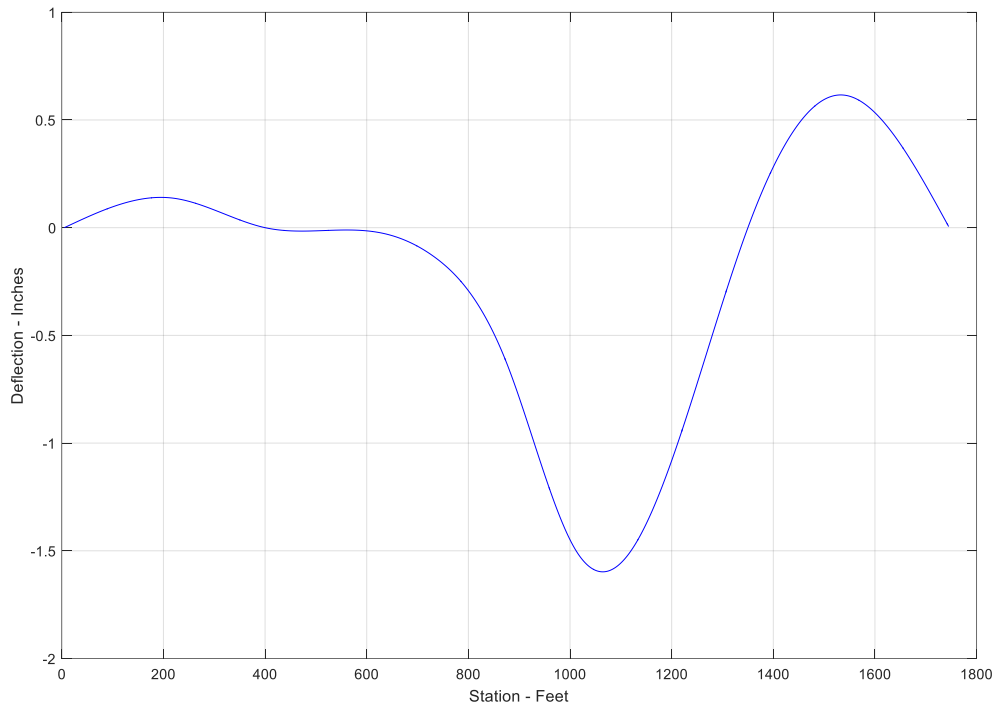


Figure 33 Final Deflection Profile for Load Pass 0_1, Including Surface Mounted Tilt Meters, with Trucks Positioned Above T_E6

It can be seen from the deflection profile in Figure 33 that the peak deflection of -1.60 inches occurs to the left of the location of tilt meter T_E6, which is located at the 1,010 ft location. Similar to the loading scenario when the trucks were positioned above tilt meter T_E4, this is expected as this is not a symmetric load case.

8.2.1.2 Comparison of Deflection Profiles With and Without Surface Mounted Tilt Meters

In order to fully understand the benefit of including the two surface mounted tilt meters during data collection, comparisons of the rotation and deflection profiles computed with and without the inclusion of data from the additional surface mounted tilt meters are provided. The comparisons of the rotation and deflection profiles are

only provided for the loading scenario with trucks positioned above tilt meter T_E5. This is because, as stated previously, the loading scenario with trucks at the midspan location is the most critical scenario and is the main focus of this research.

The comparison of the rotation profiles for the midspan loading scenario is shown in Figure 34, with the red line representing the deflection profile with the surface mounted tilt meters included and the blue line representing the deflection profile without the surface mounted tilt meters.

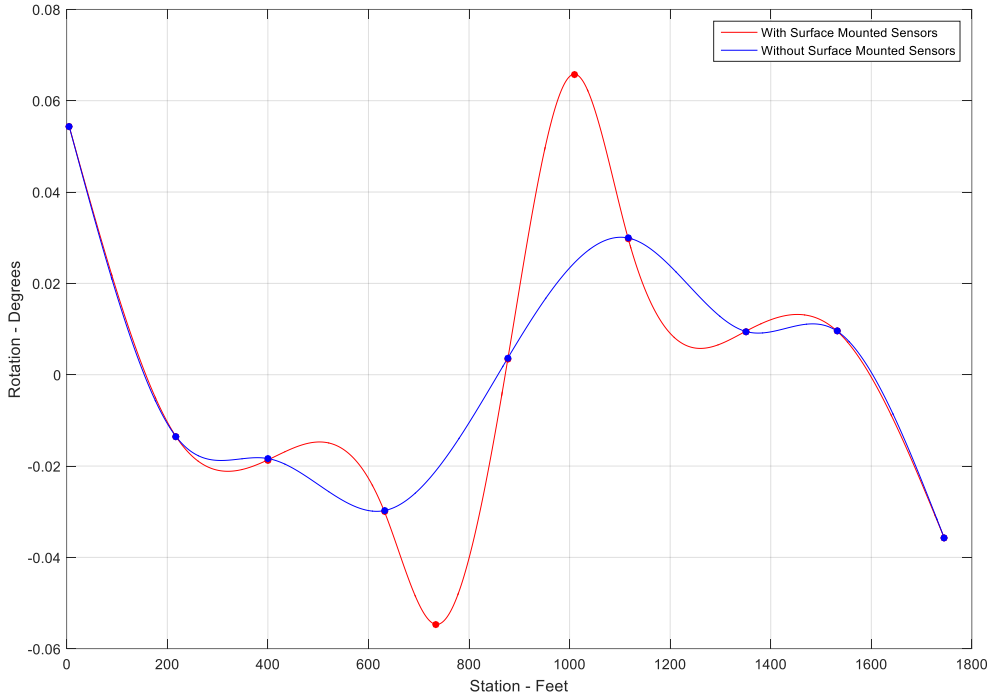


Figure 34 Rotation Profile Comparison Between Inclusion of Surface Mounted Tilt Meters and Exclusion of Surface Mounted Tilt Meters

The comparison of the deflection profiles for the midspan loading scenario is shown in Figure 35, with the red line representing the deflection profile with the

surface mounted tilt meters included and the blue line representing the deflection profile without the surface mounted tilt meters. In order to visualize the increased accuracy of the deflection results when the surface mounted tilt meters are included, the survey midspan deflection is indicated in Figure 35, represented by the black asterisk. A complete comparison of survey deflection values to the calculated deflection values will be presented in Chapter 9.

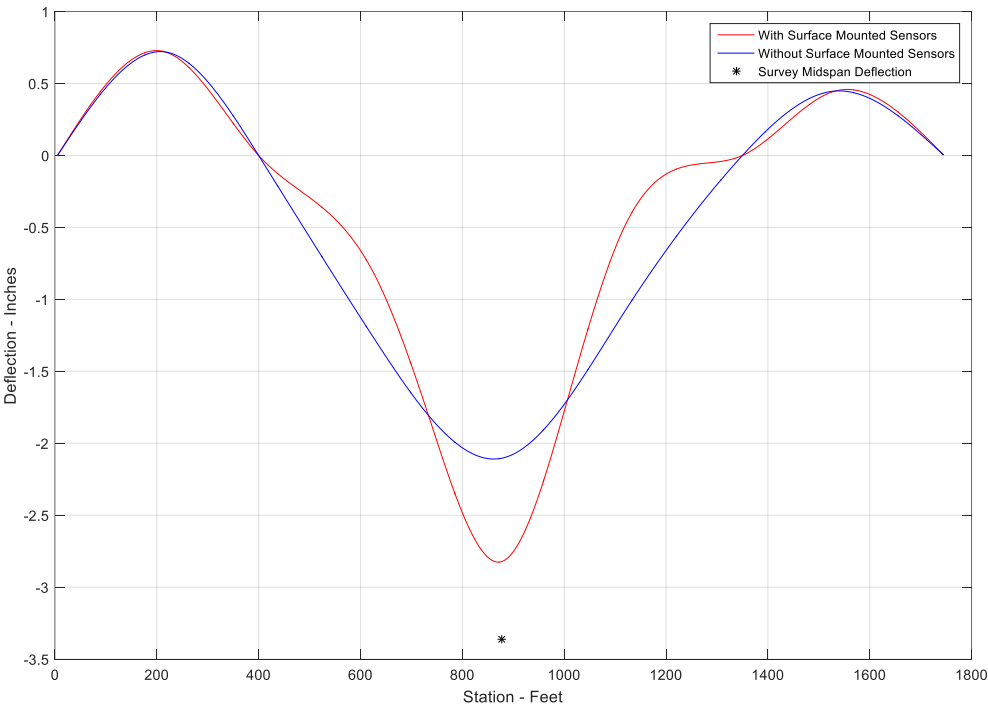


Figure 35 Deflection Profile Comparison Between Inclusion of Surface Mounted Tilt Meters and Exclusion of Surface Mounted Tilt Meters

As stated before, the peak midspan deflection when the surface mounted tilt meters are included is approximately -2.82 inches, and the peak midspan deflection when the surface mounted tilt meters are excluded is approximately -2.12 inches. This

results in a percent difference of about 33% when comparing the midspan deflections with and without the surface mounted tilt meters. A comparison of the deflections at each of the remaining locations is shown in Table 6.

Table 6 Comparison of Final Deflection Values With and Without Surface Mounted Tilt Meters

Tilt Location (Feet)	Without Surface Mounted Deflection (Inches)	With Surface Mounted Deflection (Inches)	Percent Difference
5	0	0	0
217	0.719	0.719	0
400	0	0	0
632	-1.30	-0.859	-40.9
734	-	-1.81	-
877	-2.12	-2.82	-28.3
1010	-	-1.66	-
1117	-1.10	-0.507	-73.8
1350	0	0	0
1532	0.448	0.448	0
1745	0	0	0

From the percent difference values presented in Table 6, it is evident that the surface mounted tilt meters significantly change the deflection values in only the mainspan of the bridge. With percent difference values ranging from about 28% to 73% in the mainspan, it is clear that including the two surface mounted tilt meters during data collection is extremely beneficial for the accuracy of rotation monitoring and deflection calculations. The increased accuracy of the deflection calculations will be presented in the next chapter when the deflection profiles are compared to measured deflections from the survey, and also to FEA results.

8.2.2 Load Pass 0_2

As mentioned before, Load Pass 0_2 focused on investigating the midspan rotation and deflection of the bridge. As done with Load Pass 0_1, the system data from Load Pass 0_2 was combined with the data from the surface mounted tilt meters and the estimated data for tilt meters T_E2 and T_E8, in order to analyze the combined rotation data for the bridge. The combined rotation data was again analyzed using the necessary adjustments that were introduced in Chapter 7. Therefore, the Load Pass 0_2 results presented in the following section are produced from the boundary condition corrected calculation using data from both system tilt meters and surface mounted tilt meters. The results when surface mounted tilt meters are included will be compared to the results found when only using the permanently mounted tilt meters.

8.2.2.1 Final Rotation and Deflection Profile Plots

The final results for Load Pass 0_2 with the inclusion of the surface mounted tilt meters consist of a rotation profile and deflection profile of the bridge. The rotation and deflection profiles are for a stationary loading above the midspan critical location, which is above tilt meter T_E5. The final rotation and deflection profiles with the inclusion of the surface mounted tilt meters are shown in Figure 36.

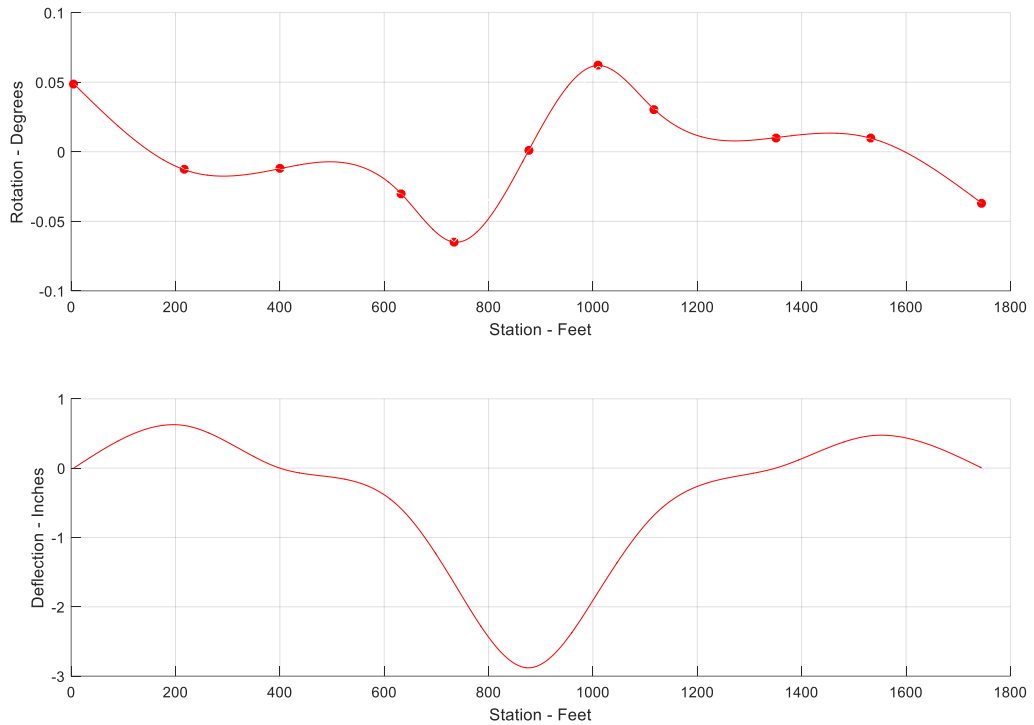


Figure 36 Final Rotation and Deflection Profiles for Load Pass 0_2, Including Surface Mounted Tilt Meters, with Trucks Positioned Above T_E5

From the final deflection profile shown in Figure 36, with the two surface mounted tilt meters included, it can be seen that the pylon deflections and bridge end deflections are zero. Additionally, it can be seen that the midspan peak deflection is larger and more distinct. In order to better see the details of the final deflection profile, the deflection profile including the surface mounted tilt meters is presented individually in Figure 37.

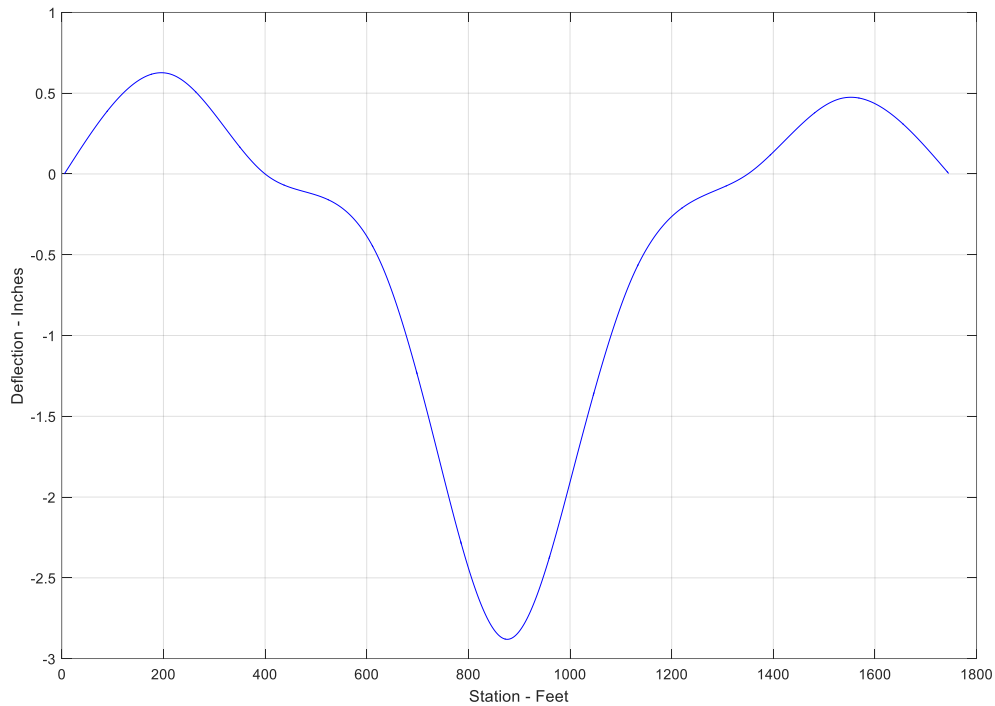


Figure 37 Final Deflection Profile for Load Pass 0_2, Including Surface Mounted Tilt Meters, with Trucks Positioned Above T_E5

The final deflection profile presented in Figure 37 shows that the two surface mounted tilt meters significantly change the shape of the deflection profile. The deflection profile including the surface mounted tilt meters corresponds much better with the shape of the model deflection profile, shown in Figure 20, than the original deflection profile, shown in Figure 25. Additionally, the maximum peak deflection is larger in magnitude when the surface mounted tilt meters are included. The maximum peak deflection occurs at the midspan location, above tilt meter T_E5, as expected. The deflection values at each of the tilt meter locations are presented in Table 7. The deflection values presented in Table 7 will be used for future comparisons.

Table 7 Final Deflection Values for Load Pass 0_2, Including Surface Mounted Tilt Meters, with Trucks Positioned Above T_E5

Tilt Location (Feet)	Deflection (Inches)
5	0
217	0.614
400	0
632	-0.583
734	-1.66
877	-2.88
1010	-1.79
1117	-0.681
1350	0
1532	0.466
1745	0

From the tabulated deflection values shown in Table 7, it can be seen that the maximum peak deflection at the midspan location is approximately -2.88 inches. This peak deflection is significantly larger than the peak deflection that excluded the surface mounted tilt meters, which was presented in Table 4. A comparison of the deflection values and deflection profiles from the exclusion and inclusion of the surface mounted tilt meters will be presented in the following section. The peak deflection for the inclusion of the surface mounted tilt meters will be compared with that of the FEA model and survey in the following chapter.

Similar to the results from the automated Matlab code, presented in Section 8.1.2, the results including surface mounted tilt meters can also be used to verify the repeatability and reliability of the data collected during the May 2016 Load Test. In order to demonstrate the repeatability of the results, a comparison of the deflection profiles from Load Pass 0_1 and Load Pass 0_2 is shown in Figure 38.

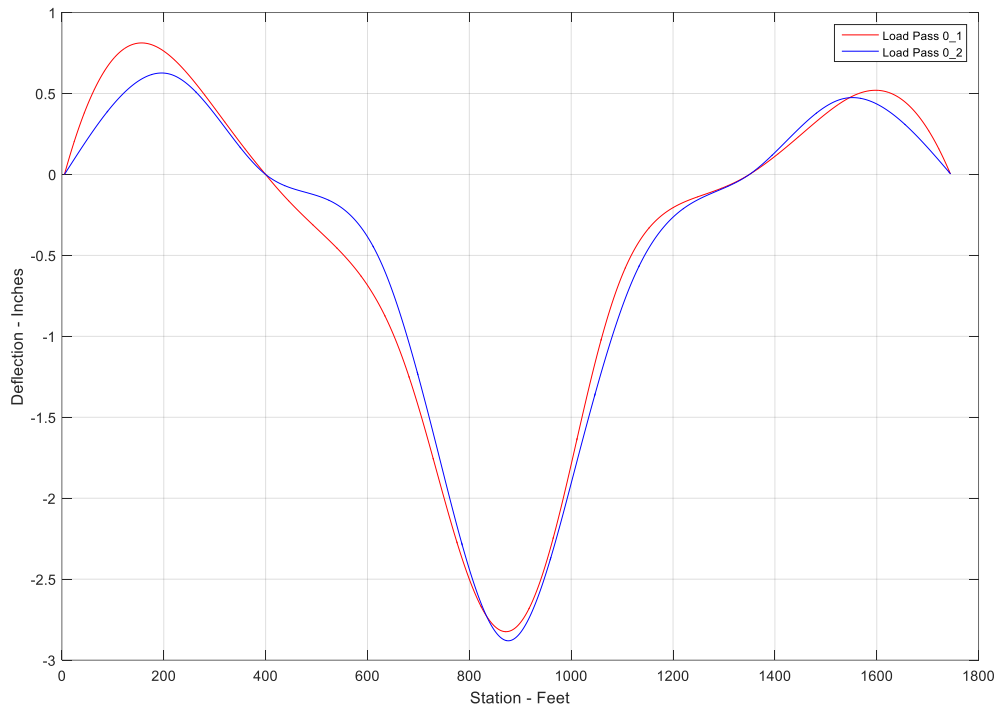


Figure 38 Comparison of Load Pass 0_1 and Load Pass 0_2 Deflection Profiles, Including Surface Mounted Tilt Meters

While there are some inconsistencies between the two deflection profiles, the shapes of the deflection profiles compare very well. The percent difference between the midspan deflection values is about 2.07%, with midspan deflection values for Load Pass 0_1 and Load Pass 0_2 of -2.82 inches and -2.88 inches, respectively. While the deflection results from Load Pass 0_1 and Load Pass 0_2 are very similar, they are not identical, which is common when replicate tests are conducted.

8.2.2.2 Comparison of Deflection Profiles With and Without Surface Mounted Tilt Meters

Similar to Load Pass 0_1, a comparison of the rotation and deflection profiles with and without the surface mounted tilt meters are provided for Load Pass 0_2. The

comparison of the rotation profiles for Load Pass 0_2 is shown in Figure 39, with the red line representing the deflection profile with the surface mounted tilt meters included and the blue line representing the deflection profile without the surface mounted tilt meters.

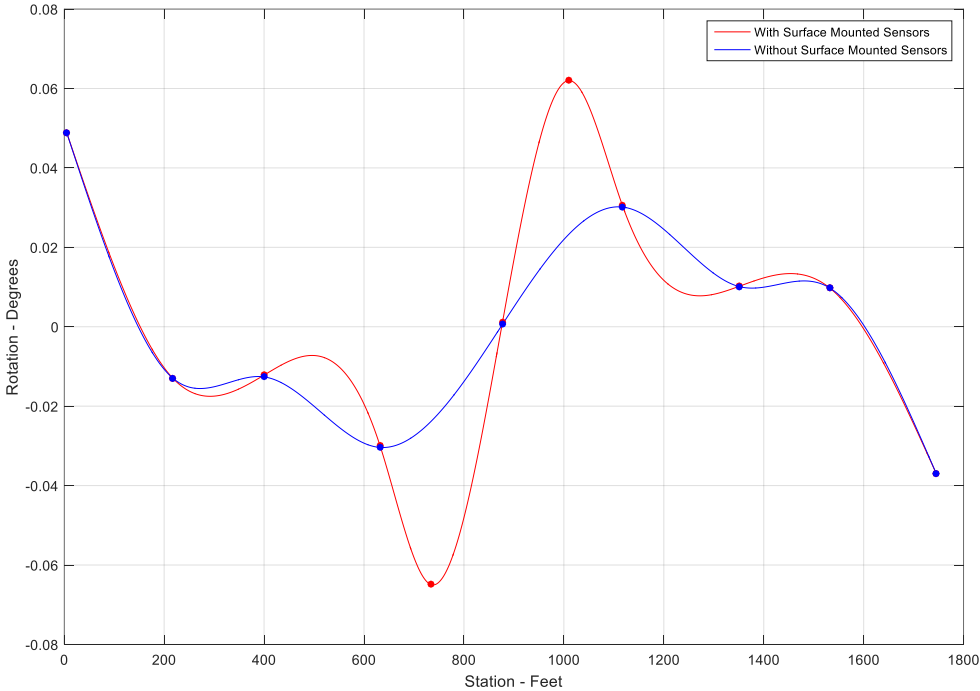


Figure 39 Rotation Profile Comparison Between Inclusion of Surface Mounted Tilt Meters and Exclusion of Surface Mounted Tilt Meters

The comparison of the deflection profiles is shown in Figure 40, with the red line representing the deflection profile with the surface mounted tilt meters included and the blue line representing the deflection profile without the surface mounted tilt meters. In order to visualize the increased accuracy of the deflection results when the surface mounted tilt meters are included, the survey midspan deflection is indicated in

Figure 40, represented by the black asterisk. A complete comparison of survey deflection values to the calculated deflection values will be presented in Chapter 9.

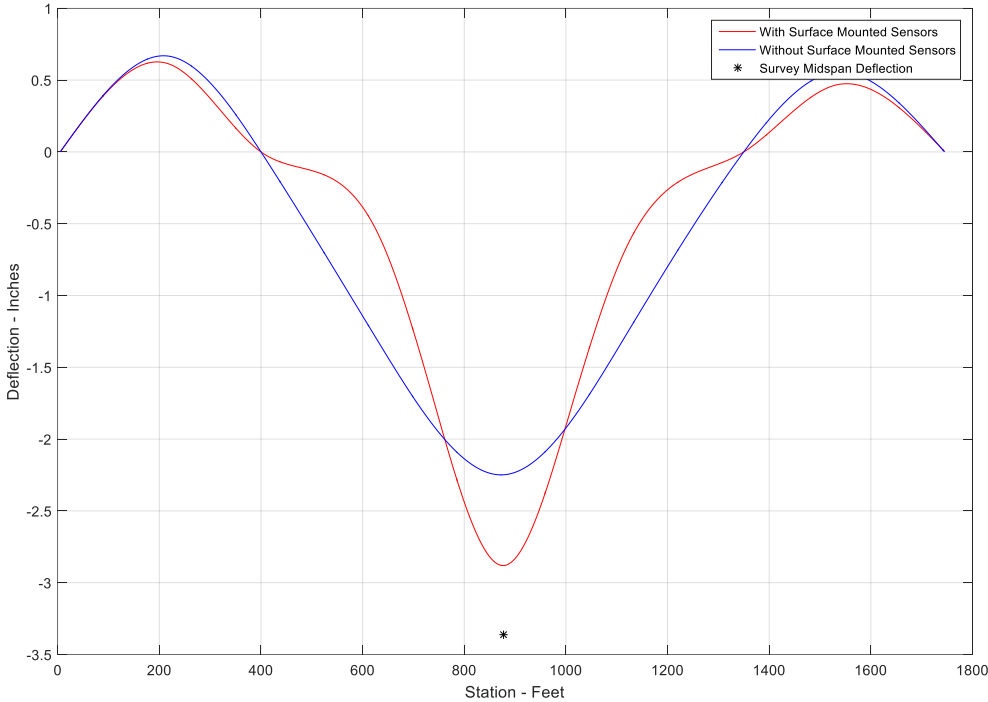


Figure 40 Deflection Profile Comparison Between Inclusion of Surface Mounted Tilt Meters and Exclusion of Surface Mounted Tilt Meters

As stated before, the peak midspan deflection when the surface mounted tilt meters are included is approximately -2.88 inches, and the peak midspan deflection when the surface mounted tilt meters are excluded is approximately -2.25 inches. This results in a percent difference of about 25% when comparing the midspan deflections with and without the surface mounted tilt meters. A comparison of the deflection values at each of the remaining locations is shown in Table 8.

Table 8 Comparison of Final Deflection Values With and Without Surface Mounted Tilt Meters

Tilt Location (Feet)	Without Surface Mounted Deflection (Inches)	With Surface Mounted Deflection (Inches)	Percent Difference
5	0	0	0
217	0.667	0.614	8.27
400	0	0	0
632	-1.33	-0.583	-78.1
734	-	-1.66	-
877	-2.25	-2.88	-24.6
1010	-	-1.79	-
1117	-1.28	-0.681	-61.1
1350	0	0	0
1532	0.556	0.466	17.6
1745	0	0	0

From the percent difference values presented in Table 8, it is evident that the surface mounted tilt meters significantly change the deflection values in the mainspan of the bridge, with only slight changes in the two backspans. With percent difference values ranging from about 25% to 78% in the mainspan, it is clear that including the two surface mounted tilt meters during data collection has a significant impact on the final results. The accuracy of the deflection calculations will be presented in the next chapter.

Chapter 9

ACCURACY OF CALCULATED DEFLECTIONS

The following chapter focuses on investigating the accuracy of the calculated deflections that were presented in the previous chapter. First, the accuracy of the deflections that were calculated using the automated Matlab code will be determined for both Load Pass 0_1 and Load Pass 0_2 of Load Test 5. To do this, the calculated deflections will be compared to both FEA model deflections and survey deflections. The accuracy of the deflections that were calculated when including the surface mounted tilt meters will then be analyzed, again for Load Pass 0_1 and Load Pass 0_2. Similar to the deflections that were calculated by integrating measured rotation values using the automated Matlab code, the deflections that were calculated when the surface mounted tilt meters are included will be compared to the FEA model deflections and survey deflections.

9.1 Automated Matlab Code for Load Test System Data

After presenting the final computed deflection results from Load Pass 0 in Chapter 8, those results will be used to evaluate their accuracy. Analyzing the accuracy of the calculated deflections will help to establish the validity of the methodology developed to calculate deflections using the SHM system rotation data. The calculated deflections for Load Pass 0_1 and Load Pass 0_2, which were calculated using the automated Matlab code, with adjustments for known boundary condition deflections, are compared to both the FEA model deflections and survey deflections in the following sections. The raw rotation data for Load Pass 0_1 and Load Pass 0_2 can be found in Appendix D.

9.1.1 Load Pass 0_1

The final results from Load Pass 0_1 consisted of rotation and deflection profiles for the midspan loading scenario, with the trucks positioned above tilt meter T_E5. While Load Pass 0_1 produced rotations and deflections of the bridge when trucks were positioned at each tilt meter location, the automated Matlab code simply focused on analyzing the rotation and calculating the deflection for the case when the trucks were at the midspan location, as this loading produces the largest midspan deflection. With that being said, the deflection values from the midspan loading scenario for Load Pass 0_1, which were calculated using the automated Matlab code, are compared to both the FEA model deflections and survey deflections in the following two sections.

9.1.1.1 Comparison to FEA Model

As introduced in Chapter 3, a FEA model was created for the IRIB in order to better analyze the static and dynamic behavior of the bridge. The FEA model that was used for this research is a 3-D CSiBridge model with beam elements. The model was used to analyze the rotations and deflections of the bridge, as well as to verify the recorded SHM system rotation data and the calculated deflection values. The FEA model serves as one of two available ways to verify the recorded rotation data and calculated deflection values. Because of this, the calculated deflection results from the automated Matlab code for Load Pass 0_1 were compared to the FEA model deflections results. The deflection results are compared using a percent error, which is shown in Table 9. Both the calculated deflection values and the model deflection values can be found in Table 9 also.

Table 9 Comparison of Load Pass 0_1 Calculated Deflections with FEA Model Deflections

Tilt Meter	Station (Feet)	Calculated Deflection (Inches)	Model Deflection (Inches)	Percent Error (%)
T_E1	5	0	0	0
T_E2	217	0.719	0.525	37.0
T_E3	400	0	0	0
T_E4	632	-1.30	-0.750	73.3
T_E5	877	-2.12	-3.66	-42.1
T_E6	1117	-1.10	-0.696	58.0
T_E7	1350	0	0	0
T_E8	1532	0.448	0.513	-12.7
T_E9	1745	0	0	0

From the error values presented in Table 9, it is evident that the deflection results from the automated Matlab code for Load Pass 0_1 differ rather significantly from the FEA model deflection values. The error values between the calculated deflections and the FEA model deflections range from approximately 13% to 73% at the nonzero deflection locations. At the midspan critical location, the location of tilt meter T_E5, the error between the calculated deflection and the FEA model deflection is approximately 42%.

The calculated deflection values from Load Pass 0_1 and the FEA model deflections are also compared graphically, in order to better visualize the comparison. The plot of the deflection comparison is shown in Figure 41, with the red line representing the Load Pass 0_1 calculated deflection values and the blue line representing the FEA model deflection values.

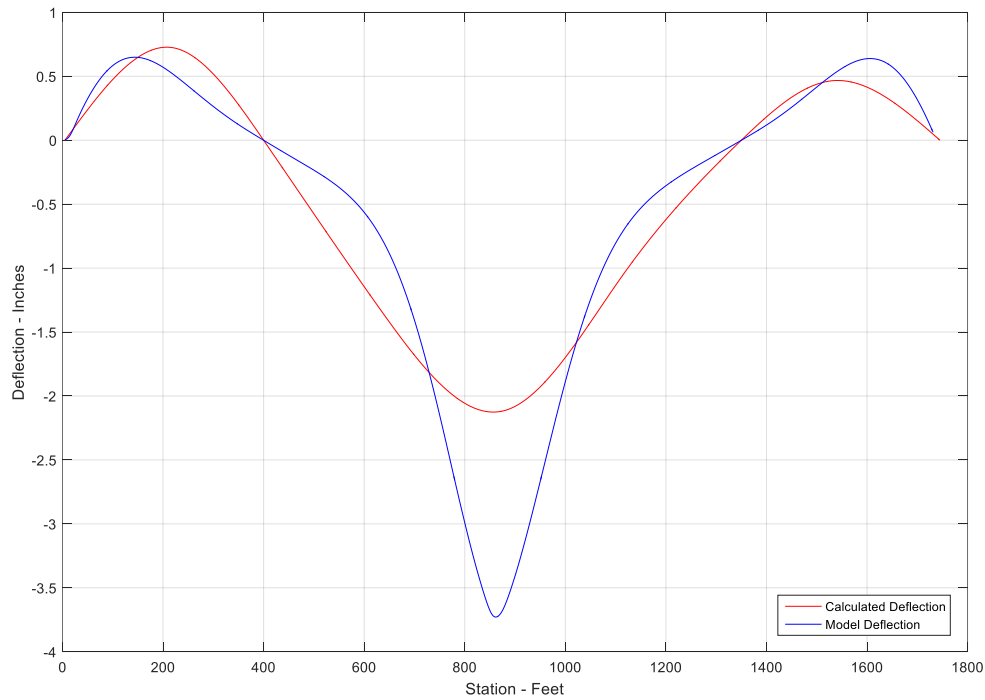


Figure 41 Graphical Comparison of Load Pass 0_1 Calculated Deflections and FEA Model Deflections

From the comparison plot in Figure 41, it can be seen that the calculated deflection values and the FEA model deflection values, in general, differ the greatest in the mainspan section of the bridge. The shapes of the deflection profiles compare well with each other, with the main shape difference again occurring in the mainspan section. While the difference in the midspan deflection values seems significantly large, with a calculated deflection value of -2.12 inches and a FEA model deflection value of -3.66 inches, it is important to note that the FEA model does not serve as the optimum comparison tool. Since the FEA model was created with some assumptions and simplifications, which were discussed in Chapter 3, the model does not provide the most accurate deflection values. A more accurate way to compare the calculated

deflection values is through the survey deflection values, which are discussed in the following section.

9.1.1.2 Comparison to Survey

As described in Chapter 5, a survey crew was brought out during the May 2016 Load Test. Survey measurements taken by the survey crew provided accurate and reliable deflections for the bridge, which could be used to validate the deflections that were calculated using the SHM system rotation data. The calculated deflections from the automated Matlab code for Load Pass 0_1 were compared to survey deflections. Similar to the FEA model comparison, the deflection results are compared using a percent error. The calculated deflection values, survey deflection values, and the error between them are shown in Table 10.

Table 10 Comparison of Load Pass 0_1 Calculated Deflections with Survey Deflections

Tilt Meter	Station (Feet)	Calculated Deflection (Inches)	Survey Deflection (Inches)	Percent Error (%)
T_E1	5	0	0	0
T_E2	217	0.719	0.360	99.7
T_E3	400	0	-	-
T_E4	632	-1.30	-0.720	80.6
T_E5	877	-2.12	-3.36	-36.9
T_E6	1117	-1.10	-0.840	31.0
T_E7	1350	0	-	-
T_E8	1532	0.448	0.600	-25.3
T_E9	1745	0	0.120	-100

It is evident from the error values presented in Table 10 that the deflection results from the automated Matlab code for Load Pass 0_1 differ significantly from

survey deflection values. The error values between the calculated deflections and survey deflections range from approximately 25% to 100%. At the midspan critical location, the error between the calculated deflection and survey deflection is approximately 37%.

In order to visually compare the deflections, the calculated deflection values from Load Pass 0_1 and survey deflection values are compared graphically. The plot of the deflection comparison is shown in Figure 42. The red line represents the Load Pass 0_1 calculated deflection values and the blue asterisks represent survey deflection values.

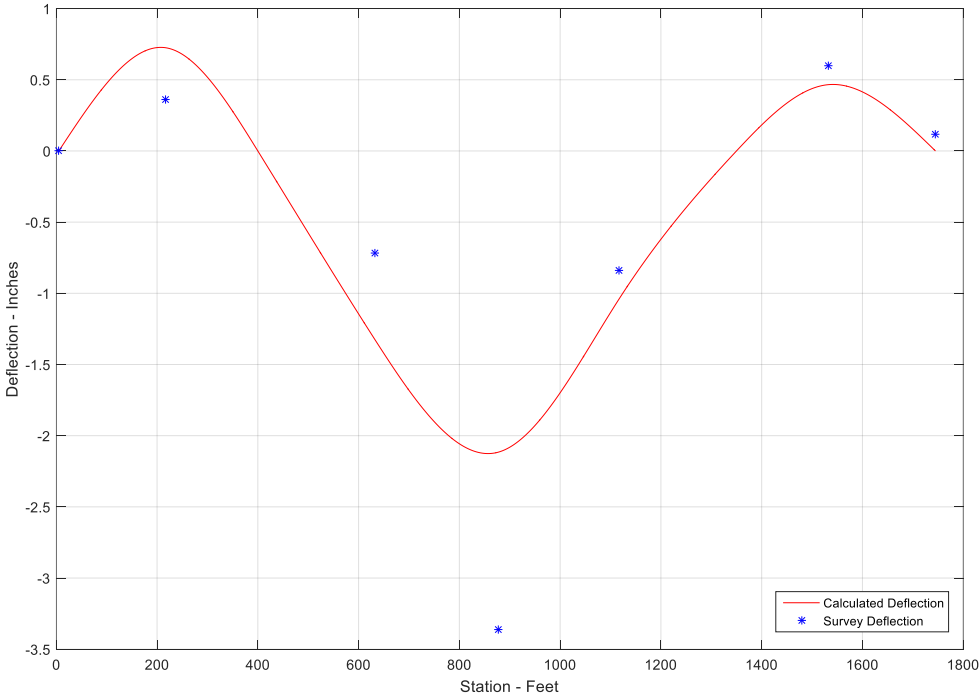


Figure 42 Graphical Comparison of Load Pass 0_1 Calculated Deflections and Survey Deflections

From the comparison plot shown in Figure 42, it can be seen that the calculated deflection values and survey deflection values, in general, differ the greatest in the beginning half of the bridge, from 0 to 877 ft along the bridge. The locations of the peaks in the calculated deflection profile compare well with the locations of the peak survey deflections. Focusing on the midspan peak deflection, the difference in the deflection values is significant, with a calculated deflection value of -2.12 inches and survey deflection value of -3.36 inches. Although this deflection difference is still rather large, this deflection difference is less than the deflection difference experienced when comparing the calculated midspan deflection to the FEA model midspan deflection.

9.1.2 Load Pass 0_2

The final results from Load Pass 0_2 consisted of rotation and deflection profiles from the midspan critical loading scenario, with the trucks positioned above tilt meter T_E5. The deflection values from the midspan loading scenario for Load Pass 0_2, which were calculated using the automated Matlab code, are compared to both the FEA model deflection values and survey deflection values in the following two sections.

9.1.2.1 Comparison to FEA Model

Similar to Load Pass 0_1, the calculated deflection results from the automated Matlab code for Load Pass 0_2 were compared to the FEA model deflection results, using a percent error approach. The Load Pass 0_2 calculated deflection values, the model deflection values, and the error between them are shown in Table 11.

Table 11 Comparison of Load Pass 0_2 Calculated Deflections with FEA Model Deflections

Tilt Meter	Station (Feet)	Calculated Deflection (Inches)	Model Deflection (Inches)	Percent Error (%)
T_E1	5	0	0	0
T_E2	217	0.667	0.525	27.0
T_E3	400	0	0	0
T_E4	632	-1.33	-0.750	77.3
T_E5	877	-2.25	-3.66	-38.5
T_E6	1117	-1.28	-0.696	83.9
T_E7	1350	0	0	0
T_E8	1532	0.556	0.513	8.38
T_E9	1745	0	0	0

From the error values presented in Table 11, it is evident that the deflection results from the automated Matlab code for Load Pass 0_2 differ significantly from the FEA model deflection values. The error values between the calculated deflections and the FEA model deflections range from approximately 8% to 84% at the nonzero deflection locations. At the midspan critical location, the error between the calculated deflection and the FEA model deflection is approximately 39%.

For a visual comparison, the calculated deflection values from Load Pass 0_2 and the FEA model deflections are also compared graphically. The plot of the deflection comparison is shown in Figure 43, with the red line representing the Load Pass 0_2 calculated deflection values and the blue line representing the FEA model deflection values.

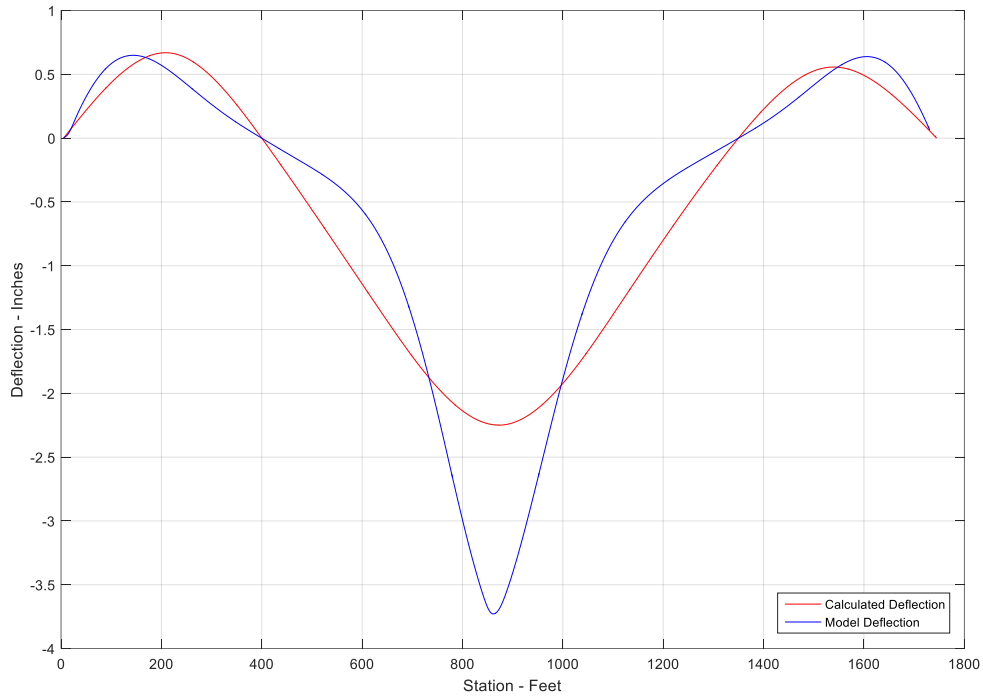


Figure 43 Graphical Comparison of Load Pass 0_2 Calculated Deflections and FEA Model Deflections

Similar to Load Pass 0_1, it can be seen that the calculated deflection values and the FEA model deflection values, in general, differ the greatest in the mainspan section of the bridge. The shapes of the deflection profiles compare well with each other, with the main shape difference again occurring in the mainspan section. The difference in the peak midspan deflection values seems significantly large, with a calculated deflection value of -2.25 inches and a FEA model deflection value of -3.66 inches. However, the calculated deflections will be compared to the survey deflections in the following section, in order to get a more accurate comparison.

9.1.2.2 Comparison to Survey

Similar to Load Pass 0_1, the calculated deflections from the automated Matlab code for Load Pass 0_2 were compared to survey deflections, using a percent error approach. The calculated deflection values, survey deflection values, and the error between them are shown in Table 12.

Table 12 Comparison of Load Pass 0_2 Calculated Deflections with Survey Deflections

Tilt Meter	Station (Feet)	Calculated Deflection (Inches)	Survey Deflection (Inches)	Percent Error (%)
T_E1	5	0	0	0
T_E2	217	0.667	0.360	85.3
T_E3	400	0	-	-
T_E4	632	-1.33	-0.720	84.7
T_E5	877	-2.25	-3.36	-33.0
T_E6	1117	-1.28	-0.840	52.4
T_E7	1350	0	-	-
T_E8	1532	0.556	0.600	-7.33
T_E9	1745	0	0.120	-100

From the error values presented in Table 12, it is evident that the deflection results from the automated Matlab code for Load Pass 0_2 differ considerably from survey deflection values. The error values between the calculated deflections and survey deflections range from approximately 7% to 100%. At the midspan critical location, the error between the calculated deflection and survey deflection is approximately 33%.

In order to visually compare the deflections, the calculated deflection values from Load Pass 0_2 and survey deflection values are compared graphically. The plot of the deflection comparison is shown in Figure 44. The red line represents the Load

Pass 0_2 calculated deflection values and the blue asterisks represent survey deflection values.

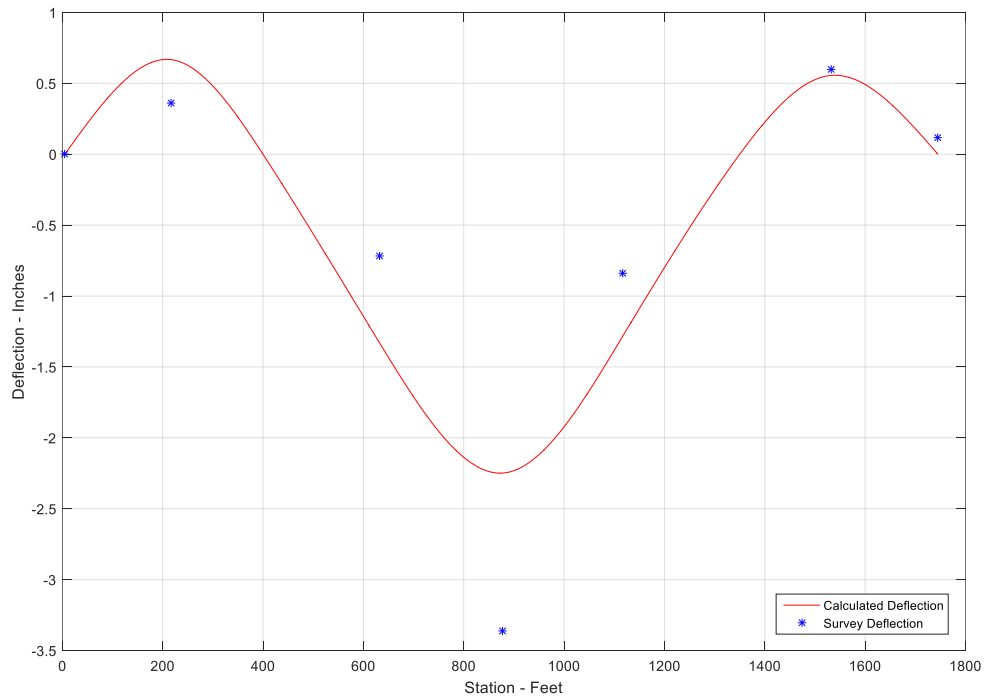


Figure 44 Graphical Comparison of Load Pass 0_2 Calculated Deflections and Survey Deflections

From the comparison plot shown in Figure 44, it can be seen that the calculated deflection values and survey deflection values, in general, differ the greatest in the mainspan section of the bridge. The locations of the peaks in the calculated deflection profile compare well with the locations of the peak survey deflections. Focusing on the midspan peak deflection, the difference in the deflection values is significant, with a calculated deflection value of -2.25 inches and survey deflection value of -3.36 inches. Although this deflection difference is still rather large, this deflection

difference is less than the deflection difference experienced when comparing the Load Pass 0_1 calculated midspan deflection to the survey midspan deflection.

9.1.3 Comparison of Final Results

In order to better visualize the accuracy of the calculated deflection results, the calculated deflection results for Load Pass 0_1 and Load Pass 0_2 are compared to both survey deflection values and the FEA model deflection results in Figure 45. The red solid line represents the calculated Load Pass 0_1 deflections, the blue solid line represents the calculated Load Pass 0_2 deflections, the black asterisks represent survey deflection values, and the solid green line represents the FEA model deflections.

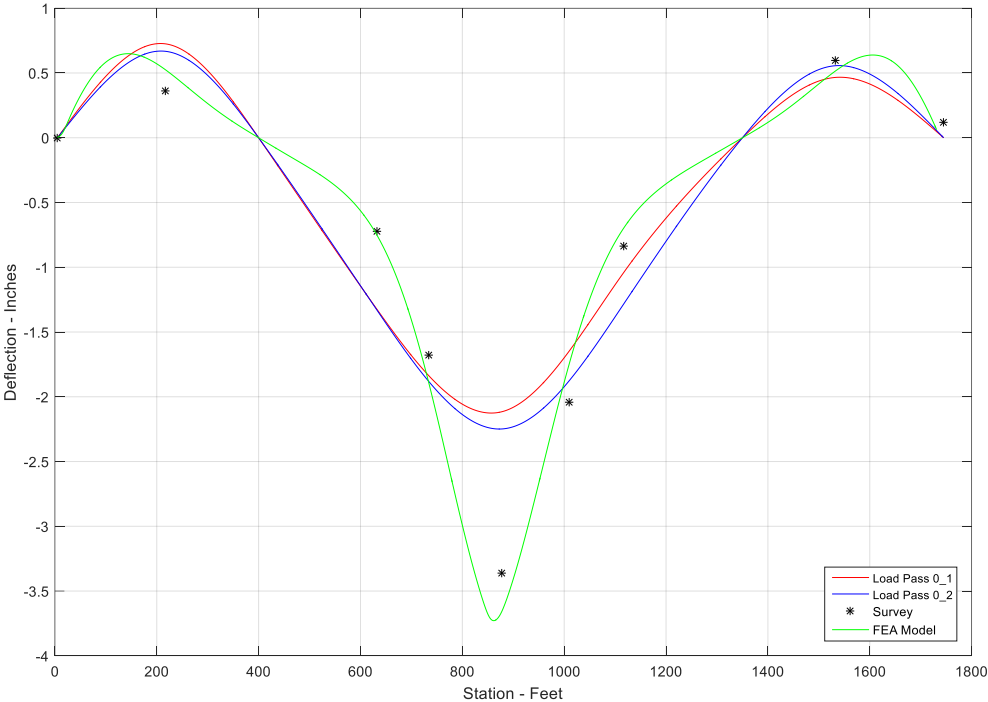


Figure 45 Comparison of Calculated Load Pass 0_1, Calculated Load Pass 0_2, Survey, and FEA Model Deflections

It can be seen from the comparison in Figure 45 that the Load Pass 0_1 and Load Pass 0_2 deflection results compare well with each other. However, the calculated Load Pass 0_1 and Load Pass 0_2 results differ significantly from survey deflection values and the FEA model deflection results, specifically in the mainspan section of the bridge. To numerically compare the deflection results, the deflection values at each tilt meter location are presented in Table 13.

Table 13 Comparison of Calculated Load Pass 0_1, Calculated Load Pass 0_2, Survey, and FEA Model Deflections

Tilt Meter	Station (Feet)	Deflection (Inches)			
		Calculated Load Pass 0_1	Calculated Load Pass 0_2	Survey	FEA Model
T_E1	5	0	0	0	0
T_E2	217	0.719	0.667	0.360	0.525
T_E3	400	0	0	-	0
T_E4	632	-1.30	-1.33	-0.720	-0.750
T_E5	877	-2.12	-2.25	-3.36	-3.66
T_E6	1117	-1.10	-1.28	-0.840	-0.696
T_E7	1350	0	0	-	0
T_E8	1532	0.448	0.556	0.600	0.513
T_E9	1745	0	0	0.120	0

From the tabulated deflection values shown in Table 13, it can be seen that the calculated Load Pass 0_1 and calculated Load Pass 0_2 midspan deflection values are significantly smaller than the survey midspan deflection, whereas the FEA model midspan deflection is considerably larger than the survey midspan deflection. Therefore, it is evident that the automated Matlab code underestimates the midspan deflection, given the current number and placement of the permanent tilt meters. On the other hand, it is evident that the FEA model overestimates the midspan deflection.

9.2 Surface Mounted Tilt Meters for Load Test Data

Similar to the automated Matlab code results, the final results from the surface mounted tilt meters, which were presented in Chapter 8, were used to analyze the accuracy of the calculated deflections. As mentioned previously, the validity of the methodology used to calculate deflections from SHM system data is confirmed by analyzing the accuracy of the calculated deflections. The calculated deflections for Load Pass 0_1 and Load Pass 0_2, with the surface mounted tilt meters included, are compared to both the FEA model deflections and survey deflections in the following few sections. The raw rotation data for Load Pass 0_1 and Load Pass 0_2 can be found in Appendix D.

9.2.1 Load Pass 0_1

The final results from Load Pass 0_1, with the surface mounted tilt meters included, consisted of rotation and deflection profiles at the locations of tilt meters T_E4 through T_E6, which are located on the mainspan of the bridge. While the Load Pass 0_1 final results were presented for tilt meters T_E4 through T_E6, the accuracy of the calculated deflections will only be analyzed for the T_E5 loading scenario. The midspan T_E5 loading scenario is the most critical location to monitor, and the FEA model deflections and survey deflections were only recorded for the midspan loading scenario. Therefore, only the deflection values from the midspan loading scenario for Load Pass 0_1, which were calculated including the surface mounted tilt meters, are compared to both the FEA model deflections and survey deflections in the following two sections.

9.2.1.1 Comparison to FEA Model

Similar to the results from the automated Matlab code, the results from the surface mounted tilt meters were compared to the FEA model deflection results. The calculated deflection results for Load Pass 0_1, including the surface mounted tilt meters, were compared to the FEA model deflection results using a percent error approach. The calculated deflection values, the model deflection values, and the error values are shown in Table 14.

Table 14 Comparison of Load Pass 0_1 Calculated Deflections, Including Surface Mounted Tilt Meters, with FEA Model Deflections

Tilt Meter	Station (Feet)	Calculated Deflection (Inches)	Model Deflection (Inches)	Percent Error (%)
T_E1	5	0	0	0
T_E2	217	0.719	0.525	37.0
T_E3	400	0	0	0
T_E4	632	-0.859	-0.750	14.5
SM_1	734	-1.81	-1.89	-4.23
T_E5	877	-2.82	-3.66	-23.0
SM_2	1010	-1.66	-1.74	-4.60
T_E6	1117	-0.507	-0.696	-27.2
T_E7	1350	0	0	0
T_E8	1532	0.448	0.513	-12.7
T_E9	1745	0	0	0

From the error values presented in Table 14, it is evident that the deflection results from the SHM system and surface mounted tilt meters for Load Pass 0_1 differ much less from the FEA model deflection values than the original automated Matlab code results. The error values between the calculated deflections and the FEA model deflections range from approximately 4% to 37% at the nonzero deflection locations.

At the midspan critical location, the error between the calculated deflection and the FEA model deflection is approximately 23%.

In order to better visualize the comparison, the calculated deflection values from Load Pass 0_1, with the surface mounted tilt meters included, and the FEA model deflections are also compared graphically. The plot of the deflection comparison is shown in Figure 46. In the comparison plot, the red line represents the Load Pass 0_1 calculated deflection values and the blue line represents the FEA model deflection values.

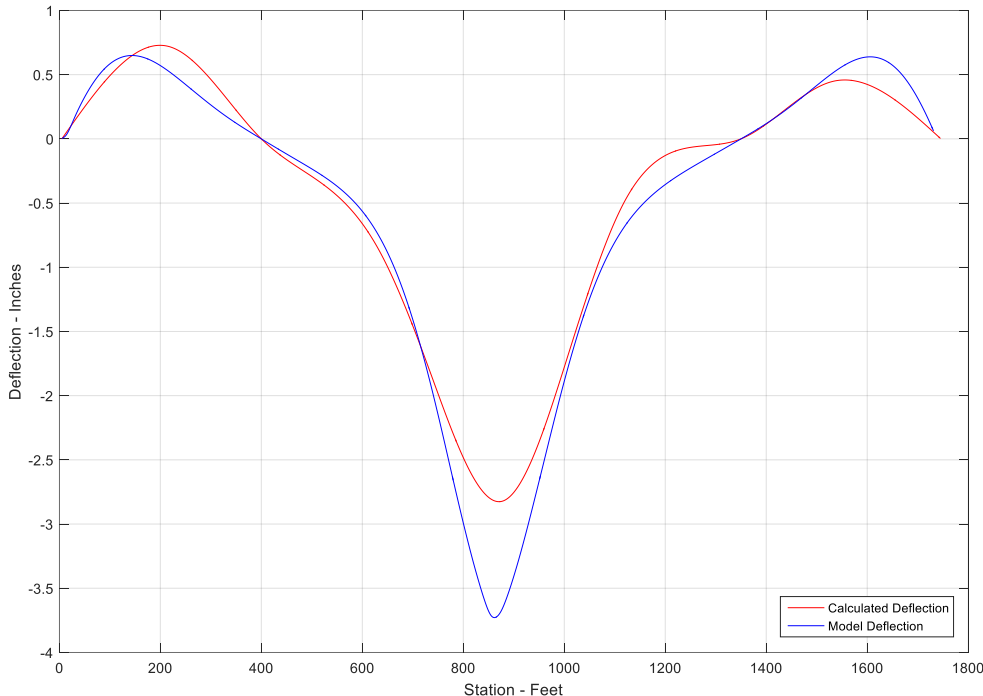


Figure 46 Graphical Comparison of Load Pass 0_1 Calculated Deflections, Including Surface Mounted Tilt Meters, and FEA Model Deflections

From the comparison plot shown in Figure 46, it can be seen that the calculated deflection values and the FEA model deflection values, in general, differ the greatest at the peaks in the deflection profiles. The shapes of the deflection profiles compare very well with each other, with the main shape differences occurring at the peaks in the deflection profiles due to the deflection magnitude differences. The difference in the peak midspan deflection values seems large, with a calculated deflection value of -2.82 inches and a FEA model deflection value of -3.66 inches. However, this deflection difference is considerably lower than the deflection difference seen when comparing the Load Pass 0_1 automated Matlab code deflection results and the FEA model deflection results.

9.2.1.2 Comparison to Survey

Similar to the results from the automated Matlab code, the calculated deflections from the SHM system and surface mounted tilt meters for Load Pass 0_1 were compared to survey deflections, using a percent error approach. The calculated deflection values, survey deflection values, and the error between them are shown in Table 15.

Table 15 Comparison of Load Pass 0_1 Calculated Deflections, Including Surface Mounted Tilt Meters, with Survey Deflections

Tilt Meter	Station (Feet)	Calculated Deflection (Inches)	Survey Deflection (Inches)	Percent Error (%)
T_E1	5	0	0	0
T_E2	217	0.719	0.360	99.7
T_E3	400	0	-	-
T_E4	632	-0.859	-0.720	19.3
SM_1	734	-1.81	-1.68	7.74
T_E5	877	-2.82	-3.36	-16.1
SM_2	1010	-1.66	-2.04	-18.6
T_E6	1117	-0.507	-0.840	-39.6
T_E7	1350	0	-	-
T_E8	1532	0.448	0.600	-25.3
T_E9	1745	0	0.120	-100

From the error values presented in Table 15, it is evident that the deflection results from the surface mounted tilt meters for Load Pass 0_1 differ considerably from survey deflection values at some points along the bridge. The error values between the calculated deflections and survey deflections range from approximately 8% to 100%. At the midspan critical location, the error between the calculated deflection and survey deflection is approximately 16%.

For a visual comparison, the calculated deflection values, including the surface mounted tilt meters, from Load Pass 0_1 and survey deflection values are compared graphically. The plot of the deflection comparison is shown in Figure 47, with the red line representing the Load Pass 0_1 calculated deflection values and the blue asterisks representing survey deflection values.

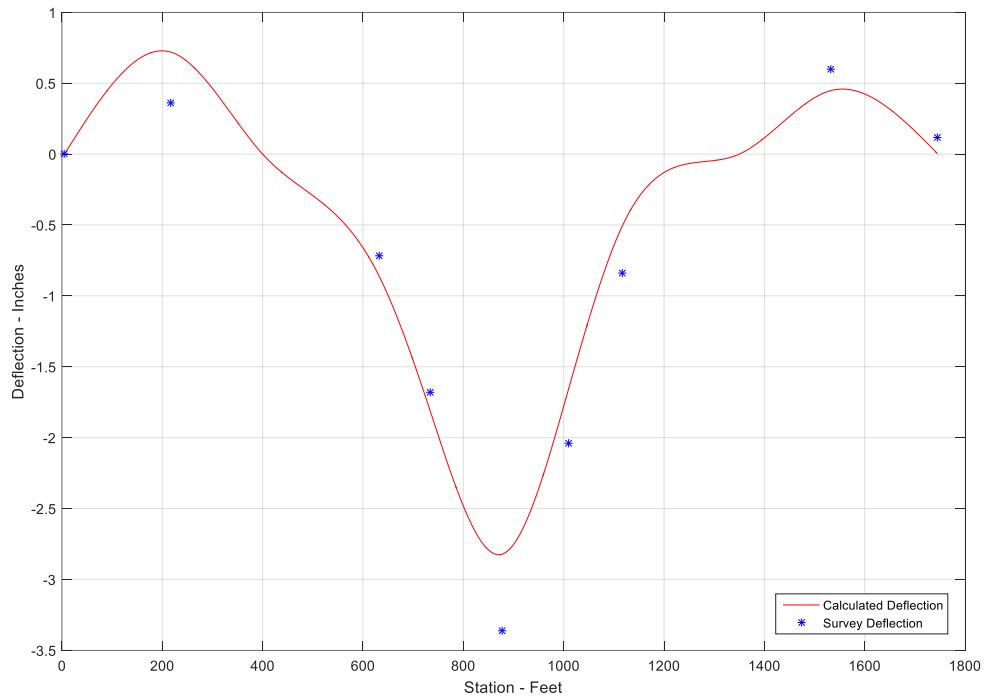


Figure 47 Graphical Comparison of Load Pass 0_1 Calculated Deflections, Including Surface Mounted Tilt Meters, and Survey Deflections

It can be seen from the comparison plot that the calculated deflection values and survey deflection values, in general, differ the greatest at the peaks in the deflection profile. Although the magnitudes of the peak deflections differ, the locations of the peaks in the calculated deflection profile compare well with the locations of the peak survey deflections. Focusing on the midspan peak deflection, the difference in the deflection values is notable, with a calculated deflection value of -2.82 inches and survey deflection value of -3.36 inches. While this deflection difference is still sizeable, similar to the automated Matlab code results, this deflection difference is less than the deflection difference experienced when comparing the calculated midspan deflection to the FEA model midspan deflection.

9.2.2 Load Pass 0_2

The final results from Load Pass 0_2, with the surface mounted tilt meters included, consisted of rotation and deflection profiles from the midspan critical loading scenario. The Load Pass 0_2 deflection values from the midspan loading scenario, with the trucks positioned above tilt meter T_E5, are compared to both the FEA model deflection values and survey deflection values in the following two sections.

9.2.2.1 Comparison to FEA Model

Similar to Load Pass 0_1, the calculated deflection results from the SHM system and surface mounted tilt meters for Load Pass 0_2 were compared to the FEA model deflection results. The comparison was done using a percent error approach. The Load Pass 0_2 calculated deflection values, the model deflection values, and the error between them are shown in Table 16.

Table 16 Comparison of Load Pass 0_2 Calculated Deflections, Including Surface Mounted Tilt Meters, with FEA Model Deflections

Tilt Meter	Station (Feet)	Calculated Deflection (Inches)	Model Deflection (Inches)	Percent Error (%)
T_E1	5	0	0	0
T_E2	217	0.614	0.525	17.0
T_E3	400	0	0	0
T_E4	632	-0.583	-0.750	-22.3
SM_1	734	-1.66	-1.89	-12.2
T_E5	877	-2.88	-3.66	-21.3
SM_2	1010	-1.79	-1.74	2.87
T_E6	1117	-0.681	-0.696	-2.16
T_E7	1350	0	0	0
T_E8	1532	0.466	0.513	-9.16
T_E9	1745	0	0	0

It is evident from the error values, presented in Table 16, that the deflection results from the SHM system and surface mounted tilt meters for Load Pass 0_2 differ much less from the FEA model deflection values than the original automated Matlab code results. The error values between the calculated deflections and the FEA model deflections range from approximately 2% to 22% at the nonzero deflection locations. At the midspan critical location, the error between the calculated deflection and the FEA model deflection is approximately 21%.

In order to better visualize the comparison, the calculated deflection values from Load Pass 0_2, with the surface mounted tilt meters included, and the FEA model deflections are also compared graphically. The plot of the deflection comparison is shown in Figure 48. In the comparison plot, the red line represents the Load Pass 0_2 calculated deflection values and the blue line represents the FEA model deflection values.

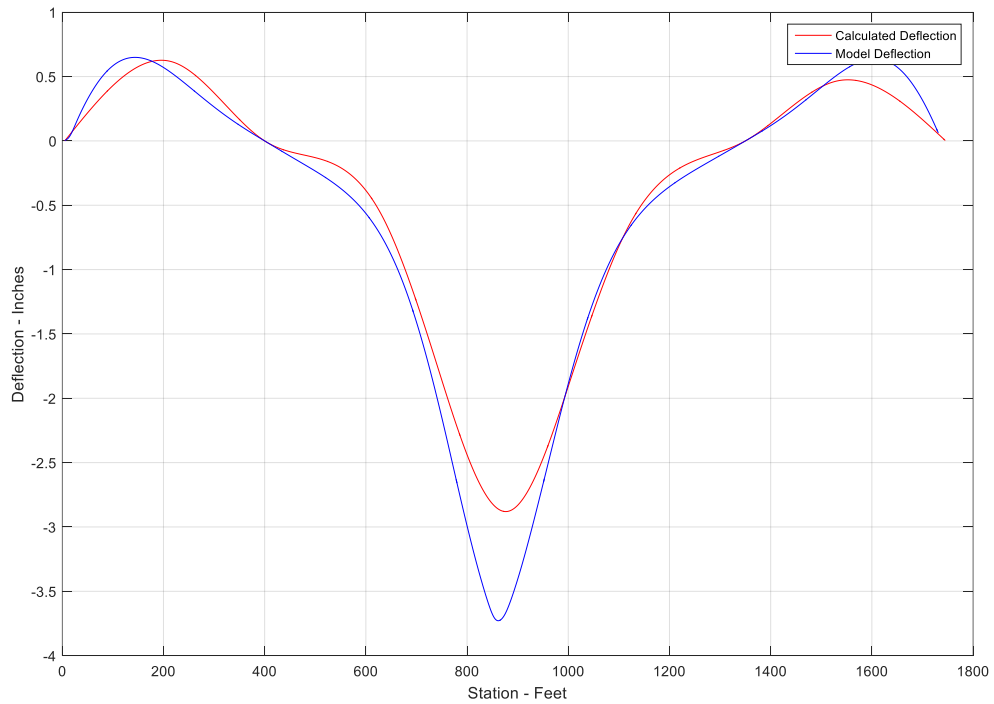


Figure 48 Graphical Comparison of Load Pass 0_2 Calculated Deflections, Including Surface Mounted Tilt Meters, and FEA Model Deflections

From the comparison plot shown in Figure 48, it can be seen that the calculated deflection values and the FEA model deflection values, in general, differ the greatest near the midspan location of the bridge. The shapes of the deflection profiles compare very well with each other, with the main shape differences occurring at the peaks of the deflection profiles. There is a slight difference in the peak midspan deflection, with a calculated deflection value of -2.88 inches and a FEA model deflection value of -3.66 inches. Although this deflection difference is still evident, this deflection difference is considerably lower than the deflection difference seen when comparing the Load Pass 0_2 automated Matlab code deflection results and the FEA model deflection results.

9.2.2.2 Comparison to Survey

Similar to Load Pass 0_1, the calculated deflections from the SHM system and surface mounted tilt meters for Load Pass 0_2 were compared to survey deflections. The comparison between the calculated deflections and survey deflections was done using a percent error approach. The calculated deflection values, survey deflection values, and the error between them are shown in Table 17.

Table 17 Comparison of Load Pass 0_2 Calculated Deflections, Including Surface Mounted Tilt Meters, with Survey Deflections

Tilt Meter	Station (Feet)	Calculated Deflection (Inches)	Survey Deflection (Inches)	Percent Error (%)
T_E1	5	0	0	0
T_E2	217	0.614	0.360	70.6
T_E3	400	0	-	-
T_E4	632	-0.583	-0.720	-19.0
SM_1	734	-1.66	-1.68	-1.19
T_E5	877	-2.88	-3.36	-14.3
SM_2	1010	-1.79	-2.04	-12.3
T_E6	1117	-0.681	-0.840	-18.9
T_E7	1350	0	-	-
T_E8	1532	0.466	0.600	-22.3
T_E9	1745	0	0.120	-100

From the error values presented in Table 17, it is evident that the deflection results from the surface mounted tilt meters for Load Pass 0_2 differ considerably from survey deflection values at numerous points along the bridge. The error values between the calculated deflections and survey deflections range from approximately 1% to 100%. At the midspan critical location, the error between the calculated deflection and survey deflection is approximately 14%.

For a visual comparison, the calculated deflection values, including the surface mounted tilt meters, from Load Pass 0_2 and survey deflection values are compared graphically. The plot of the deflection comparison is shown in Figure 49, with the red line representing the Load Pass 0_2 calculated deflection values and the blue asterisks representing survey deflection values.

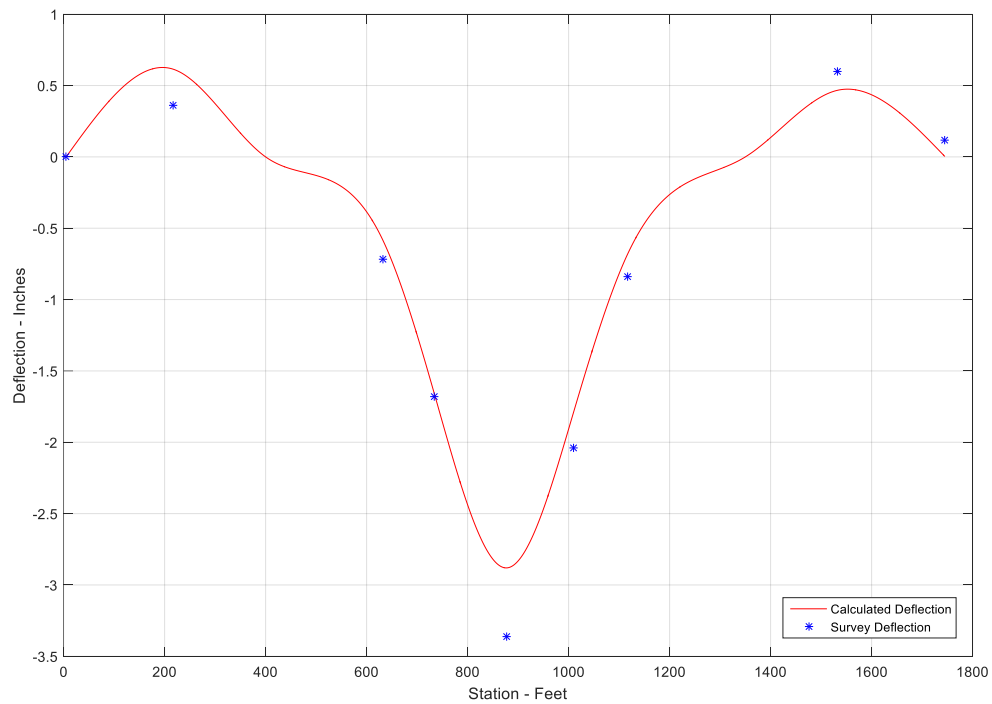


Figure 49 Graphical Comparison of Load Pass 0_2 Calculated Deflections, Including Surface Mounted Tilt Meters, and Survey Deflections

It can be seen from the comparison plot, shown in Figure 49, that the calculated deflection values and survey deflection values differ slightly at various points along the bridge. Although the magnitudes of the peak deflections differ, the locations of the peaks in the calculated deflection profile compare well with the

locations of the peak survey deflections. Focusing on the midspan peak deflection, the difference in the deflection values is minor, with a calculated deflection value of -2.88 inches and survey deflection value of -3.36 inches. This deflection difference is the smallest deflection difference of all of the comparisons and load passes that were analyzed, indicating that integrating two surface mounted tilt meters to the SHM system would provide the most accurate rotation data and deflection results. A midspan deflection difference, determined by comparing the calculated deflection and survey deflection, of only 14% proves that the methodology used to calculate deflections from SHM system rotation data is valid as a preliminary method.

9.2.3 Comparison of Final Results

In order to better visualize the accuracy of the calculated deflection results, the calculated deflection results for Load Pass 0_1 and Load Pass 0_2, including the surface mounted tilt meters, are compared to both survey deflection values and the FEA model deflection results in Figure 50. The red solid line represents the calculated Load Pass 0_1 deflections, the blue solid line represents the calculated Load Pass 0_2 deflections, the black asterisks represent survey deflection values, and the solid green line represents the FEA model deflections.

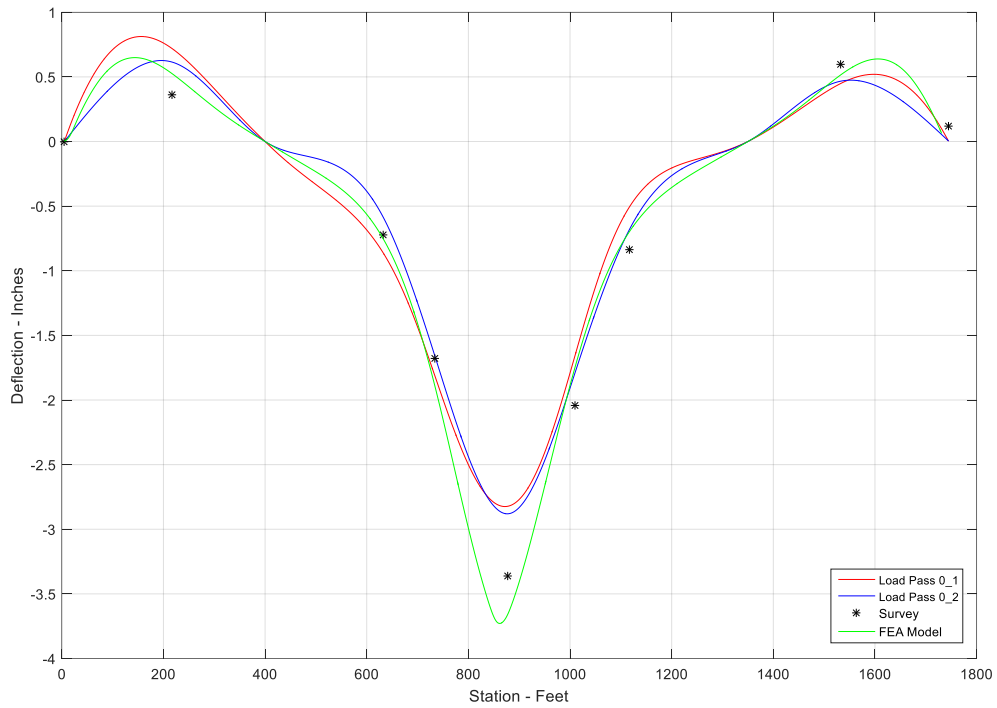


Figure 50 Comparison of Calculated Load Pass 0_1, Calculated Load Pass 0_2, Survey, and FEA Model Deflections

It can be seen from the comparison in Figure 50 that the Load Pass 0_1 and Load Pass 0_2 deflection results compare well with each other. Both the Load Pass 0_1 and Load Pass 0_2 results differ slightly from survey deflection values and the FEA model deflection results. The most significant differences in the deflection values occur in the mainspan section of the bridge. To numerically compare the deflection results, the deflection values at each tilt meter location are presented in Table 18.

Table 18 Comparison of Calculated Load Pass 0_1, Calculated Load Pass 0_2, Survey, and FEA Model Deflections

Tilt Meter	Station (Feet)	Deflection (Inches)			
		Calculated Load Pass 0_1	Calculated Load Pass 0_2	Survey	FEA Model
T_E1	5	0	0	0	0
T_E2	217	0.719	0.614	0.360	0.525
T_E3	400	0	0	-	0
T_E4	632	-0.859	-0.583	-0.720	-0.750
SM_1	734	-1.81	-1.66	-1.68	-1.89
T_E5	877	-2.82	-2.88	-3.36	-3.66
SM_2	1010	-1.66	-1.79	-2.04	-1.74
T_E6	1117	-0.507	-0.681	-0.840	-0.696
T_E7	1350	0	0	-	0
T_E8	1532	0.448	0.466	0.600	0.513
T_E9	1745	0	0	0.120	0

From the tabulated deflection values shown in Table 18, it can be seen that the calculated Load Pass 0_1 and calculated Load Pass 0_2 midspan deflection values are smaller than the survey midspan deflection, whereas the FEA model midspan deflection is larger than the survey midspan deflection. Both of the calculated load pass midspan deflections compare well with the midspan survey deflection. The Load Pass 0_2 midspan deflection is the closest calculated deflection to the survey midspan deflection, and is therefore the most accurate deflection calculated thus far. From looking at the comparisons in Table 18, it is evident that the method used to calculate deflections from rotation data underestimates the midspan deflection, given the current number and placement of tilt meters. On the other hand, it is evident that the FEA model overestimates the midspan deflection.

Chapter 10

CONCLUSIONS AND RECOMMENDATIONS

The following chapter focuses on discussing the conclusions that were drawn from this research. Some of the key final results are summarized, and the conclusions drawn from the results are introduced. The recommendations for future work are provided towards the end of the chapter.

10.1 Conclusions

The research discussed in this paper focused on using SHM system rotation data from the IRIB to compute bridge deflections. Five load tests were conducted on the IRIB; however, this research focused specifically on analyzing the rotation data from Load Test 5, which took place in May 2016. Load Test 5 differed from all previous load tests in that a survey crew was onsite during the load test, in order to measure the actual bridge deflections caused by loaded test trucks. While numerous truck configurations were used during Load Test 5, the work reported herein focuses on a six-truck side-by-side loading configuration in which the trucks were located at midspan, which results in the largest midspan deflection, and survey deflections were recorded. In terms of the Load Test 5, Load Passes 0_1 and 0_2 were the ones in which survey deflections were recorded. The collected rotation data for these passes was integrated using Matlab to obtain deflection profiles for the bridge. The accuracy of the calculated deflections was then evaluated by comparing the calculated deflections to both survey deflections and to deflections predicted by a finite element analysis. The finite element analysis utilized a 3-D CSiBridge model with beam elements.

Research has shown the importance of accounting for known displacement boundary conditions, as well as the need for a sufficient number and distribution of tilt meters, in order to properly capture the deflection profile. Having done this, the final deflection values for Load Pass 0_1 and Load Pass 0_2 were computed. Using only the system tilt meters, the Load Pass 0_1 and Load Pass 0_2 midspan deflection results differed by approximately 6%, with a Load Pass 0_1 midspan deflection of -2.12 inches and a Load Pass 0_2 midspan deflection of -2.25 inches. With the surface mounted tilt meters included, the Load Pass 0_1 and Load Pass 0_2 midspan deflection results differed by approximately 2%, with a Load Pass 0_1 midspan deflection of -2.82 inches and a Load Pass 0_2 midspan deflection of -2.88 inches. While the midspan deflection results from Load Pass 0_1 and Load Pass 0_2 are comparable in both cases, the results are not identical, which is common when replicate tests are conducted.

By comparing the calculated deflection values, using only the system tilt meters, with survey deflection values, it was concluded that additional tilt meters were needed in order to accurately capture a complete deflection profile. Focusing on the midspan deflection caused by six trucks located at midspan (which is the largest and most critical deflection to consider), the survey deflection was measured as -3.36 inches. The Load Pass 0_1 calculated midspan deflection of -2.12 inches is off from the survey midspan deflection by approximately 37%. The Load Pass 0_2 calculated midspan deflection of -2.25 inches is off from the survey midspan deflection by approximately 33%. These relatively large differences between the midspan computed deflections found by integrating the rotation data and the survey midspan deflection

value indicate that additional tilt meters are necessary to obtain more accurate deflection results.

Therefore, two surface mounted tilt meters were utilized during the May 2016 Load Test. The final deflection results from Load Pass 0_1 and Load Pass 0_2, including the surface mounted tilt meters, were computed. By comparing the calculated deflection values with survey deflection values, it was concluded that the procedure used to calculate deflections from SHM system rotation data is a viable method for computing bridge deflections. The main focus is the midspan survey deflection, caused by six trucks located at midspan, of -3.36 inches. The Load Pass 0_1 calculated midspan deflection of -2.82 inches is off from the survey midspan deflection by approximately 16%. The Load Pass 0_2 calculated midspan deflection of -2.88 inches is off from the survey midspan deflection by approximately 14%. These relatively small differences between the midspan computed deflections found by integrating the rotation data and the survey midspan deflection value indicate that the methodology has significant promise.

For reference, the FEA model deflection at the midspan location was predicted to be -3.66 inches, which is off from the survey midspan deflection by approximately 9%. This small difference indicates that FEA can be used to produce both rotations and deflections. FEA of the bridge can be useful in determining where sensors need to be located for future SHM implementations or for additional sensors on the IRIB. Generally, FEA results are used for design and are taken to be accurate values, which suggests that the level of accuracy from integrating tilt meter rotations should be accurate as well.

10.2 Recommendations for Future Work

By using the methodology that was introduced here, it is recommended that future load test rotation data be used to compute deflection profiles for the bridge. All rotation data and deflection values from future load tests can be compared to survey and FEA model data, as well as to previous load test data, to monitor the structural health of the IRIB. During future load tests, if survey is going to be conducted, data should be collected with trucks in stationary positions. However, based on looking at data from load tests with moving trucks, rotation profiles from quasi-static passes should be acceptable to use for deflection analyses.

It is also recommended that two additional tilt meters be integrated into the existing SHM system. The two surface mounted tilt meters that were used during Load Test 5 verified the benefit of having additional tilt meters. The additional tilt meters were positioned specifically for a midspan truck loading and resulting rotation profile. Other truck loadings will change the rotation profile and the locations of the peak rotations, which will ultimately change the deflection profile. While the surface mounted tilt meters can be reused for future load tests, the automated Matlab code that is used for analysis cannot account for the surface mounted tilt meters. Therefore, it is recommended to include the two tilt meters in the SHM system, so that the automated Matlab code can analyze the complete set of tilt meters together. This will result in more accurate deflections results and an easier analysis process.

Another recommendation for future work is to expand the methodology introduced through this research to analyze all SHM system rotation data, rather than solely the data collected during load tests. This will require various revisions to the Matlab code, in order to account for the countless loading scenarios that are encountered on a daily basis. Having a Matlab code that could analyze the SHM

system rotation data that is continuously collected will open the door for many other areas of analysis and research. For example, the effects of temperature change, whether it be daily fluctuations or seasonal changes, on the rotations along the IRIB could be analyzed. This could ultimately lead to valuable information and observations that have not yet been considered for the IRIB.

REFERENCES

- Al-Khateeb, H. T. (2016). *Bridge Evaluation Utilizing Structural Health Monitoring Data*.
- Ashkenazi, V., & Roberts, G. W. (1997). Experimental monitoring of the Humber Bridge using GPS. *ICE Proceedings Civil Engineering*, 120, 177–182. <https://doi.org/10.1680/icien.1997.29810>
- Google Maps. (2017). Charles W Cullen Bridge. Retrieved from <https://www.google.com/maps/place/Charles+W+Cullen+Bridge,+Delaware/@38.6095365,-75.0638358,14.9z/data=!4m5!3m4!1s0x89b8c9550626f6a1:0xa284d1ba8e6b6604!8m2!3d38.607852!4d-75.0635975>
- Hibbeler, R. C. (2012). *Structural Analysis* (8th ed.). Upper Saddle River: Pearson Prentice Hall.
- Hou, X., Yang, X., & Huang, Q. (2005). Using Inclinometers to Measure Bridge Deflection. *Journal of Bridge Engineering*, 10(5), 564–569. [https://doi.org/10.1061/\(ASCE\)1084-0702\(2005\)10:5\(564\)](https://doi.org/10.1061/(ASCE)1084-0702(2005)10:5(564))
- Marquez, P. (2013). *Load Rating of the Indian River Inlet Bridge Using a Structural Health Monitoring System*.
- Nassif, H. H., Gindy, M., & Davis, J. (2005). Comparison of laser Doppler vibrometer with contact sensors for monitoring bridge deflection and vibration. In *NDT and E International* (Vol. 38, pp. 213–218). <https://doi.org/10.1016/j.ndteint.2004.06.012>
- Roberts, G. W., Brown, C. J., Meng, X., Ogundipe, O., Atkins, C., & Colford, B. (2012). Deflection and frequency monitoring of the Forth Road Bridge, Scotland, by GPS. *Proceedings of the Institution of Civil Engineers - Bridge Engineering*, 165(2), 105–123. <https://doi.org/10.1680/bren.9.00022>
- Shenton, H., Fernandez, M., Ramanna, N., Chajes, M., & Wenczel, G. (2013). Structural Health Monitoring of a Cable-Stayed Bridge : Using Tiltmeter Data to Determine Edge Girder Deflections, (1).
- Watson, C., Watson, T., & Coleman, R. (2007). Structural monitoring of cable-stayed bridge: Analysis of GPS versus modeled deflections. *Journal of Surveying Engineering*, 133(1), 23–28. [https://doi.org/10.1061/\(ASCE\)0733-9453\(2007\)133:1\(23\)](https://doi.org/10.1061/(ASCE)0733-9453(2007)133:1(23))

Appendix A

LOAD PASS 0_1 RESULTS, INCLUDING SURFACE MOUNTED TILT METERS

A.1 Rotation and Deflection Profiles for Loading Scenarios

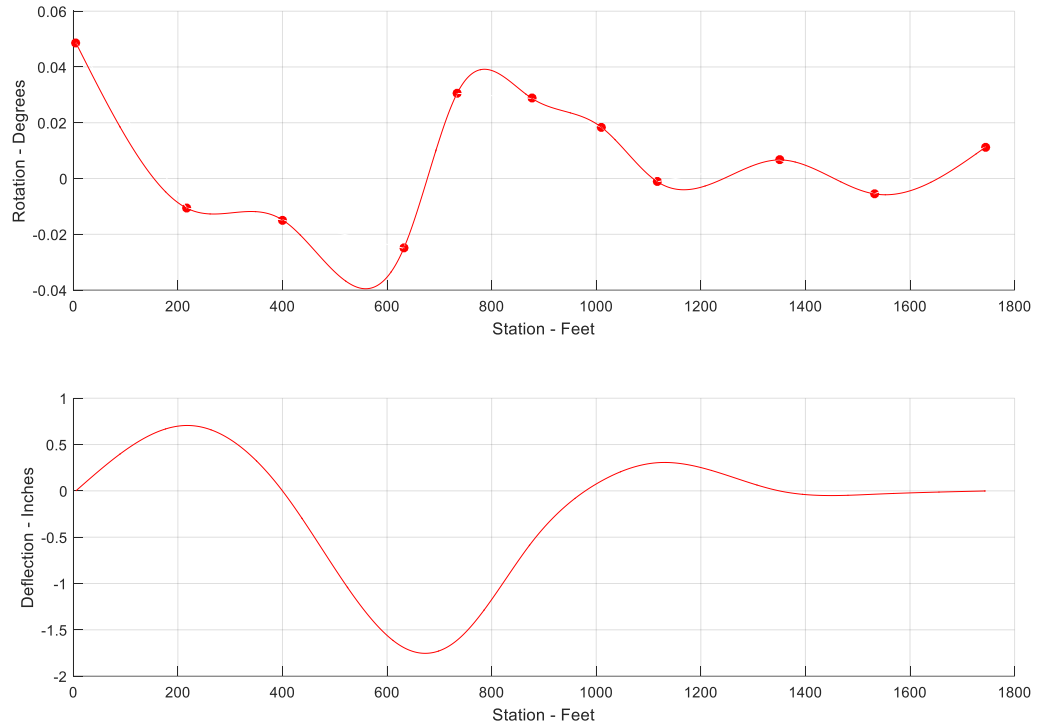


Figure A.1 Rotation and Deflection Profiles for Trucks Positioned Above Tilt Meter T_E4

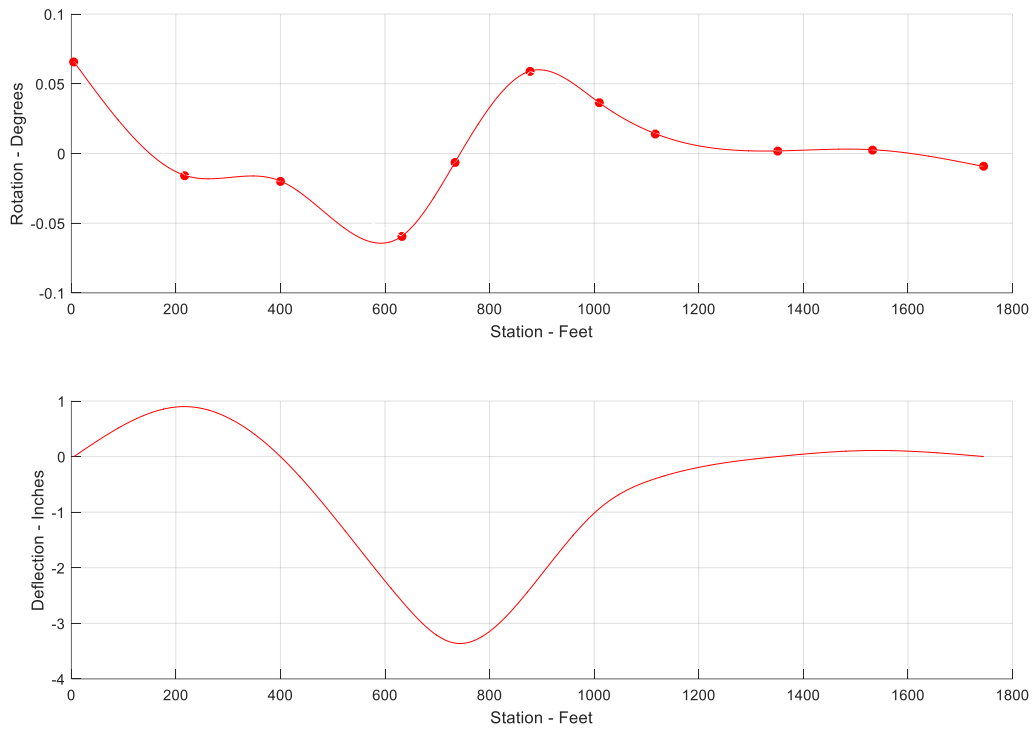


Figure A.2 Rotation and Deflection Profiles for Trucks Positioned Above Tilt Meter SM_1

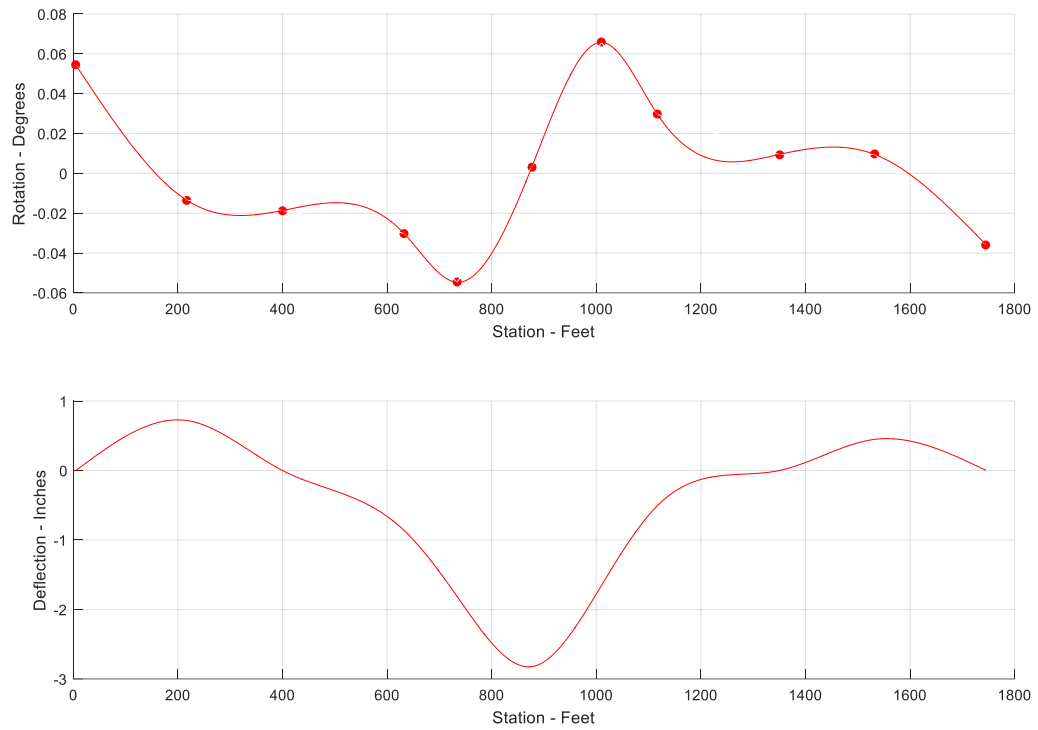


Figure A.3 Rotation and Deflection Profiles for Trucks Positioned Above Tilt Meter T_E5

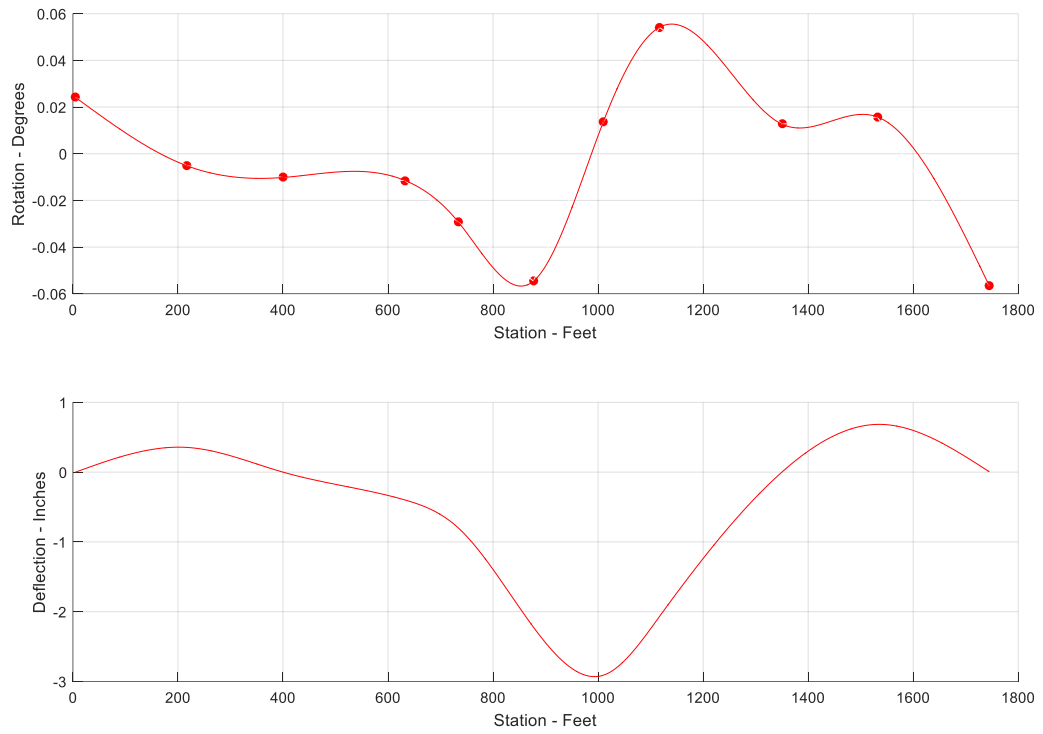


Figure A.4 Rotation and Deflection Profiles for Trucks Positioned Above Tilt Meter SM_2

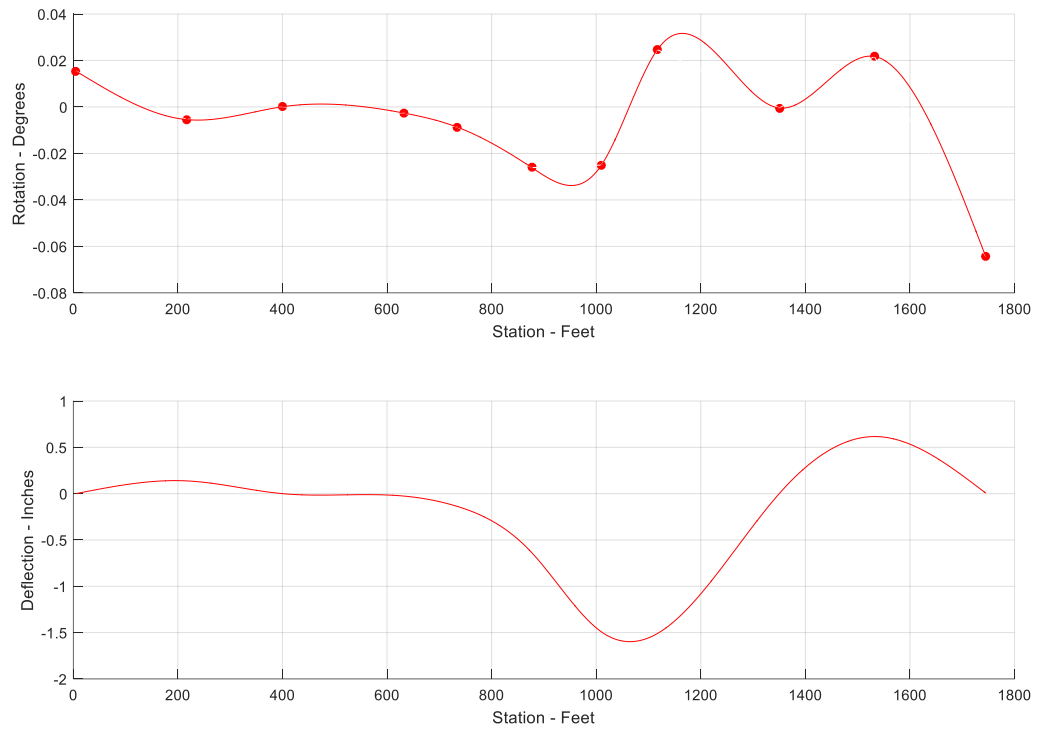
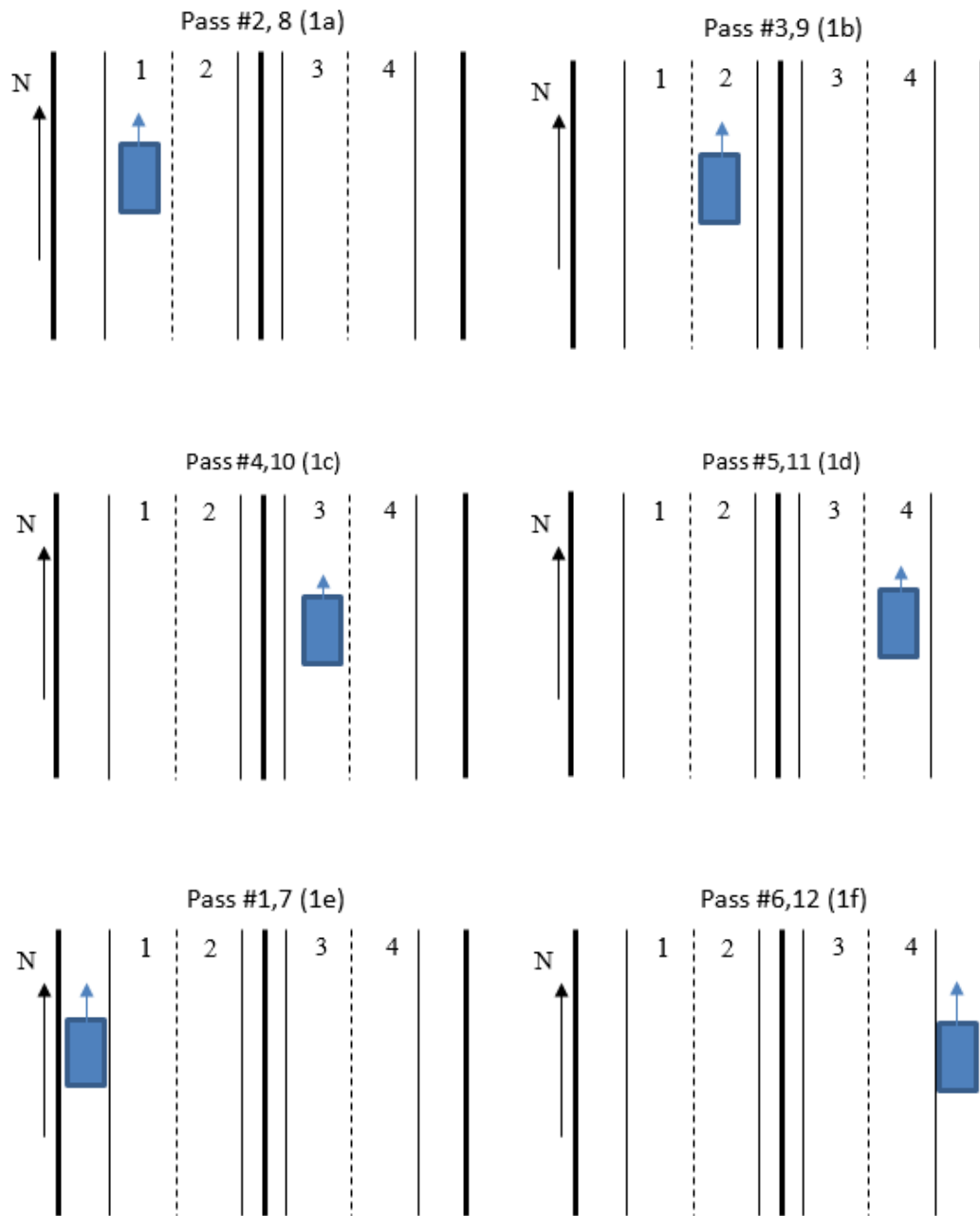


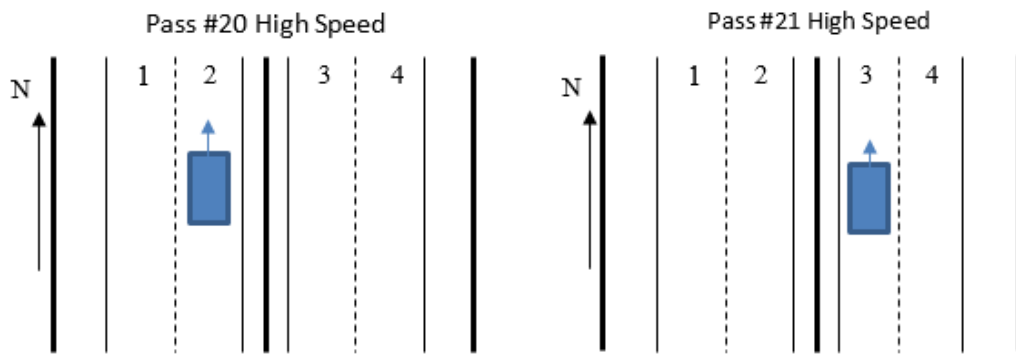
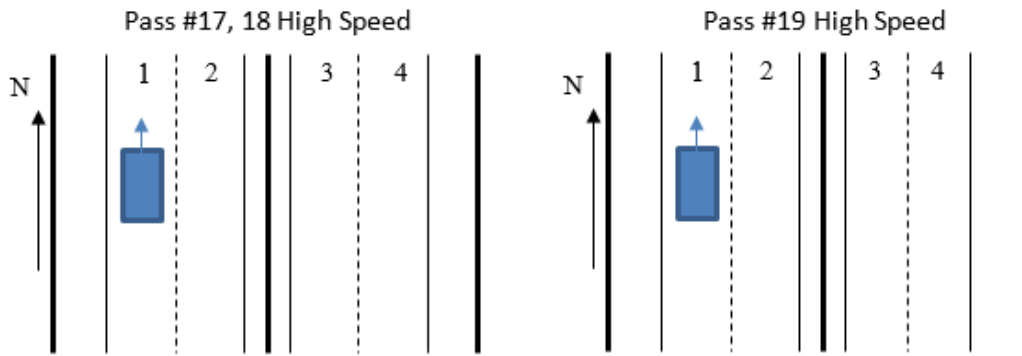
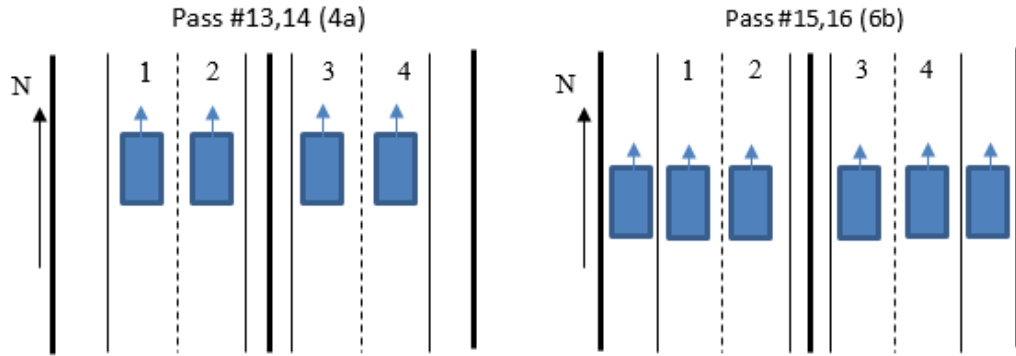
Figure A.5 Rotation and Deflection Profiles for Trucks Positioned Above Tilt Meter T_E6

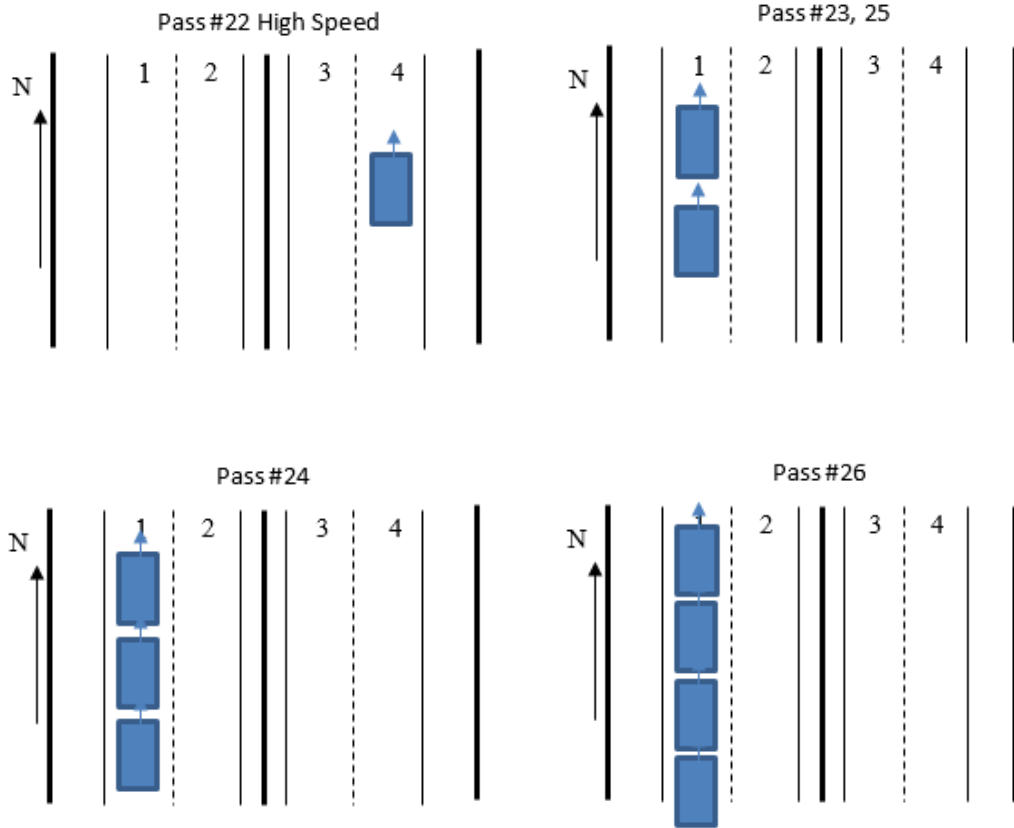
Appendix B

LOAD TEST 5 TRUCK CONFIGURATIONS

B.1 Truck Configurations and Respective Load Pass Numbers







Appendix C

AUTOMATED MATLAB CODE USED TO CALCULATE DEFLECTIONS FROM SHM SYSTEM ROTATION DATA

C.1 Matlab Code Used to Automatically Analyze Load Test Data

```
%This code is used to automatically generate the rotation and
deflection plots for selected Load Test Data files.
uiwait(msgbox('This code is used to automatically calculate the final
deflection profile of the bridge for selected Load Test data
files.', 'Purpose of the Code'));

%Before running the code, be sure to save the Text Files containing
the raw data as Excel Workbooks. Both System A and System B data must
be saved as separate Excel Workbooks.
uiwait(msgbox('Be sure to save the Text Files containing the raw data
as Excel workbooks. System A and System B data must both be saved as
separate workbooks.', 'Before Running the Code'));

%-----%

%This section of the code is used to retrieve the Excel data files
that need to be analyzed. Both System A and System B files need to be
selected. You will be prompted to select the System A Excel file
first, and then you will be prompted to select the System B Excel file.
uiwait(msgbox('First select the Excel workbook containing the System
A data.', 'System A Data Selection'));
[FileName,PathName] = uigetfile('*.xlsx','Select the System A data
Excel file');
[num,txt] = xlsread([PathName '/' FileName]);

uiwait(msgbox('Next select the Excel workbook containing the System B
data.', 'System B Data Selection'));
[FileName2,PathName2] = uigetfile('*.xlsx','Select the System B data
Excel file');
[num2,txt2] = xlsread([PathName2 '/' FileName2]);

%This section of the code is used to warn users that the results will
be less accurate if any sensors are lost for the specific data
collection that is being analyzed.
uiwait(msgbox('In the event that a sensor is lost during the time
frame of data that is being analyzed, the results for the deflection
will be less accurate. The code will still run, but keep in mind that
the results will be affected.', 'Warning','warn'));
```

%This section of the code is used to extract the timestamp, rotation, and midspan strain data from the Excel data file. The data is organized into individual matrices, which are named according to the corresponding sensor name. The remaining sensors in the system are not needed for this code.

```

headers = txt(1,:);
headers2 = txt2(1,:);

Timestamp = strmatch('Timestamp',headers);
Timestamp2 = strmatch('Timestamp',headers2);
S_E7 = strmatch('S_E7',headers);
S_E8 = strmatch('S_E8',headers);
T_E1 = strmatch('T_E1',headers2);
T_E2 = strmatch('T_E2',headers);
T_E3 = strmatch('T_E3',headers);
T_E4 = strmatch('T_E4',headers);
T_E5 = strmatch('T_E5',headers);
T_E6 = strmatch('T_E6',headers);
T_E7 = strmatch('T_E7',headers);
T_E8 = strmatch('T_E8',headers);
T_E9 = strmatch('T_E9',headers2);

Timestamp = num(:,[Timestamp]);
Timestamp2 = num2(:,[Timestamp2]);
S_E7 = num(:,[S_E7]);
S_E8 = num(:,[S_E8]);
T_E1 = num2(:,[T_E1]);
T_E2 = num(:,[T_E2]);
T_E3 = num(:,[T_E3]);
T_E4 = num(:,[T_E4]);
T_E5 = num(:,[T_E5]);
T_E6 = num(:,[T_E6]);
T_E7 = num(:,[T_E7]);
T_E8 = num(:,[T_E8]);
T_E9 = num2(:,[T_E9]);

if isempty(S_E7);
    S_E7 = nan(length(Timestamp),1);
end
if isempty(S_E8);
    S_E8 = nan(length(Timestamp),1);
end
if isempty(T_E1);
    T_E1 = nan(length(Timestamp2),1);
end
if isempty(T_E2);
    T_E2 = nan(length(Timestamp),1);
end
if isempty(T_E3);

```

```

    T_E3 = nan(length(Timestamp),1);
end
if isempty(T_E4);
    T_E4 = nan(length(Timestamp),1);
end
if isempty(T_E5);
    T_E5 = nan(length(Timestamp),1);
end
if isempty(T_E6);
    T_E6 = nan(length(Timestamp),1);
end
if isempty(T_E7);
    T_E7 = nan(length(Timestamp),1);
end
if isempty(T_E8);
    T_E8 = nan(length(Timestamp),1);
end
if isempty(T_E9);
    T_E9 = nan(length(Timestamp2),1);
end

```

%This section of the code is used to demean the data to account for any differences in the zeroing of the system. The demeaning takes place over the first 10 readings, which represent the timeframe when the trucks were off of the bridge. The steps of the demeaning process are: extracting the first 10 readings from each matrix, calculating the average of those first 10 readings for each sensor, and subtracting the averages from the corresponding matrices.

```

BeginS_E7 = S_E7(1:10,1:1);
BeginS_E8 = S_E8(1:10,1:1);
BeginT_E1 = T_E1(1:10,1:1);
BeginT_E2 = T_E2(1:10,1:1);
BeginT_E3 = T_E3(1:10,1:1);
BeginT_E4 = T_E4(1:10,1:1);
BeginT_E5 = T_E5(1:10,1:1);
BeginT_E6 = T_E6(1:10,1:1);
BeginT_E7 = T_E7(1:10,1:1);
BeginT_E8 = T_E8(1:10,1:1);
BeginT_E9 = T_E9(1:10,1:1);

AverageS_E7 = mean(BeginS_E7);
AverageS_E8 = mean(BeginS_E8);
AverageT_E1 = mean(BeginT_E1);
AverageT_E2 = mean(BeginT_E2);
AverageT_E3 = mean(BeginT_E3);
AverageT_E4 = mean(BeginT_E4);
AverageT_E5 = mean(BeginT_E5);
AverageT_E6 = mean(BeginT_E6);
AverageT_E7 = mean(BeginT_E7);
AverageT_E8 = mean(BeginT_E8);

```

```

AverageT_E9 = mean(BeginT_E9);

DemeanS_E7 = S_E7 - AverageS_E7;
DemeanS_E8 = S_E8 - AverageS_E8;
DemeanT_E1 = T_E1 - AverageT_E1;
DemeanT_E2 = T_E2 - AverageT_E2;
DemeanT_E3 = T_E3 - AverageT_E3;
DemeanT_E4 = T_E4 - AverageT_E4;
DemeanT_E5 = T_E5 - AverageT_E5;
DemeanT_E6 = T_E6 - AverageT_E6;
DemeanT_E7 = T_E7 - AverageT_E7;
DemeanT_E8 = T_E8 - AverageT_E8;
DemeanT_E9 = T_E9 - AverageT_E9;

%The section of the code is used to smooth the data in order to
eliminate any noise from the signal.
smoothS_E7 = smooth(DemeanS_E7, 5);
smoothS_E8 = smooth(DemeanS_E8, 5);
smoothT_E1 = smooth(DemeanT_E1, 5);
smoothT_E2 = smooth(DemeanT_E2, 5);
smoothT_E3 = smooth(DemeanT_E3, 5);
smoothT_E4 = smooth(DemeanT_E4, 5);
smoothT_E5 = smooth(DemeanT_E5, 5);
smoothT_E6 = smooth(DemeanT_E6, 5);
smoothT_E7 = smooth(DemeanT_E7, 5);
smoothT_E8 = smooth(DemeanT_E8, 5);
smoothT_E9 = smooth(DemeanT_E9, 5);

%The section of the code is used to plot the rotation graph for each
tilt sensor. These graphs serve as a visual check that everything is
working properly.
subplot(3, 3, 1)
plot(Timestamp2, smoothT_E1, 'b-');
% Label axes
xlabel 'Timestamp'
ylabel 'Rotation - Degrees'
grid on

subplot(3, 3, 2)
plot(Timestamp, smoothT_E2, 'b-');
% Label axes
xlabel 'Timestamp'
ylabel 'Rotation - Degrees'
grid on

subplot(3, 3, 3)
plot(Timestamp, smoothT_E3, 'b-');

```

```

% Label axes
xlabel 'Timestamp'
ylabel 'Rotation - Degrees'
grid on

subplot(3, 3, 4)
plot(Timestamp, smoothT_E4, 'b-');
% Label axes
xlabel 'Timestamp'
ylabel 'Rotation - Degrees'
grid on

subplot(3, 3, 5)
plot(Timestamp, smoothT_E5, 'b-');
% Label axes
xlabel 'Timestamp'
ylabel 'Rotation - Degrees'
grid on

subplot(3, 3, 6)
plot(Timestamp, smoothT_E6, 'b-');
% Label axes
xlabel 'Timestamp'
ylabel 'Rotation - Degrees'
grid on

subplot(3, 3, 7)
plot(Timestamp, smoothT_E7, 'b-');
% Label axes
xlabel 'Timestamp'
ylabel 'Rotation - Degrees'
grid on

subplot(3, 3, 8)
plot(Timestamp, smoothT_E8, 'b-');
% Label axes
xlabel 'Timestamp'
ylabel 'Rotation - Degrees'
grid on

subplot(3, 3, 9)
plot(Timestamp2, smoothT_E9, 'b-');
% Label axes
xlabel 'Timestamp'
ylabel 'Rotation - Degrees'
grid on

%This section of the code is used to find the maximum midspan strain.
Finding the maximum midspan strain helps determine the timestamp at

```

which the midspan rotation profile occurs. The midspan strain, at either S_E7 or S_E8, is maximum when the trucks are at the midspan location on the bridge.

```
[M,I] = max(smoothS_E8(:));  
if M == NaN  
    [M,I] = min(smoothS_E7(:));  
end
```

%This section of the code is used to account for the timestamp differences in System A and System B. Due to the manual start of the systems and the delays in the systems themselves, the timestamp for System A and the timestamp for System B are not exactly the same. This affects the final rotation and deflection results if not accounted for.

```
SystemDiff = Timestamp(1,1) - Timestamp2(1,1);  
FrequencyB = (Timestamp2(end,:) - Timestamp2(1,:))/size(Timestamp2,  
1);  
ShiftB = SystemDiff / FrequencyB;  
T = round(I + ShiftB);
```

%This section of the code is used to select the corresponding rotation data for all tilt sensors at the maximum strain location. This data makes up the rotation profile that will be used to calculate the deflection profile of the bridge. The rotation data is also converted from degrees to radians during this section of the code. Rotations in radians are needed in order to integrate and obtain deflections.

```
RotationDegrees1 =  
[smoothT_E1(T,1), smoothT_E2(I,1), smoothT_E3(I,1)]';  
RotationRadians1 = RotationDegrees1 * (pi/180);  
RotationDegrees2 =  
[smoothT_E3(I,1), smoothT_E4(I,1), smoothT_E5(I,1), smoothT_E6(I,1), smoo  
thT_E7(I,1)]';  
RotationRadians2 = RotationDegrees2 * (pi/180);  
RotationDegrees3 =  
[smoothT_E7(I,1), smoothT_E8(I,1), smoothT_E9(T,1)]';  
RotationRadians3 = RotationDegrees3 * (pi/180);
```

%This section of the code is used to input the location of each tilt sensor, in feet. The locations of each tilt sensor are known and should never vary, as the tilt sensors are permanently attached to the bridge.

```
TiltLocation1 = [5,217,400]';  
TiltLocation2 = [400,632,877,1117,1350]';  
TiltLocation3 = [1350,1532,1745]';
```

```

%This section of the code is used to fit a smoothing spline through
the rotation profile data for Section 1 of the bridge. The data used
for the smoothing spline are the TiltLocation1 as the X Input and the
RotationDegrees1 as the Y Input. The smoothing parameter is set to
0.4 to ensure that the goodness of fit reaches 1.0.
%% Fit: 'Fitted Curve'.
[xData, yData] = prepareCurveData( TiltLocation1, RotationDegrees1 );

% Set up fittype and options.
ft = fittype( 'smoothingspline' );
opts = fitoptions( 'Method', 'SmoothingSpline' );
opts.SmoothingParam = 0.4;

% Fit model to data.
[fitresult, gof] = fit( xData, yData, ft, opts );

% Plot fit with data.
figure('visible','off', 'Name', 'Rotation Plot - Section 1' );
h = plot( fitresult, xData, yData );
legend( h, 'RotationDegrees1 vs. TiltLocation1', 'Fitted Curve',
'Location', 'NorthEast' );
% Label axes
xlabel 'Station - Feet'
ylabel 'Rotation - Degrees'
grid on
savefig('Rotation Plot - Section 1')

%This section of the code is used to integrate the rotation profile
of the bridge for Section 1, in order to obtain the deflection
profile for Section 1. A smoothing spline was again fit through the
rotation profile data. However, the data used for the smoothing
spline this time are the TiltLocation1 as the X Input and the
RotationRadians1 as the Y Input. The smoothing parameter is again set
to 0.4.
%% Fit: 'Fitted Curve'.
[xData, yData] = prepareCurveData( TiltLocation1, RotationRadians1 );

% Set up fittype and options.
ft2 = fittype( 'smoothingspline' );
opts2 = fitoptions( 'Method', 'SmoothingSpline' );
opts2.SmoothingParam = 0.4;

% Fit model to data.
[fitresult2, gof2] = fit( xData, yData*12, ft2, opts2 );

```

```

figure('visible','off', 'Name', 'Deflection Plot - Section 1' );
plot(fitresult2,xData,yData,{'integral'});
xlabel 'Station - Feet'
ylabel 'Deflection - Inches'
grid on
legend('Integration')
savefig('Deflection Plot - Section 1')

%This section of the code is used to export the data from the
Deflection Plot for Section 1, which will later be used to create the
final deflection profile plot for the bridge.
o = openfig('Deflection Plot - Section 1.fig');
F = findobj(o, 'type', 'line');
x_points1 = get(F, 'xData');
x_points1 = x_points1';
y_points1 = get(F, 'yData');
y_points1 = y_points1';

%This section of the code is used to force both ends of the
deflection profile graph for Section 1 to zero.
DeflectionDiff1 = y_points1(end,:);
TotalLength1 = x_points1(end,:) - x_points1(1,:);
RotationCorrection1 = DeflectionDiff1 / (TotalLength1 * 12);

RotationRadiansCorrected1 = RotationRadians1 - RotationCorrection1;
RotationDegreesCorrected1 = RotationRadiansCorrected1 * (180/pi());

%This section of the code is used to fit a smoothing spline through
the rotation profile data for Section 1, using the corrected data to
force the ends of the graph to zero. The data used for the smoothing
spline are the TiltLocation1 as the X Input and the
RotationDegreesCorrected1 as the Y Input. The smoothing spline
parameter is set to 0.4 to ensure that the goodness of fit reaches
1.0.
%% Fit: 'Fitted Curve'.
[xData, yData] = prepareCurveData( TiltLocation1,
RotationDegreesCorrected1 );

% Set up fitype and options.
ft3 = fitype( 'smoothingspline' );
opts3 = fitoptions( 'Method', 'SmoothingSpline' );
opts3.SmoothingParam = 0.4;

% Fit model to data.

```

```

[fitresult3, gof3] = fit( xData, yData, ft3, opts3 );

% Plot fit with data.
figure('visible','off','Name', 'Rotation and Deflection' );
subplot(2, 1, 1)
h = plot( fitresult3, xData, yData );
legend( h, 'RotationDegreesCorrected1 vs. TiltLocation1', 'Fitted
Curve', 'Location', 'NorthEast' );
% Label axes
xlabel 'Station - Feet'
ylabel 'Rotation - Degrees'
grid on

%This section of the code is used to integrate the corrected rotation
profile of the bridge for Section 1, in order to obtain the final
deflection profile for Section 1. A smoothing spline was again fit
through the rotation profile data. However, the data used for the
smoothing spline this time are the TiltLocation1 as the X Input and
the RotationRadiansCorrected1 as the Y Input. The smoothing parameter
is again set to 0.4.
%% Fit: 'Fitted Curve'.
[xData, yData] = prepareCurveData( TiltLocation1,
RotationRadiansCorrected1 );

% Set up fittype and options.
ft4 = fittype( 'smoothingspline' );
opts4 = fitoptions( 'Method', 'SmoothingSpline' );
opts4.SmoothingParam = 0.4;

% Fit model to data.
[fitresult4, gof4] = fit( xData, yData*12, ft4, opts4 );

figure('visible','off', 'Name', 'Corrected Plots - Section 1' );
subplot(2, 1, 2)
plot(fitresult4,xData,yData,{'integral'})
xlabel 'Station - Feet'
ylabel 'Deflection - Inches'
grid on
legend('Integration')
savefig('Corrected Plots - Section 1')

figure('visible','off', 'Name', 'Final Deflection - Section 1' );
plot(fitresult4,xData,yData,{'integral'});
xlabel 'Station - Feet'
ylabel 'Deflection - Inches'
grid on
legend('Integration')
savefig('Final Deflection - Section 1')

```

```

%This section of the code is used to fit a smoothing spline through
the rotation profile data for Section 2 of the bridge. The data used
for the smoothing spline are the TiltLocation2 as the X Input and the
RotationDegrees2 as the Y Input. The smoothing parameter is set to
0.4 to ensure that the goodness of fit reaches 1.0.
%% Fit: 'Fitted Curve'.
[xData, yData] = prepareCurveData( TiltLocation2, RotationDegrees2 );

% Set up fitype and options.
ft5 = fitype( 'smoothingspline' );
opts5 = fitoptions( 'Method', 'SmoothingSpline' );
opts5.SmoothingParam = 0.4;

% Fit model to data.
[fitresult5, gof5] = fit( xData, yData, ft5, opts5 );

% Plot fit with data.
figure('visible','off', 'Name', 'Rotation Plot - Section 2' );
h = plot( fitresult5, xData, yData );
legend( h, 'RotationDegrees2 vs. TiltLocation2', 'Fitted Curve',
'Location', 'NorthEast' );
% Label axes
xlabel 'Station - Feet'
ylabel 'Rotation - Degrees'
grid on
savefig('Rotation Plot - Section 2')

%This section of the code is used to integrate the rotation profile
of the bridge for Section 2, in order to obtain the deflection
profile for Section 2. A smoothing spline was again fit through the
rotation profile data. However, the data used for the smoothing
spline this time are the TiltLocation2 as the X Input and the
RotationRadians2 as the Y Input. The smoothing parameter is again set
to 0.4.
%% Fit: 'Fitted Curve'.
[xData, yData] = prepareCurveData( TiltLocation2, RotationRadians2 );

% Set up fitype and options.
ft6 = fitype( 'smoothingspline' );
opts6 = fitoptions( 'Method', 'SmoothingSpline' );
opts6.SmoothingParam = 0.4;

% Fit model to data.
[fitresult6, gof6] = fit( xData, yData*12, ft6, opts6 );

figure('visible','off', 'Name', 'Deflection Plot - Section 2' );

```

```

plot(fitresult6,xData,yData,{'integral'});
xlabel 'Station - Feet'
ylabel 'Deflection - Inches'
grid on
legend('Integration')
savefig('Deflection Plot - Section 2')

%This section of the code is used to export the data from the
Deflection Plot for Section 2, which will later be used to create the
final deflection profile plot for the bridge.
o = openfig('Deflection Plot - Section 2.fig');
F = findobj(o,'type','line');
x_points2 = get(F,'xData');
x_points2 = x_points2';
y_points2 = get(F,'yData');
y_points2 = y_points2';

%This section of the code is used to force both ends of the
deflection profile graph for Section 2 to zero.
DeflectionDiff2 = y_points2(end,:);
TotalLength2 = x_points2(end,:) - x_points2(1,:);
RotationCorrection2 = DeflectionDiff2 / (TotalLength2 * 12);

RotationRadiansCorrected2 = RotationRadians2 - RotationCorrection2;
RotationDegreesCorrected2 = RotationRadiansCorrected2 * (180/pi());

%This section of the code is used to fit a smoothing spline through
the rotation profile data for Section 2, using the corrected data to
force the ends of the graph to zero. The data used for the smoothing
spline are the TiltLocation2 as the X Input and the
RotationDegreesCorrected2 as the Y Input. The smoothing spline
parameter is set to 0.4 to ensure that the goodness of fit reaches
1.0.
%% Fit: 'Fitted Curve'.
[xData, yData] = prepareCurveData( TiltLocation2,
RotationDegreesCorrected2 );

% Set up fittype and options.
ft7 = fittype( 'smoothingspline' );
opts7 = fitoptions( 'Method', 'SmoothingSpline' );
opts7.SmoothingParam = 0.4;

% Fit model to data.
[fitresult7, gof7] = fit( xData, yData, ft7, opts7 );

```

```

% Plot fit with data.
figure('visible','off','Name', 'Rotation and Deflection' );
subplot(2, 1, 1)
h = plot( fitresult7, xData, yData );
legend( h, 'RotationDegreesCorrected2 vs. TiltLocation2', 'Fitted
Curve', 'Location', 'NorthEast' );
% Label axes
xlabel 'Station - Feet'
ylabel 'Rotation - Degrees'
grid on

%This section of the code is used to integrate the corrected rotation
profile of the bridge for Section 2, in order to obtain the final
deflection profile for Section 2. A smoothing spline was again fit
through the rotation profile data. However, the data used for the
smoothing spline this time are the TiltLocation2 as the X Input and
the RotationRadiansCorrected2 as the Y Input. The smoothing parameter
is again set to 0.4.
%% Fit: 'Fitted Curve'.
[xData, yData] = prepareCurveData( TiltLocation2,
RotationRadiansCorrected2 );

% Set up fittype and options.
ft8 = fittype( 'smoothingspline' );
opts8 = fitoptions( 'Method', 'SmoothingSpline' );
opts8.SmoothingParam = 0.4;

% Fit model to data.
[fitresult8, gof8] = fit( xData, yData*12, ft8, opts8 );

figure('visible','off', 'Name', 'Corrected Plots - Section 2' );
subplot(2, 1, 2)
plot(fitresult8,xData,yData,{'integral'})
xlabel 'Station - Feet'
ylabel 'Deflection - Inches'
grid on
legend('Integration')
savefig('Corrected Plots - Section 2')

figure('visible','off', 'Name', 'Final Deflection - Section 2' );
plot(fitresult8,xData,yData,{'integral'});
xlabel 'Station - Feet'
ylabel 'Deflection - Inches'
grid on
legend('Integration')
savefig('Final Deflection - Section 2')

```

```

%This section of the code is used to fit a smoothing spline through
the rotation profile data for Section 3 of the bridge. The data used
for the smoothing spline are the TiltLocation3 as the X Input and the
RotationDegrees3 as the Y Input. The smoothing parameter is set to
0.4 to ensure that the goodness of fit reaches 1.0.
%% Fit: 'Fitted Curve'.
[xData, yData] = prepareCurveData( TiltLocation3, RotationDegrees3 );

% Set up fitype and options.
ft9 = fitype( 'smoothingspline' );
opts9 = fitoptions( 'Method', 'SmoothingSpline' );
opts9.SmoothingParam = 0.4;

% Fit model to data.
[fitresult9, gof9] = fit( xData, yData, ft9, opts9 );

% Plot fit with data.
figure('visible','off', 'Name', 'Rotation Plot - Section 3' );
h = plot( fitresult9, xData, yData );
legend( h, 'RotationDegrees3 vs. TiltLocation3', 'Fitted Curve',
'Location', 'NorthEast' );
% Label axes
xlabel 'Station - Feet'
ylabel 'Rotation - Degrees'
grid on
savefig('Rotation Plot - Section 3')

%This section of the code is used to integrate the rotation profile
of the bridge for Section 3, in order to obtain the deflection
profile for Section 3. A smoothing spline was again fit through the
rotation profile data. However, the data used for the smoothing
spline this time are the TiltLocation3 as the X Input and the
RotationRadians3 as the Y Input. The smoothing parameter is again set
to 0.4.
%% Fit: 'Fitted Curve'.
[xData, yData] = prepareCurveData( TiltLocation3, RotationRadians3 );

% Set up fitype and options.
ft10 = fitype( 'smoothingspline' );
opts10 = fitoptions( 'Method', 'SmoothingSpline' );
opts10.SmoothingParam = 0.4;

% Fit model to data.
[fitresult10, gof10] = fit( xData, yData*12, ft10, opts10 );

figure('visible','off', 'Name', 'Deflection Plot - Section 3' );

```

```

plot(fitresult10,xData,yData,{'integral'});
xlabel 'Station - Feet'
ylabel 'Deflection - Inches'
grid on
legend('Integration')
savefig('Deflection Plot - Section 3')

%This section of the code is used to export the data from the
Deflection Plot for Section 3, which will later be used to create the
final deflection profile plot for the bridge.
o = openfig('Deflection Plot - Section 3.fig');
F = findobj(o,'type','line');
x_points3 = get(F,'xData');
x_points3 = x_points3';
y_points3 = get(F,'yData');
y_points3 = y_points3';

%This section of the code is used to force both ends of the
deflection profile graph for Section 3 to zero.
DeflectionDiff3 = y_points3(end,:);
TotalLength3 = x_points3(end,:) - x_points3(1,:);
RotationCorrection3 = DeflectionDiff3 / (TotalLength3 * 12);

RotationRadiansCorrected3 = RotationRadians3 - RotationCorrection3;
RotationDegreesCorrected3 = RotationRadiansCorrected3 * (180/pi());

%This section of the code is used to fit a smoothing spline through
the rotation profile data for Section 3, using the corrected data to
force the ends of the graph to zero. The data used for the smoothing
spline are the TiltLocation3 as the X Input and the
RotationDegreesCorrected3 as the Y Input. The smoothing spline
parameter is set to 0.4 to ensure that the goodness of fit reaches
1.0.
%% Fit: 'Fitted Curve'.
[xData, yData] = prepareCurveData( TiltLocation3,
RotationDegreesCorrected3 );

% Set up fittype and options.
ft11 = fittype( 'smoothingspline' );
opts11 = fitoptions( 'Method', 'SmoothingSpline' );
opts11.SmoothingParam = 0.4;

% Fit model to data.
[fitresult11, gof11] = fit( xData, yData, ft11, opts11 );

```

```

% Plot fit with data.
figure('visible','off','Name', 'Rotation and Deflection' );
subplot(2, 1, 1)
h = plot( fitresult11, xData, yData );
legend( h, 'RotationDegreesCorrected3 vs. TiltLocation3', 'Fitted
Curve', 'Location', 'NorthEast' );
% Label axes
xlabel 'Station - Feet'
ylabel 'Rotation - Degrees'
grid on

%This section of the code is used to integrate the corrected rotation
profile of the bridge for Section 3, in order to obtain the final
deflection profile for Section 3. A smoothing spline was again fit
through the rotation profile data. However, the data used for the
smoothing spline this time are the TiltLocation3 as the X Input and
the RotationRadiansCorrected3 as the Y Input. The smoothing parameter
is again set to 0.4.
%% Fit: 'Fitted Curve'.
[xData, yData] = prepareCurveData( TiltLocation3,
RotationRadiansCorrected3 );

% Set up fittype and options.
ft12 = fittype( 'smoothingspline' );
opts12 = fitoptions( 'Method', 'SmoothingSpline' );
opts12.SmoothingParam = 0.4;

% Fit model to data.
[fitresult12, gof12] = fit( xData, yData*12, ft12, opts12 );

figure('visible','off', 'Name', 'Corrected Plots - Section 3' );
subplot(2, 1, 2)
plot(fitresult12,xData,yData,{'integral'})
xlabel 'Station - Feet'
ylabel 'Deflection - Inches'
grid on
legend('Integration')
savefig('Corrected Plots - Section 3')

figure('visible','off', 'Name', 'Final Deflection - Section 3' );
plot(fitresult12,xData,yData,{'integral'});
xlabel 'Station - Feet'
ylabel 'Deflection - Inches'
grid on
legend('Integration')
savefig('Final Deflection - Section 3')

```

```

% This section of the code is used to combine the Final Deflection
figures from each of the three sections of the bridge, to create the
final deflection plot. The data points are loaded from each Final
Deflection figure.
A = openfig('Final Deflection - Section 1.fig');
B = findobj(A, 'type', 'line');
x_points = get(B, 'xData');
x_points = x_points';
y_points = get(B, 'yData');
y_points = y_points';

C = openfig('Final Deflection - Section 2.fig');
D = findobj(C, 'type', 'line');
x_points2 = get(D, 'xData');
x_points2 = x_points2';
y_points2 = get(D, 'yData');
y_points2 = y_points2';

E = openfig('Final Deflection - Section 3.fig');
F = findobj(E, 'type', 'line');
x_points3 = get(F, 'xData');
x_points3 = x_points3';
y_points3 = get(F, 'yData');
y_points3 = y_points3';

xvalues = [x_points(1:end-1); x_points2(1:end-1); x_points3(1:end)];
yvalues = [y_points(1:end-1); y_points2(1:end-1); y_points3(1:end)];

figure('Name', 'Final Combined Deflection', 'visible', 'off' );
plot(xvalues, yvalues)
xlabel 'Station - Feet'
ylabel 'Deflection - Inches'
grid on
savefig('Final Deflection Plot')

%This section of the code is used to output the final deflection
values for the data. The data points are loaded from the Final
Combined Deflection figure. The specific station values needed are
then pulled from the data, and they are filtered to ensure that
multiple values do not exist for one station. The station and
deflection values are then outputted.
p = openfig('Final Deflection Plot.fig');
F = findobj(p, 'type', 'line');
x_points = get(F, 'xData');
x_points = x_points';
y_points = get(F, 'yData');
y_points = y_points';

```

```

[~, Station1] = min(abs(x_points-5));
[~, Station2] = min(abs(x_points-217));
[~, Station3] = min(abs(x_points-400));
[~, Station4] = min(abs(x_points-632));
[~, Station5] = min(abs(x_points-877));
[~, Station6] = min(abs(x_points-1117));
[~, Station7] = min(abs(x_points-1350));
[~, Station8] = min(abs(x_points-1532));
[~, Station9] = min(abs(x_points-1745));

Deflection =
[y_points(Station1),y_points(Station2),y_points(Station3),y_points(St
ation4),y_points(Station5),y_points(Station6),y_points(Station7),y_po
ints(Station8),y_points(Station9)'];

format shortG
[FinalValues] =
[TiltLocation1(1,:),Deflection(1,:);TiltLocation1(2,:),Deflection(2,:
);TiltLocation2(1,:),Deflection(3,:);TiltLocation2(2,:),Deflection(4,
:);TiltLocation2(3,:),Deflection(5,:);TiltLocation2(4,:),Deflection(6
,:);TiltLocation3(1,:),Deflection(7,:);TiltLocation3(2,:),Deflection(
8,:);TiltLocation3(3,:),Deflection(9,:)]
uiwait(msgbox('The final Tilt Location and Deflection results are
displayed in the Command Window as an output. The Tilt Location
values are presented in feet, and the Deflection values are displayed
in inches.', 'Final Results'));

%This section of the code is used to plot the final deflection
profile for the selected data. The plot also indicates the locations
of the system tilt meters, which are the locations that the
deflection values were outputted for.
TiltLocation =
[TiltLocation1(1:2,:);TiltLocation2(1:4,:);TiltLocation3(1:3,:)];

%% Fit: 'Fitted Curve'.
[xData, yData] = prepareCurveData( TiltLocation, Deflection );

% Set up fittype and options.
ft13 = fittype( 'smoothingspline' );
opts13 = fitoptions( 'Method', 'SmoothingSpline' );
opts13.SmoothingParam = 0.4;

% Fit model to data.
[fitresult13, gof13] = fit( xData, yData, ft13, opts13 );

% Plot fit with data.
figure( 'Name', 'Final Deflection Profile');
% plot(xData, yData , 'r.', 'MarkerSize',15)

```

```

% hold on
plot(fitresult13, 'r-');
legend(gca, 'off');
% Label axes
xlabel 'Station - Feet'
ylabel 'Deflection - Inches'
grid on
savefig('Final Deflection Profile')

RotationDegrees =
[RotationDegrees1(1:2,:);RotationDegrees2(1:4,:);RotationDegrees3(1:3
,:)];

%% Fit: 'Fitted Curve'.
[xData, yData] = prepareCurveData( TiltLocation, RotationDegrees );

% Set up fitype and options.
ft14 = fitype( 'smoothingspline' );
opts14 = fitoptions( 'Method', 'SmoothingSpline' );
opts14.SmoothingParam = 0.4;

% Fit model to data.
[fitresult14, gof14] = fit( xData, yData, ft14, opts14 );

% Plot fit with data.
figure( 'Name', 'Final Plots', 'visible', 'off');
h = plot( fitresult14, xData, yData, 'w');
set(h, 'DisplayName', 'Fitted Curve');
legend(gca, 'off');
% Label axes
xlabel 'Station - Feet'
ylabel 'Rotation - Degrees'
grid on
savefig('Final Combined Rotation Plot')

% Load saved figures
w=hgload('Final Combined Rotation Plot.fig');
z=hgload('Final Deflection Profile.fig');
% Prepare subplots
figure
h(1)=subplot(2,1,1);
grid on
h(2)=subplot(2,1,2);
grid on
% Paste figures on the subplots
copyobj(allchild(get(w, 'CurrentAxes')),h(1));

```

```
copyobj(allchild(get(z, 'CurrentAxes')),h(2));  
% Add axis labels  
xlabel(h(1), 'Station - Feet');  
ylabel(h(1), 'Rotation - Degrees');  
xlabel(h(2), 'Station - Feet');  
ylabel(h(2), 'Deflection - Inches');
```

Appendix D

RAW ROTATION DATA COLLECTED DURING LOAD TEST 5

D.1 Raw Rotation Data from SHM System and Surface Mounted Tilt Meters

Table D.1 Raw Rotation Data from Load Pass 0_1 and Load Pass 0_2

Tilt Meter	Station (Feet)	Rotation (Degrees)	
		Load Pass 0_1	Load Pass 0_2
T_E1	5	0.05432	0.04887
T_E2	217	-0.01349	-0.01291
T_E3	400	-0.01865	-0.01218
T_E4	632	-0.03004	-0.02994
SM_1	734	-0.05466	-0.06493
T_E5	877	0.003325	0.001042
SM_2	1010	0.0658	0.06199
T_E6	1117	0.02969	0.03085
T_E7	1350	0.009488	0.01014
T_E8	1532	0.00954	0.009771
T_E9	1745	-0.03572	-0.03691

Appendix E

PERMISSIONS

E.1 Permission to Use Figure 2 and Figure 5



Ashley Bechtold <albech@udel.edu>

Permission for Photos in Thesis

3 messages

Ashley Bechtold <albech@udel.edu>
To: Hadi Al-Khateeb <khateeb@udel.edu>

Thu, Apr 13, 2017 at 2:08 PM

Hadi,

I hope you are doing well and enjoying your job. I am finishing up my thesis for submission next week. After talking to Chris about my thesis, she brought to my attention that I will need to get your permission to use a couple of your photos from your dissertation. I had cited your dissertation next to the photos (because I did not know where the photos originally came from so I thought they were originally yours), but she said that I will need an email from you granting your permission for each photo. The photos that I used are below. If you would be willing to provide permission for each of the two photos below, I'd greatly appreciate it!

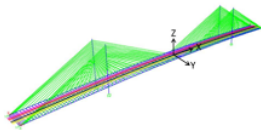
Thank you so much Hadi!

--
Ashley L. Bechtold, E.I.T.
Civil Engineering - Structural
University of Delaware, Newark, DE 19716

2 attachments



AE5C282A91694365A69F88E6E2061BCF.png
434K



51C98178C6D946D8BF4C41814D6F59BA.png
84K

Hadi Al-Khateeb <khateeb@udel.edu>
To: Ashley Bechtold <albech@udel.edu>

Thu, Apr 13, 2017 at 2:38 PM

Ashley,

Sure. I am officially give you the permission to include those photos and other photos from my dissertation if you need them. Good luck in your new career and life. Stay in touch on LinkedIn.

Thank you,
Hadi

[Quoted text hidden]

--
Hadi Al-khateeb, Ph.D.
Research Associate II
Department of Civil & Environmental Engineering
University of Delaware
Newark, DE 19716

Ashley Bechtold <albech@udel.edu>
To: Hadi Al-Khateeb <khateeb@udel.edu>

Fri, Apr 14, 2017 at 3:26 PM

Thank you Hadi!

--

Ashley L. Bechtold, E.I.T.
Civil Engineering - Structural
University of Delaware, Newark, DE 19716
[Quoted text hidden]